Thermal Processing for Gear Solutions
Spring/Summer 2016

Thermal processing
for Gear Solutions

Company Profile: Houghton International

Improved Materials and Enhanced Fatigue Resistance for Gear Components

Analysis of Heat Treat Growth on Carburized Ring Gear and Multivariate Regression Model Development

Coupling CFD and Oil Quench Hardening Analysis of a Gear Component

Residual Stress Distribution in an Induction Hardened Gear

Case Study: Laser Hardening

Spring/Summer 2016
thermalprocessing.com


Ipsen


Ipsen

FEATURES Spring/Summer 2016

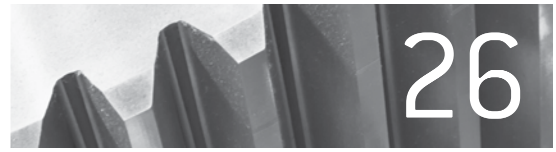

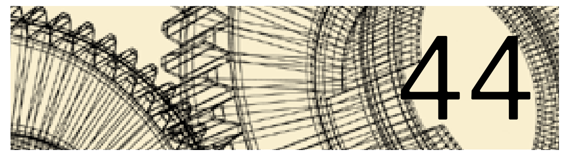

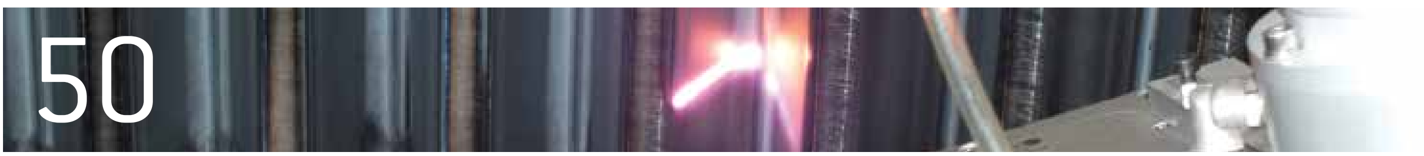

DEPARTMENTS

Spring/Summer 2016
Volume 5 / Number 1

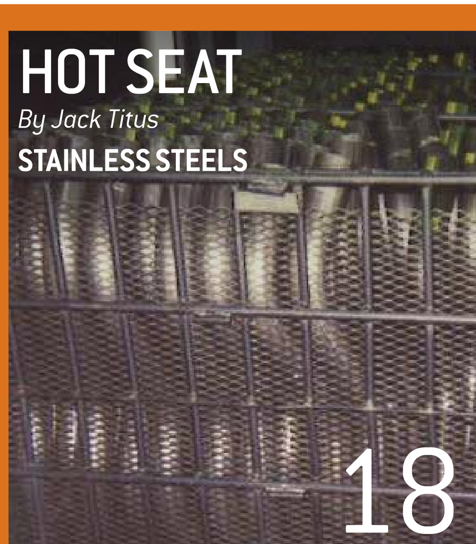

RESOURCES

Cover photo: McInnes Rolled Rings

Thermal Processing for Gear Solutions is published semi-annually by Media Solutions, Inc., 266D Yeager Parkway Pelham, AL 35124. Phone (205) 380-1573 Fax (205) 380-1580 International subscription rates: $105.00 per year. Postage Paid at Pelham AL and at additional mailing offices. Printed in the USA. POSTMASTER: Send address changes to *Thermal Processing for Gear Solutions* magazine, P.O. Box 1210 Pelham AL 35124. Return undeliverable Canadian addresses to P.O. Box 503 RPO West Beaver Creek Richmond Hill, ON L4B4R6.

LETTER FROM THE EDITOR

Welcome to the Spring/Summer issue of *Thermal Processing for Gear Solutions.*

In *Thermal Processing*, we bring you the latest advancements within the heat treating industry, as they are so critical to the manufacturing of gears and other components. For a process that's been around since antiquity, it's impressive that heat treatment techniques seem to progress on a daily basis, and the selection of articles in this issue are all reflective of those new developments.

First, Dr. Ing. Volker Heuer, Klaus Loeser, and Gunther Schmitt from ALD Vacuum Technologies GmbH discuss the advances of steel grades and case hardening technology that enhance fatigue resistance especially for transmission components. Another advancement is presented by Olga Rowan and Thomas Yaniak with the Advanced Materials Technology division at Caterpillar — a development of a better tool for predicting heat treat changes during carburizing that could lead to reduced post–heat treat gear machining.

Authors Dr. Zhichao (Charlie) Li and Dr. B. Lynn Ferguson from DANTE Solutions present an analysis to predict latent heat release, which has a significant effect on the temperature distribution during quenching. In addition, Dr. Dmitry Ivanov, John Inge Asperheim, and Leif Markegård from EFD Induction use simulation software to evaluate residual stress distribution in an induction hardened aeronautic gear.

Our *Thermal Processing* columnists return to share their expertise as well. Jim Oakes from Super Systems Inc. talks about gas nitriding, and Jack Titus presents a discussion on stainless steels. And we are thrilled to welcome our new Metal Urgency columnist, March Li, a metallurgist from Lufkin Industries, part of GE Oil & Gas, who begins with an introduction on carburizing.

For the company profile, I had the pleasure of speaking with Houghton International, a leading developer of metalworking fluids. You may have met them at ASM's 2015 Heat Treat expo in Detroit (their booth's plush vibrant-orange carpet was certainly memorable). Houghton's first lubricant product was invented in 1865, so today, the company is excited to celebrate its anniversary of over 150 years.

I also had an enjoyable conversation with Bill Stuehr of Induction Tooling for this issue's Q&A. Remarkably, with only 20 employees, the company is the largest facility in the world that engineers induction hardening tooling for selective hardening.

Lastly, we feature a case study from Laserline by Markus A. Ruetering, who shares success stories and results of customers using the fast-growing process of laser hardening.

We've covered the gamut of heat treat processes in this issue, but if there is an area you'd like to see more of, please feel free to reach out to me. I would love to hear from you.

Also, we invite you to visit our recently redesigned *Thermal Processing* website. With a brand-new look and easier navigation, the site highlights current content on the home page and features an expansive keyword-searchable technical library, an events calendar, a rotating banner ad display, and a complete archives with all past articles and downloadable issues. We are proud of our design team and the hard work that they've put into the site, and we'll continue to enhance and improve it, offering more content and benefits to you.

I hope you enjoy the new website and this issue of *Thermal Processing*.

Thanks for reading!

Molly J. Rogers

Molly J. Rogers
Editor
Thermal Processing magazine
editor@thermalprocessing.com
(800) 366-2185 x205

Thermal processing for Gear Solutions

David C. Cooper
PUBLISHER

Chad Morrison
ASSOCIATE PUBLISHER

EDITORIAL

Molly J. Rogers
EDITOR

Anna Claire Howard
ASSOCIATE EDITOR

SALES

Chad Morrison
ASSOCIATE PUBLISHER

Dave Gomez
REGIONAL SALES MANAGER

CIRCULATION

Teresa Cooper
MANAGER

Kassie Boggan
COORDINATOR

Jamie Willett
ASSISTANT

ART

Shane Bell
CREATIVE DIRECTOR

Michele Hall
GRAPHIC DESIGNER

CONTRIBUTING WRITERS

JOHN INGE ASPERHEIM
B. LYNN FERGUSON
VOLKER HEUER
DMITRY IVANOV
MARCH LI
ZHICHAO (CHARLIE) LI
KLAUS LOESER
LEIF MARKEGÅRD
JIM OAKES
OLGA ROWAN
MARKUS A. RUETERING
GUNTHER SCHMITT
JACK TITUS
THOMAS YANIAK

Media Solutions

PUBLISHED BY MEDIA SOLUTIONS, INC.
P. O. BOX 1987 • PELHAM, AL 35124
(800) 366-2185 • (205) 380-1580 FAX

David C. Cooper
PRESIDENT

Chad Morrison
VICE PRESIDENT

Teresa Cooper
OPERATIONS

Laserline LDF

The New Benchmark for Diode Lasers

Source: Lasertherm

Lasers for
Hardening
Heat Treatment
Thermal Processing

and more applications in industrial materials processing

How can superior technology be improved? By making it more versatile to use while preserving all proven properties. The new Laserline LDF diode laser of the 6th generation sets new standards for industrial applications in the multi-kilowatts range: with more power, more mobility, more efficiency and easier maintenance.

Laserline Inc.
1800 Wyatt Drive, Suite 9
Santa Clara, CA 95054, USA
Tel. +1 408 834 4660

46025 Port Street
Plymouth MI 48170, USA
Tel. +1 248 826 5041

info@laserline-inc.com
www.laserline-inc.com

New Grip Smart System for Hot Workpieces by Wickert

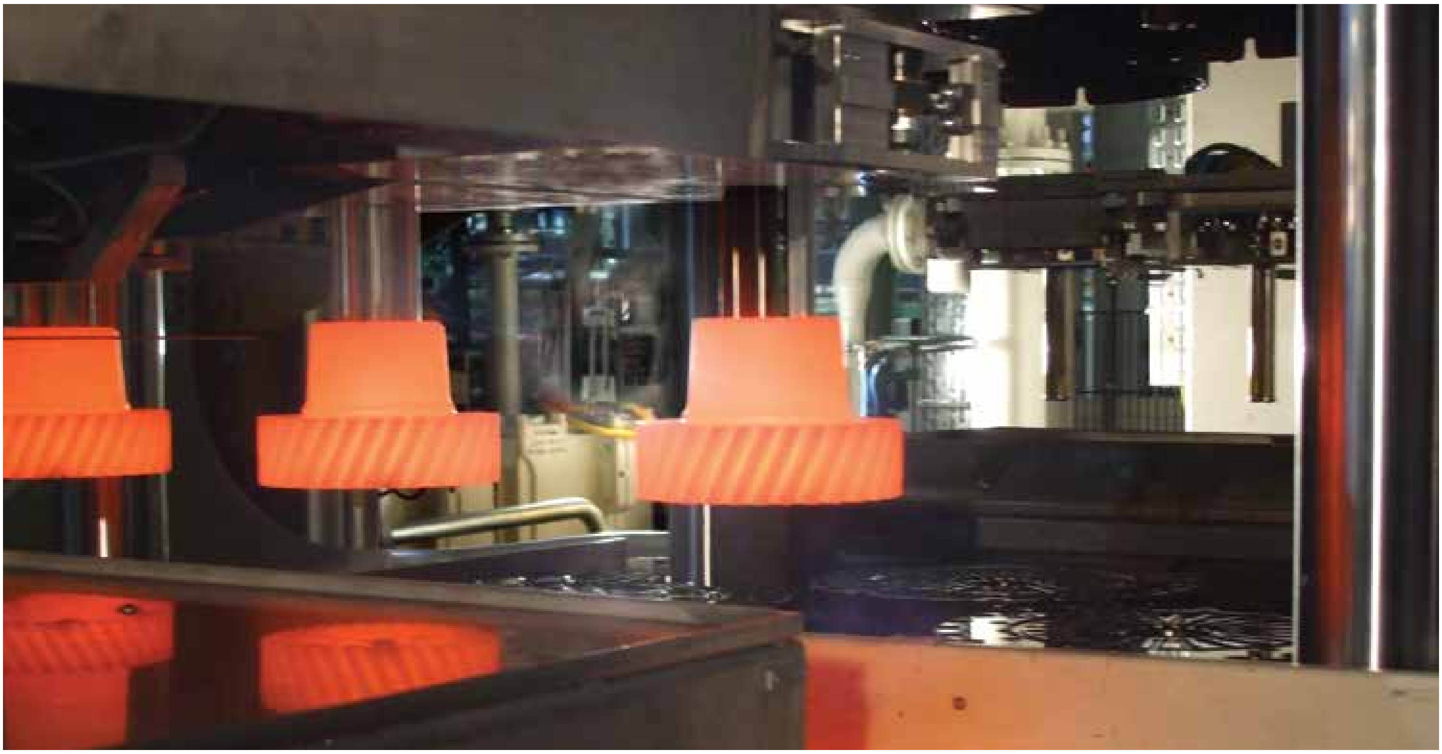

Wickert Hydraulic Presses is a global manufacturer of fixture hardening systems for heat treated high-tolerance parts, such as the carburization of gears or parts requiring forming and hardening. Wickert's 110 years of in-depth knowledge of the process has led it to develop a new and innovative technology — Grip Smart System (GSS) grippers. Wickert's GSS has been developed to minimize the risk of defective goods caused by tilt and/or mislocation of production hardening masks. Moreover, the GSS avoids pressure points and prevents damage to delicately interlocked components that are often encountered with conventional grippers in a heat treat system.

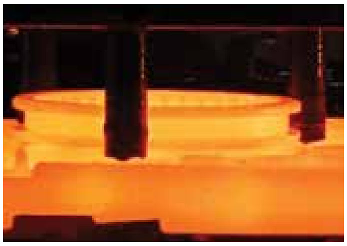

Wickert's GSS provides the ability to directly check the position of the rings during closing. This alleviates the tilting of the component — a common issue in the hardening press. As a result, the Wickert GSS prevents damages to the hardening mask, as well as manufacturing errors.

An additional advantage with the GSS is that workpieces are treated gently after hardening. Compared to current off-the-shelf type grippers, the new GSS has a specialized surface treatment to create a damping effect that improves the gripper reliability. When working with delicate gears and intricate workpieces, these smart grippers provide up to a 50-percent increase in productivity with reduced rejects.

Wickert delivers custom-engineered fixture hardening systems. Its turnkey packages provide tooling, including automatic tool-change function, ovens, and preheating stations with component buffers. Wickert also offers a single control package for the entire system with component tracking, production data monitoring, and SPC, including pre-selectable testing reports. Installation and worldwide service are included in a complete service package.

FOR MORE INFORMATION: wickert-usa.com

Heat Treat Expansion Complete at McInnes Rolled Rings

McInnes Rolled Rings recently completed an $8 million, 25,000-square-foot expansion to its current manufacturing facility. The addition expands its present heat treat size capabilities by providing the ability to quench and temper forgings up to 144 inches in diameter. With separate high agitation water and polymer quench tanks, this new state-of-the-art bay will significantly expand the daily tonnage capacity to ensure the fastest delivery times available in the industry.

McInnes contracted with Can-Eng Furnaces Intl. Ltd. to design and install the most advanced technology to process large diameter products. The furnace and quench tank designs are augmented by a customized material handling system by Dango & Dienthal Hollerbach GmbH capable of processing loads up to 25 tons. The system's fast transfer from furnace to quench tank provides optimal and repeatable process controls.

"This new bay nearly doubles our quenched and tempered offerings to the power transmission industry and adds the ability to solution anneal large diameter stainless steel rings," said Shawn O'Brien, vice president of sales and marketing. "Also, the addition of water quenching improves our ability to meet the high property demands of the custom flange markets."

FOR MORE INFORMATION:
mcinnesrolledrings.com

Thermex Metal Treating Expands Plant Capacity with Seco/Warwick's ZeroFlow Technology

Thermex Metal Treating is expanding capacity at its facility in Canada with the purchase of a gas nitrider with vertical pit-style loading and Seco/Warwick's proprietary ZeroFlow™ control technology and ferritic nitrocarburizing capability.

Thermex offers a wide range of ferrous metal heat treating processes and services in Western Canada from its base in Edmonton, Alberta. The purchase of this state-of-the-art equipment keeps with Thermex's ongoing commitment to continuous improvement, integration of new technology, and high-quality customer service.

"Combined with Seco/Warwick's R&D testing capabilities and its experience in gas nitriding, we felt this was our best option to offer exacting nitriding solutions for our customers and our large load requirements," said Norm Hanson, Thermex's president.

Seco/Warwick is a technology leader with the proprietary ZeroFlow method of economical gas flow and precision nitrided layer control. The furnace is being designed and manufactured in Seco/Warwick's facility in Meadville, Pennsylvania.

"We are pleased to partner with Thermex to provide this new technology alternative to traditional nitriding methods, designed specifically to reduce process costs while improving process efficiency," said Jonathan Markley, Seco/Warwick's managing director.

FOR MORE INFORMATION: secowarwick.com

Grieve's 2000°F Inert Atmosphere, Heavy-Duty Furnace Used for Turbine Components

No. 1039 is a 2000°F (1093°C) inert atmosphere, heavy-duty furnace from Grieve that is currently being used for heat treating turbine components at the customer's facility. Workspace dimensions of this furnace measure 36" w x 60" d x 36" h. Also, 73 kW are installed in ICA wire coils supported by vacuum-formed ceramic fiber installed on all interior surfaces, including the door and beneath the hearth.

This Grieve inert atmosphere furnace has a roof-mounted, heat-resisting alloy circulating fan powered by a 1-hp motor with V-belt drive, water cooled bearings, and inert atmosphere shaft seal. Furnace features include: 9-inch-thick insulated walls comprised of 5 inches of 2300°F ceramic fiber and 4 inches of 1900°F block insulation and 8½-inch floor insulation comprised of 4 ½ inches of 2300°F firebrick and 4 inches of 1900°F block insulation. Other features include ¼-inch plate exterior reinforced with structural steel and ½-inch steel face plate at doorway with air-operated vertical lift door. Inert atmosphere construction includes continuously welded outer shell, high-temperature door gasket, sealed heater terminal boxes, inert atmosphere inlet, inert atmosphere outlet, inert atmosphere flow meter, and manual gas valve.

Controls on No. 1039 include a digital programming temperature controller, a manual reset excess temperature controller with separate contactors, paperless event recorder, and SCR power controller.

FOR MORE INFORMATION:
grievecorp.com

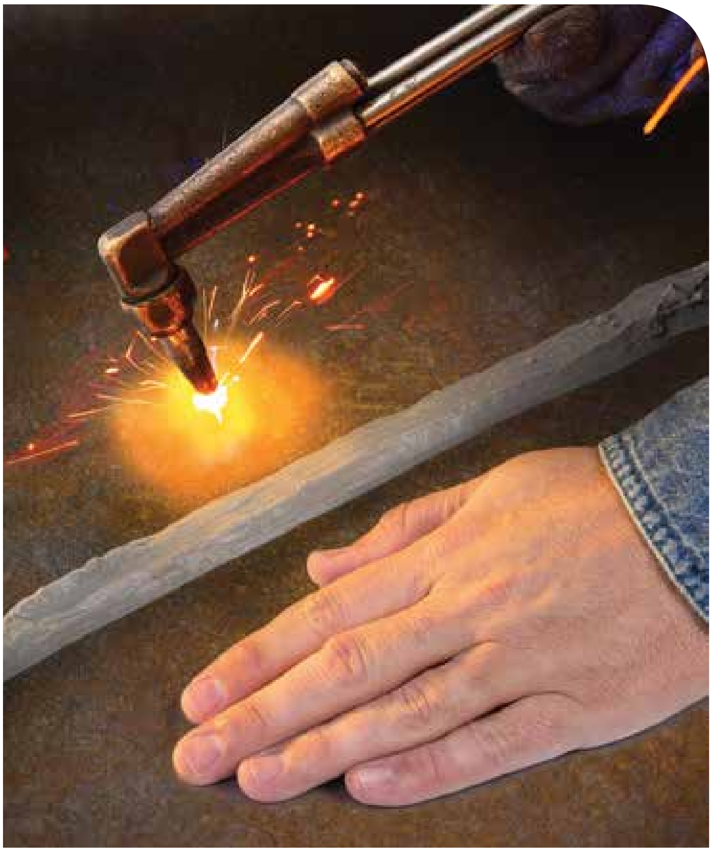

Heat-Absorbing Compound Blocks Heat Transfer Through Metal

Alvin Products of Everett, Massachusetts, recently released its heat-absorbing compound that protects metal from heat damage and prevents heat from traveling through the metal surface and potentially damaging or discoloring parts.

Alvin® Heat-Block is a compound formulated to eliminate and protect metal against heat damage and discoloration during brazing, soldering, welding, and other procedures. It is simple to use — just apply the heat-absorbing paste directly from the container onto the metal, and it will absorb and dissipate heat, preventing it from traveling through the metal surface.

Protecting parts in close proximity such as pipes, valves, internal gaskets, and other components that could be damaged during installation or repair work requiring heat applied by torch or a soldering iron, Alvin Heat-Block is a reusable water-based compound. This heat sink compound stops heat-related damages, including buckling, cracking, warping, and discoloration.

Alvin Heat-Block is offered in pint, quart, 1-gallon, and 5-gallon sizes. It cleans up with soap and water.

FOR MORE INFORMATION: dampney.com

Thermo-Calc Software

Thermodynamic and Diffusion Simulation Software

With Thermo-Calc you gain deep insights into the behaviour of materials that allow you to:

- ✓ Reduce costly, time-consuming experiments
- ✓ Base decisions on scientifically supported predictions and data
- ✓ Shorten development time and accelerate materials development while reducing risk
- ✓ Improve the quality and consistency of your products through deeper understanding of your materials and processes

Thermo-Calc

Powerful software for thermodynamic calculations for multicomponent systems

- ✓ Calculate furnace gas chemistry based on composition, temperature and pressure, along with activity coefficients in the gas.
- ✓ Predict formation of precipitate phases within an alloy as a function of composition and temperature.
- ✓ Plot multicomponent phase diagrams for alloys that allow a quick overview of optimal regions for a heat treat process.

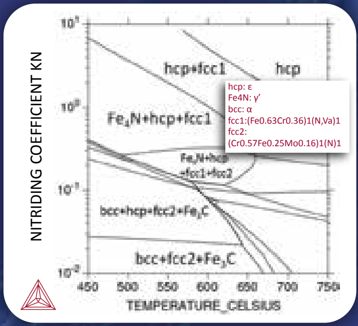

Lehrer diagram for steel

DICTRA

Unique software for the simulation of diffusion controlled transformations in multicomponent systems

- ✓ Predict case depth profiles, for example during carburization, as a function of time and activity or flux at the surface, even for highly alloyed materials.
- ✓ Model the growth, coarsening and dissolution of precipitates.
- ✓ Predict the homogenization of multicomponent alloys
- ✓ Model post weld heat treatment.

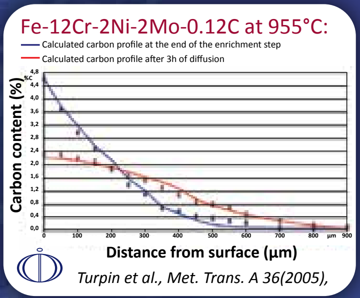

Simulation of carbon evolution in high alloyed steels

TC-PRISMA

Software for simulating precipitation kinetics in multicomponent systems

- ✓ Simulate the concurrent nucleation, growth, dissolution and coarsening of precipitate phases as a function of alloy chemistry, temperature and time, during an isothermal/non-isothermal heat-treat cycle.
- ✓ Predict the fraction of precipitate phases and the number density and size distribution of the precipitates.
- ✓ Calculate TTT diagrams for precipitate phases.

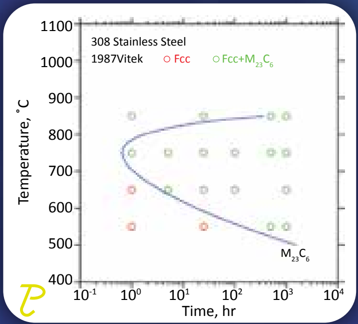

Calculated TTT diagram for precipitate phases

Watch our free webinar

Reliable Simulation of Heat Treating Using CALPHAD-Based Tools

Thermo-Calc Software AB
Email: info@thermocalc.com
Phone: +46-8-545 959 30

www.thermocalc.com

USA, Canada and Mexico
Email: paul@thermocalc.com
Phone: (724) 731 0074

Jeff Opitz Joins CeraMaterials

CeraMaterials recently announced that Jeff Opitz has joined CeraMaterials as its technical sales specialist in the Port Jervis, New York, headquarters facility.

Opitz has a B.A. from the University of Pittsburgh in economics and communications with 10 years of sales and marketing experience. Opitz honed his sales skills at Metrie, a Sauder Company, while marketing wood and trim products for home construction; at Doskocil Manufacturing where he focused on the pet product industry; and most recently, with Clarion Safety Systems where he focused on safety communication systems. Opitz brings sales expertise to CeraMaterials along with strong technical and marketing abilities. He has already contributed to improved sales and has extended the customer base in key market areas of ceramic and graphite insulation.

CeraMaterials is an international supplier of graphite and ceramic insulation, carbon composites, machined graphite, ceramics, and moly products mainly for vacuum and process furnace applications.

FOR MORE INFORMATION:
ceramaterials.com

Timken Names Roellgen, Ruel, and Connors to Executive Sales and Marketing Roles

The Timken Company, a global leader in tapered roller bearings, has named Andreas Roellgen and Brian J. Ruel to the positions of vice president of sales. Ruel leads the company's selling team across the Americas, and Roellgen will oversee the Timken sales organization for the rest of the world.

In addition, Michael J. Connors will lead the company's marketing organization as the newly appointed vice president of global marketing.

"These appointments are part of the new organization we've put in place to increase speed to market and streamline decision-making," said Christopher Coughlin, group president and executive vice president for Timken. "We expect to leverage the collective experience now captured with these bearing leadership appointments to improve both our focus and accountability with regards to driving profitable growth."

FOR MORE INFORMATION: timken.com

The success of a nitriding process depends on the ability to meet metallurgical requirements involving microstructures, surface hardness, case hardness, and, in some cases, the part's appearance.

By Jim Oakes

In general, nitriding of parts involves a thermal process that provides a tough, corrosion-resistant, and wear-resistant surface with less distortion compared to other case hardening processes due to processing temperature and no need for quenching. There are different methods of nitriding, including gas nitriding, plasma/ion nitriding, and salt-bath nitriding. This article focuses on gas nitriding.

When nitriding gears, it is common to see requirements that specify no white layer for the finished part. The white layer, also known as the compound layer, is a hard, brittle layer that is formed during nitriding but can be reduced or virtually removed through process control. Although the white layer can be machined off, the typical goal would be to reduce or even eliminate the post-nitride machining. This can be accomplished due to the fact that the part's dimensional integrity remains uncompromised from distortion through lower processing temperatures and lack of a quench.

For gas nitriding, the process variables are time, temperature, and atmosphere. Processing temperature for nitriding will most often be between 975°F and 1050°F (524°C and 566°C), but it can be as low as 650°F (343°C) for certain applications. The parts will be exposed to a non-oxygen-bearing, nitrogen-rich atmosphere typically produced by a mixture of nitrogen, ammonia, and dissociated ammonia. The furnace atmosphere will be continuously replenished with an atmosphere that provides a potential of nitrogen to diffuse into the steel and form nitrides.

In order to meet specifications for nitriding, a common control variable used to measure the amount of nitriding is K_N (nitriding potential). K_N is a derived measurement of an atmosphere's potential to allow for the diffusion of nitrogen into a material — specifically, iron, in this case.

K_N is mathematically defined in Equation 1:

$$K_N = pNH_3/(pH_2)^{3/2} \qquad \text{Equation 1}$$

where *p* denotes partial pressure.

Many specifications require tight tolerances on the amount of white layer on the surface, which requires a control system to monitor the furnace atmosphere and control the potential of nitrogen that is available to react at the surface of the part. To perform continuous closed-loop control, there must be a method of measurement for the atmosphere. In the past, the measurement was discontinuous using a water burette that would provide furnace operators with a method of measuring the percentage of residual ammonia in the atmosphere. If the residual ammonia is available, the percentage of dissociated ammonia (% DA) can be determined and then analyzed to adjust the flow rates of the process gas.

To control the gases introduced to the furnace, today's automated controls use feedback from the atmosphere being measured. For gas nitriding, process variables used in this thermochemical treatment are represented by nitrogen, dissociated ammonia (bottled or from a dissociated ammonia generator), and ammonia. Continuous measurement of the exhaust gas using a hydrogen analyzer provides a method of closed-loop control by varying the process gases to meet a desired control variable setpoint.

In this case, atmosphere control variables are K_N/DA and gas flows, which will facilitate delivery of nitrogen to the processed part. The measurement of hydrogen in the exhaust provides enough data to calculate DA or K_N. When ammonia breaks down to one-part nitrogen and three-parts hydrogen, the hydrogen can be measured to determine the percentage of uncracked ammonia in the atmosphere. For example, if we measure 30-percent hydrogen in the exhausted atmosphere, that would leave us with 10-percent nitrogen, meaning that 40-percent of the atmosphere is dissociated ammonia. Our residual 60-percent would be represented by ammonia. The assumption would be that only DA gas and ammonia were used as supply gases. If the atmosphere is using N_2 for blending, the volume of gas flowing into the retort of the furnace will be used in our calculation. By understanding the amount of ammonia dissociated in the exhaust gas, the nitrogen activity on the surface can be deduced. The greater the flow of ammonia, the greater the amount of ammonia measured in the exhaust and the more ammonia to which the parts are exposed. The higher the amount of ammonia is present, the lower the amount of dissociation (DA), and the greater the activity of nitrogen on the surface. Too much ammonia could lead to a significant compound layer, nitride networking, and a brittle surface.

Two-stage nitriding processes are used to create proper surface and case conditions. Similar to a carburizing boost and diffuse method, two-stage nitriding utilizes a nitrogen-rich atmosphere for the buildup of nitrogen concentration in the steel (a.k.a. the first stage) and a reduced nitrogen atmosphere to allow for diffusion of the nitrogen into the steel (a.k.a. the second stage). This method is most commonly used with controlling the white layer thickness. The atmosphere can be controlled to eliminate the white layer or at least reduce it to less than 0.007 mm (0.0003") for minimal post-nitride machining/grinding. Although beneficial for some applications, the white layer may not be desired in the process based on manufacturing steps and performance requirements for the finished goods.

ABOUT THE AUTHOR: Jim Oakes is vice president of business development for Super Systems Inc. (SSi), where he oversees marketing and growth in multiple business channels and helps develop product innovation strategies in conjunction with customer feedback. He has extensive experience working in the heat treating and software/IT industries. For more information, email him at joakes@supersystems.com or go to www.supersystems.com.

Among heat treatment techniques, carburizing is one of the most widely used for case hardening.

By March Li

While some heat treatments are used to soften the material or improve its machinability, most are processed to obtain strengthened or hardened properties. The majority of heat treatments apply to metallic materials and, typically, the techniques include annealing, normalizing, quenching, tempering, precipitation strengthening, surface hardening, and case hardening. Heat treatment is so critically important that we can safely say a part undergoing extensive manufacturing processes such as melting, rolling, forging, and other related machining is of little or no value without the necessary and appropriate heat treatment.

Carburizing is one of the most widely used case hardening treatments. Per AGMA 923, carburizing is defined as a heat treatment process in which an austenitized steel is brought into contact with a carbonaceous atmosphere of sufficient carbon potential to cause adsorption of carbon bearing gases at the surface where they dissociate and, by diffusion, to create a carbon concentration gradient [1].

Carburizing is generally followed by quenching and tempering. After quenching, the outer surface becomes harder via martensitic transformation due to its higher carbon content, while the core remains relatively soft and tough. Tempering is performed to increase the toughness and ductility of the quenched part. Through carburizing and quenching plus tempering the part, the results are increased surface hardness, wear resistance, fatigue, and tensile strength, as well as the desired compressive residual stress on the surface. Consequently, the part also experiences grain growth and distortion.

Carburized parts are so popular that they are used in almost every industry including aerospace, transportation, power transmission, manufacturing, and material processing. In the automobile industry, the global output of gears in 2014 was estimated to be approximately 1 billion, and most of them are carburized [2].

Per definition, carburizing material is usually low-carbon steel, normally with a carbon content of ≤ 0.25 wt.%. In the past, plain carbon steels, such as SAE 1020, were used; however, with the demand of carrying a heavier load, more alloy steels have been developed and carburized, such as SAE 4320, 8620, and 9310 and 17CrNiMo6/18CrNiMo7-6, 16MnCr5, and 20MnCr5. Carburizing temperature usually lies in the range of 900°C to 950°C. Surface hardness is in the range of 55 HRC to 64 HRC. Case depth can be anywhere between 0.4 mm and 9 mm. A very thick case can carry heavy torque and stress, which is useful in specific applications such as marine and sugar mill gears.

Figure 1: Atmosphere gas carburizing

Historically, there are three types of carburizing methods depending on the carbon source: solid carburizing, liquid carburizing, and gas carburizing. Charcoal, molten salt, and carbon-bearing gases, such as natural gas and propane, are used correspondingly. Among them, gas carburizing is the most common type and provides precise and homogeneous control of case depth with economical and cost-effective benefits. Today, most of the world's carburizing procedures are accomplished with gas carburizing. This includes both atmosphere and low pressure (vacuum) carburizing. Although vacuum carburizing is becoming more popular, atmosphere carburizing is still the most common gas carburizing procedure. (See Figure 1 for an example of atmosphere gas carburizing.)

Although atmosphere carburizing consists of several process steps [3], it can be simplified to include two major processes: carbon generation in the furnace and carbon diffusion into the workpiece. The former provides carbon atoms while the latter determines the carbon concentration gradient.

It should be noted that gas carburizing is a complicated procedure during which many chemical reactions occur simultaneously in the carburizing atmosphere. The most commonly used carbon-source gas is natural gas (methane, CH_4), while the endothermic gas is the preferred and most widely used carrier gas, which is usually produced by mixing air and natural gas in a fixed proportion, usually a 2.5-5 to 1 ratio. Reactions take place within the gas mixture when it passes through a chamber with a catalyst, e.g., NiAl. As a result, endothermic gas is composed of nitrogen (N_2), carbon monoxide (CO), carbon dioxide (CO_2), hydrogen (H_2), water (H_2O), and methane (CH_4), and enters the furnace together with carbon source gas. Among them, CO and CH_4 are carburizing agents, while CO_2 and H_2O are decarburizing agents. It is estimated that there are over one hundred reactions inside the carburizing atmosphere. However, the following three reactions are the most important and determine the rate of carbon transfer from the carburizing atmosphere to the steel surface [4]:

$$2CO \leftrightarrow C_{(\gamma\text{-}Fe)} + CO_2 \qquad \text{Reaction 1}$$

$$CH_4 \leftrightarrow C_{(\gamma\text{-}Fe)} + 2H_2 \qquad \text{Reaction 2}$$

$$CO + H_2 \leftrightarrow C_{(\gamma\text{-}Fe)} + H_2O \qquad \text{Reaction 3}$$

Reaction 3 is about two orders of magnitude faster than the other two, therefore it determines the rate of carbon adsorption during the process [5].

The balancing reaction for gas carburizing atmosphere is called water-gas reaction and can be expressed by:

$$CO + H_2O \leftrightarrow CO_2 + H_2 \qquad \text{Reaction 4}$$

Typically, these four main reactions determine the carbon potential that provides carbon atoms for carburizing. After carbon potential is detected, a furnace controlling system adjusts the gas ratio to reach the target. Once the atoms are generated and adsorbed on the surface, they diffuse into the workpiece. The diffusion velocity depends on temperature, carbon potential in the atmosphere, and chemical composition of the steel. This step takes up the majority of time in the carburizing cycle. For example, if we want to get a very thick case, e.g., 0.35" (9 mm), an SAE 9310 steel part needs to be in the carburizing furnace for more than 10 days when carburized at 940°C. To obtain a desired homogeneous carburizing case depth, it is imperative to keep all carburizing parameters (temperature, carbon potential, and cycle time) under control. In addition to the surface hardness and case depth, other characteristics — such as surface carbon content, core hardness, and microstructure (retained austenite, carbide distribution, etc.) — should also meet the related requirements.

After carburizing, the part is quenched into the appropriate quenchant (water, oil, or polymer solution), followed by tempering, typically around 180°C. Keep in mind that not all austenite transforms into martensite after quenching. If the retained austenite is within 30 percent of the product phases, the carburized and hardened part can then move to the next manufacturing processing. Otherwise, a sub-zero treatment is needed, during which retained austenite transforms into martensite so that its fraction is no higher than 30 percent. SAE 9310 is a good example for this treatment. After that, the part needs to be tempered again. Figure 2 illustrates a carburizing cycle.

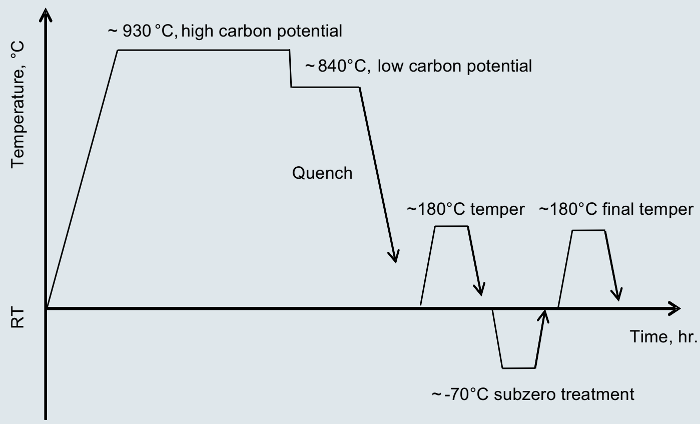

Figure 2: Schematic carburizing cycle. Temperature is lowered before quenching to reduce thermal stress and quench distortion. Low carbon potential is set to adjust the carbon/hardness profile. Subzero treatment and final temper apply to some specific steels.

REFERENCES

1. AGMA 923-B05, Metallurgical Specifications for Steel Gearing, American Gear Manufacturers Association, 500 Montgomery Street, Suite 350, Alexandria, Virginia 22314. p. 11.
2. Maciej Korecki, Emilia Wolowiec-Korecka, Doug Glenn, Single-Piece, High-Volume, Low-Distortion Case Hardening of Gears, AGMA Fall Technical Meeting, October 18-20, 2015, Detroit, Michigan.
3. Aymeric Goldsteinas and Rene Alquicer, Producing Quality Parts in an Atmosphere Furnace: How to Optimize Your Quenching and Carburizing Processes, Thermal Processing for Gear Solutions, April 15, 2015, p. 30.
4. R. Collin, S. Gunnarson and D. Thulin, Mathematical Model for Predicting Carbon Concentration Profiles of Gas-Carburized Steel, Journal of the Iron and Steel Institute, 210 (10), 1972, p. 785.
5. Olga Karabelchtchikova, Fundamentals of Mass Transfer in Gas Carburizing, Ph.D. thesis of Worcester Polytechnic Institute, November 2007, p. 7.

ABOUT THE AUTHOR: March Li is the lead metallurgist for the Power Transmission division at Lufkin Industries, LLC, part of GE Oil & Gas. He is responsible for material selection, evaluation, and application in gearboxes, heat treatment, material characterization, and failure analysis. Li has taught courses at GE Oil & Gas in material and metallurgy as well as gear failure mode and analysis. He has a Ph.D. degree in Materials Science and Engineering, over 20 years of professional experience, and has authored and co-authored over 30 technical publications in the material and metallurgy field. He is also an active AGMA committee member. For more information, email him at march.li@ge.com.

Understanding the properties, fatigue limits, and designations of stainless steels used in heat treatment processes can be helpful in selecting the right one for specific applications.

By Jack Titus

Kitchen sinks, refrigerator or oven doors, and tableware are what many people think of when they are asked what's made from stainless steel (SS). However, stainless steels encompass a wide range of products outside the home.

The more common stainless steels are iron-based alloys with chromium and sometimes nickel added to them, and they are primarily segregated into three grades: martensitic, ferritic, and austenitic. Ferritic and austenitic alloys are not hardenable by heat treatment; martensitic grades can be quenched and tempered just like ferrous or alloy steel. Austenitic stainless steels are nonmagnetic, but they can become magnetic when heavily carburized or have received severe cold work. Ferritic and martensitic stainless steels are generally magnetic.

Within the austenitic grades of stainless steel, heat-resistant (HR) alloys find application in more industrial environments such as heat treat furnaces, refineries, and chemical/pharmaceutical plants, to name a few. In addition, the food processing industry is a large consumer of the wrought form, meaning those that are transformed into plate, sheet, tube, and pipe.

While the overwhelming constituent in steel is iron with minor additions of chromium, nickel, manganese, and molybdenum, among others, stainless steels are comprised of chromium, nickel, and the balance of iron with additions of titanium, cobalt, aluminum, and other applicant-specific elements. Stainless steels are stainless because, for all practical purposes, they don't rust where iron and steel would. And like aluminum that receives its oxidation protection from the thin aluminum oxide layer formed in the air, stainless steels get their corrosion-resistant properties from chromium oxide. For an alloy to be considered stainless, it usually must have at least 10-percent chromium by weight. Figure 1 lists the composition and oxidation rate of some common austenitic stainless steels and heat-resistant alloys.

Martensitic stainless steel is, by its name, hardenable from the formation of martensite upon quenching, thus, in addition to the chromium, it has much higher carbon levels than the ferritic or austenitic grades. With much higher hardness and overall strength, it is used in applications where corrosion would attack alloy steel, such as in aircraft carrier-based airplane parts, tableware, kitchen knives, and surgical or dental instruments. Even iron golf club heads have been manufactured from investment cast martensitic stainless steel alloys such as 431 and 17-4 PH.

Ferritic stainless steels at room temperature have a ferritic microstructure due to their high chromium content and low carbon, thus no transformation to martensite can occur when quenched. Austenitic stainless steels have a high nickel concentration that forces an austenitic microstructure at ambient temperature. Both ferritic and austenitic stainless steels can only be strengthened by work hardening from such processing as cold forming into wire and rod — thin sheets, for example — but only to a limited degree.

Designations of wrought (sheet, plate, bar, pipe, and tube) stainless steel include: austenitic: 201, 202, and the more familiar 300 series, 302, 304, 309, 310, 312, 316, 321, 327, 330, and 347; ferritic: 405, 430, 442, and 446; and martensitic: 410, 414, 416, 420, 431, 440 A, B, and C.

440C, which is one of the more common aforementioned martensitic stainless steel

ALLOY	CHROMIUM %	NICKEL%	CARBON %	OXIDATION RATE, MPY*	
				1600°F (871°C)	2000°F (1093°C)
304	18.8	9.3	0.08	68.5	1571
310	23.3	19.8	0.25	<5	64
321	17.9	9.6	0.08	<5	2183
330	18.6	34.3	0.20	<5	23
INCONEL 600	15.2	75.4	0.15	37	12
22H	28.0	48.0	0.50	-	-
HH	26.8	16.6	0.20 to 0.50	0	<5
HT	18.9	34.9	0.35 to 0.75	46	12
HL	30.7	21.2	0.20 to 0.60	47	41

*MPY = 0.001 inches (0.0254 mm) penetration per year into 2 inch (50 mm) square x 1/8 inch (3.175 mm) thick coupon (in air). Data developed by writer, 1968.

Figure 1

ALLOY	THERMAL CONDUCTIVITY		LINEAR THERMAL EXPANSION	
	Btu/sq. ft./hr./°F/ft. @ 932°F	Watt/centimeter/°C [W/(cm*°C)] @500°C	10-6/in/in/°F @ 1200°F	10-6/cm/cm/°C @ 649°C
304	12.0	0.21	10.4	18.70
310	10.8	0.18	9.7	17.40
321	12.8	0.22	12.8	23.04
330	9.4	0.16	9.4	16.92
INCONEL 600	8.1	0.14	8.1	14.60
22H	16.9	0.29	21.5	38.30
HH	12.4	0.21	9.7	17.46
HT	11.9	0.20	9.1	16.38
HL	12.2	0.21	9.4	16.92
1060 STEEL	33.0	0.42	6.7	12.02
COPPER	213	3.61	9.8	17.64
ALUMINA (Al_2O_3)	10.4	0.18	4.5	8.10
SILICON CARBIDE (SiC)	23	0.39	2.8	5.10

Figure 2

grades, has a carbon level of 0.9 to 1.2 percent that's capable of creating alloy-steel-like hardness. Its maximum corrosion resistance — like all stainless steel regardless of grade — is achieved by rapid cooling from the austenitic temperature. When austenitized at 1850°F to 1950°F (1010°C to 1065°C) and quenched and tempered, trapping the alloy in solid solution 440C produces a hardness of HRC 60.

To produce the maximum corrosion resistance, stainless steel of any grade must be rapidly cooled to prevent the premature precipitation of mainly chromium carbide plus other complex precipitates. And in specific alloys — such as a fourth group of stainless steels called precipitation hardening alloys: 17-4, 17-7, and 15-7 PH — the complex precipitates after solution and rapid cooling contribute to the strengthening and hardening of the material. The low-carbon martensite formed is the result of aging to form a precipitate of mainly copper, and the hardness is more representative of bainite (20 to 48 HRC) due in part to a very low carbon level, typically 0.07 percent.

For the industrial sector as in heat treating, the two main areas for stainless steel application are furnace interiors for structural and heating element systems. Material handling is a major consumer of heat-resistant alloys for trays and fixturing. Where wrought alloys lend themselves to easier fabrication, cast alloys are the preferred material for elevated temperatures.

Cast austenitic stainless steels employed in the heat treating industry must possess four major qualities: high-temperature strength, creep resistance, carburizing, and oxidation resistance. Interior furnace cast heat-resistant alloys can sustain continuous high-temperature exposure and generally need only sufficient creep strength. Creep is the phenomenon that causes a beam, for example, to sag (over an extended time) between two support points with an applied load much lower than would normally cause it to bend. Take alloy HK as an example, which is the cast equivalent of 310 SS. Its limiting creep stress at 1800°F (982°C) for a creep rate of 0.0001 percent is 2,500 psi — compared to its 0.2 percent offset yield strength at 1800°F (982°C), which is 8,700 psi. For design purposes, we use 50 percent of the allowable creep stress, resulting in 1,250 psi as the design limit.

Cast heat-resistant alloys used in heat treating furnaces are classified via a two-letter designation beginning with the letter H, and most have a wrought equivalent. In addition, there are dozens of wrought and cast heat-resistant alloys with a myriad of designations used in aerospace and jet engine components.

Some of the more common cast stainless steels and their wrought equivalents are: HC, 446; HD, 327; HE, 312; HF, 302B; HH, 309; HK, 310; Hl, HN, HP, HT, 330; and 22H. Figure 2 lists important thermal properties of furnace materials.

Because they are cast, the H-series alloys have higher silicon and carbon content than wrought material to assist in facilitating fluid flow during casting. The major reason for choosing cast stainless steels in furnace applications is high-temperature strength — they are intrinsically more brittle, thus they have a higher hardness than wrought material due to excess carbide created by the higher base carbon.

Another advantage of cast stainless steel is a thicker chromium oxide layer compared to wrought material that is subjected to several stages of mechanical forming that can reduce or result in thinner oxides. That oxide is the primary barrier against the carburizing process that most often reduces the life of the alloy. Carbon diffused through the oxide reacts with the chromium matrix forming chromium carbide, which reduces the chromium's ability to form additional oxide, thereby accelerating the destruction of the component. Aluminum is often added to enhance the carburizing resistance of the alloy.

The second most detrimental influence on heat-resistant alloys is thermal cycling, and the combination of carburizing and thermal cycling can destroy alloy life. Thermal cycling leads to thermal fatigue and fatigue cracks and ultimately the breakdown of the protective oxide. If potential thermal cycling can't be avoided,

Figure 3: Typical load of exhaust pipes

designers must take steps to reduce direct exposure to the heat source or reduce a component's cross-section, which will reduce the temperature difference through the material attenuating the thermal stress.

An example of thermal cycling's negative effect on heat-resistant alloys occurred several years ago on a pair of load support roller rails made from cast 22H — a 28-percent chromium, 48-percent nickel, and 15-percent cobalt alloy. The furnace was a batch-type system with a top-cool chamber and accelerated gas cooling for solution annealing 304 SS automobile exhaust pipes (the pipe from the engine to the catalytic converter). See Figure 3. The cycle consisted of heating a 36" w x 72" l x 36" h load of pipes to 1950°F (1065°C), soaking one-and-a-half hours, and quenching/cooling. Immediately thereafter, another tray was charged into the hot furnace. The atmosphere consisted of nitrogen only and no carburizing gas. The unusually rapid cycling (for no other reason we can surmise) caused the roller rails (see Figure 4), to grow permanently over a six-month time period to the unbelievable length of 6 inches into the rear wall insulating fiber. The roller rails were approximately 80 inches long initially. So the 6 inches of growth was 4.6 times the 1.3 inches we expected, but surely not in just six months. It's normal for continuous furnace trays that are heated and quenched repeatedly to experience permanent growth, but again, not to the degree seen here. We knew that thermal cycling was a possible issue, but we were shocked at the magnitude of permanent growth. We removed the added growth only to see the rail continue to grow. The solution was to replace the 22H alloy rails with high-density alumina and, eventually, silicon carbide.

Finally, another classic example of thermal fatigue in heat-resistant alloys is shown in Figure 5. Recirculation fans are a consumable item in high-temperature furnaces, but they provide a necessary assist in uniformly heating parts from ambient to approximately 1400°F (760°C) where radiation becomes the dominant heat transfer mode. However, one can expect thermal fatigue when the fan is located just a few inches above the newly charged load.

Figure 4: Roller rail

Figure 5: Thermal fatigue cracks in roof fan

ABOUT THE AUTHOR: Jack Titus can be reached at (248) 668-4040 or jtitus@afc-holcroft.com. Go to www.afc-holcroft.com.

REPLACEMENT HOT ZONES

Call one of our Solar Hot Zone Specialists today for a quote or visit our website at solarmfg.com to see our full product line

Bryant Strelecki
Aftermarket Sales Manager
P 267-384-5040 x1537
E bryant@solarmfg.com

Dan Insogna
Inside Sales Engineer
P 267-384-5040 x1505
E dan@solarmfg.com

KEEP PRODUCTION FLOWING

When your vacuum furnace hot zone is unexpectedly down or nearing the end of its service life, count on Solar Manufacturing's replacement hot zones to get you back in business. Rely on our world-class engineering, outstanding customer service and reliable aftermarket support. Whether you need a straight-up replacement or an improvement of an existing design, your new hot zone will fit perfectly and keep you going.

SOLAR MANUFACTURING

PROUDLY MADE IN THE USA

www.solarmfg.com

VACUUM FURNACES

REPLACEMENT HOT ZONES

AFTERMARKET PARTS & SERVICE

THE BRIGHTEST SOLUTIONS THROUGH INGENUITY

Houghton International

Celebrating 151 years, Houghton International is a global market leader in metalworking fluids, bringing innovative and sustainable solutions that increase productivity, reduce operating costs, and improve product quality for its customers.

By Molly J. Rogers

Since its founding in 1865 by Edwin F. Houghton, the company has maintained its mission of combining environmental stewardship and social responsibility with the development, production, and management of the highest-quality specialty chemicals, oils, and lubricants. Serving the automotive, aerospace, metals, mining, machinery, offshore, and beverage industries, Houghton works with its customers to solve their unique challenges.

A FOCUS ON INNOVATION

Starting from the company's earliest days, Houghton has been at the forefront of innovation. In 1865, then-named E.F. Houghton & Co. developed its first commercial product, called Cosmoline®, a lubricant and rust preventative made from Pennsylvania crude oil. During the late 1880s to early 1900s with the birth of the automobile, transcontinental railroad, and flight and transatlantic passenger voyages, Houghton was an innovative leader with products to facilitate newly created assembly lines and steel production.

In the mid 1950s, Houghton grew its factory operations and developed new products for worldwide distribution. With the invention of Houghto-Safe® as the first water glycol hydraulic fluid, the industry had its first fire-resistant, mission-critical fluid, which quickly became the standard for the U.S. Naval Fleet.

In 1998, Houghton introduced Hocut®795, the first biostable metal-cutting coolant, and it initiated its chemical management services, Fluidcare®. In 2009, Houghton introduced its NOA™ (Non Oleic Acid) technology, an enhanced aluminum hot rolling lubricant.

A GLOBAL PORTFOLIO

Today, Houghton is headquartered in Valley Forge, Pennsylvania, employs approximately 1,900 people in 33 countries, and has 11 manufacturing facilities in 10 countries and five continents. The company was acquired by Gulf Oil International in 2012.

For the heat treating industry, Houghton offers a complete line of cold quenching oils, hot quenching oils, and aqueous quenchants. Houghton's product lines utilized in the gear manufacturing industry include lubricants for forging, metal removal (cutting, grinding, or drilling) operations, metal cleaning (fluids that remove soils and other contaminants from equipment and metal surfaces), and protection fluids used to temporarily protect metals from undesired effects caused by exposure to water, air, or other substances.

CUSTOMER VALUE

Houghton works closely with its customers to help them gain maximum value from their investments in Houghton's products and services, reduce costs, improve productivity and product quality, and mitigate risks. Customers have access to Houghton's knowledgeable and experienced product and applications specialists, as well as the opportunity to engage in projects with defined objectives and measured value-adding outcomes.

For example, one of the company's customers was using a competitive aqueous quenchant for induction hardening and experiencing maintenance issues with microbiological growth in the quenchant. Subsequent additives were required to eliminate microbiological growth and increase the pH.

"We converted the customer to Aqua-Quench® 145, one of Houghton's biostable aqueous quenchants, and eliminated the odor and additive additions," said Chuck Faulkner, product marketing manager for Heat Treatment & Metal Forming at Houghton. "This resulted in reduced operating costs and increased production for our customer."

To provide customized solutions with sustainable results to its customers, Houghton follows a four-step process. First, identify the customer's need through requirements definition and assessment. Second, design the optimal solution using Houghton's formulation expertise. Third, implement the solution, providing application support and service and aiding in implementation. And finally, provide ongoing support through technical service, ensuring effectiveness of the solutions and monitoring the customer's evolving needs.

"Houghton differentiates itself by providing value-added product technology along with technical service and support to our customers after the sale," Faulkner said. "By establishing customer intimacy, we are able to work closely with them throughout the entire process and identify process improvements and cost-reduction initiatives."

To enhance its customer relationships, Houghton is dedicated to research and development, including application field support, waste reduction, product safety and stewardship, efficiency programs, and in-house synthesis and chemical design.

INDUSTRY CHALLENGES

In the heat treating industry, Houghton has seen a substantial increase in material restrictions and regulations globally in the past decade, and it expects this trend to continue. There is an international initiative called the Globally Harmonized System (GHS) for hazard communication that is intended to align countries around the world in the classification and labeling of chemicals.

"This effort should ultimately simplify things, but for the next few years, it will increase the burden on manufacturers such as Houghton as nations around the world have taken different routes and timelines to bring their local systems into alignment with GHS," said Dr. Dave Slinkman, senior vice president of Global Research & Technology.

"Houghton takes its role as the leader in the field of metalworking fluids seriously, and we have devoted significant resources to ensure that we will be completely GHS compliant by all deadlines," Slinkman said. "This is no small effort when you consider that we have manufacturing operations on five continents."

FURTHER INVESTMENTS

According to Slinkman, Houghton will continue its efforts in the development of value-added biostable technology across product lines to provide fluids that will last longer in-use. The company is also making a significant investment in laboratory equipment to further enhance its capability in simulating the customer's process, evaluate performance, and optimize new products as they are developed.

"The better we can replicate the customer's process at the lab scale, the more effective and efficient we can be in quickly bringing innovative high-performing solutions to our customers," Slinkman said.

FOR MORE INFORMATION about Houghton International, go to www.houghtonintl.com.

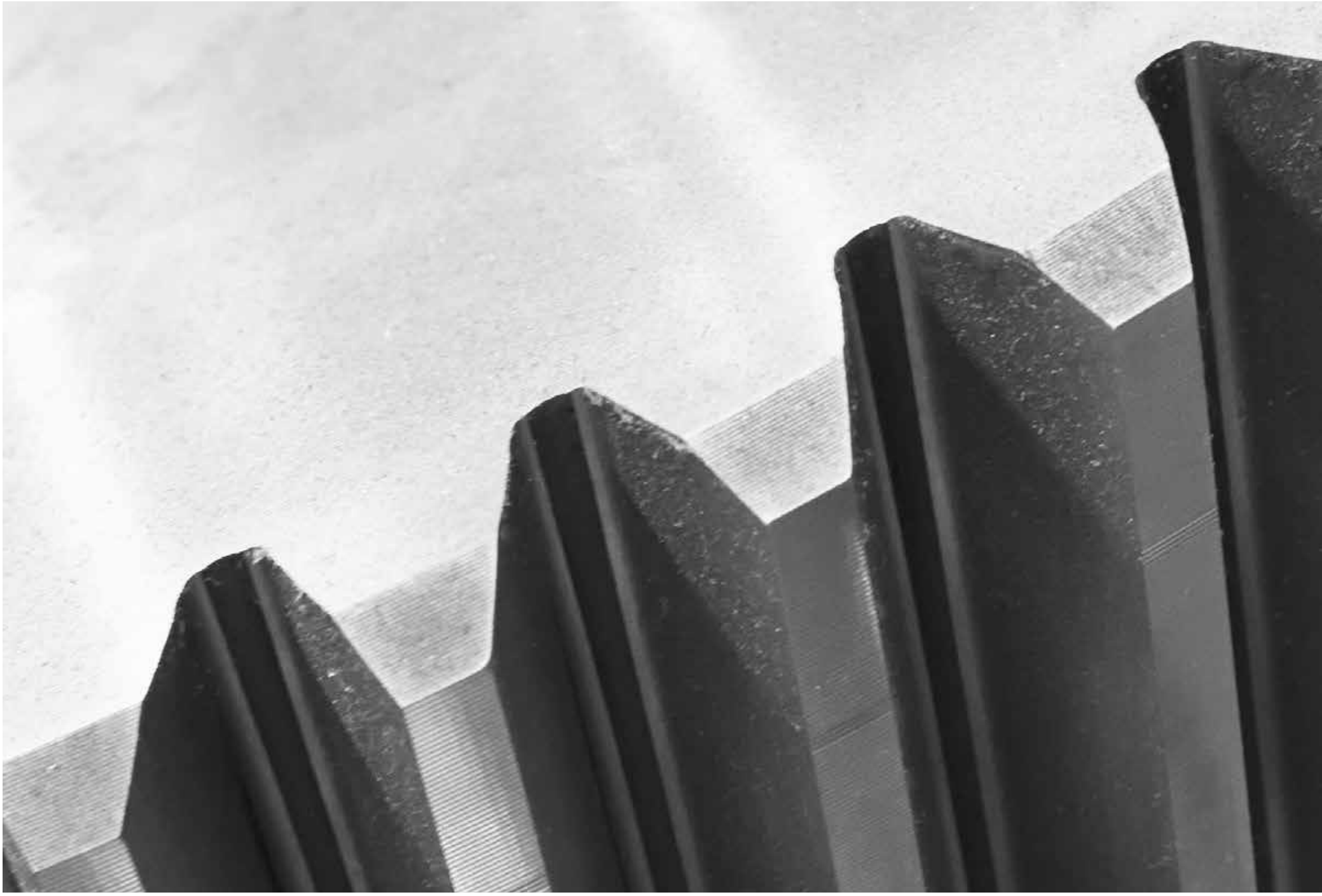

Improved Materials and Enhanced Fatigue Resistance for Gear Components

By Volker Heuer, Klaus Loeser, and Gunther Schmitt

The latest advancements in steel grades and in case hardening technology are of key importance to meet the demand for improved fatigue properties of gear components.

For decades, the gear industry has addressed the challenge to produce high-performance components in a cost-effective manner. To meet design intent, vehicle transmission components need to be heat treated. In many applications, the high demands regarding service life of components can be reached only by the application of a customized case hardening. This case hardening process results in a wear-resistant surface layer in combination with a tough core of the component.

Enhanced fatigue resistance of the components has become even more important. This is mainly driven by the need for weight reduction and by the introduction of higher durability claims. Some vehicle OEMs have introduced a 100,000-mile warranty for the powertrain.

When trying to improve fatigue properties, two important areas need to be addressed: improvements of material and improvements in heat treatment technology. This paper describes the advances in these fields over recent years.

IMPROVED MATERIAL

Traditionally, gear components are made of case hardening steels such as 8620H, 8625H, 5120H, 5130H, 9310H, 16MnCr5, 20MnCr5, 27MnCr5, 18CrNiMo7-6, and others. The chemical composition of a steel grade defines its hardenability — with the most important elements being carbon, manganese, chromium, nickel, boron, and molybdenum. The hardenability of a steel grade can be quantified either with "DI-values" or with "Jominy-curves."

The use of DI-values is popular in North America. DI (ideal diameter) is the largest diameter of a given steel composition that, under

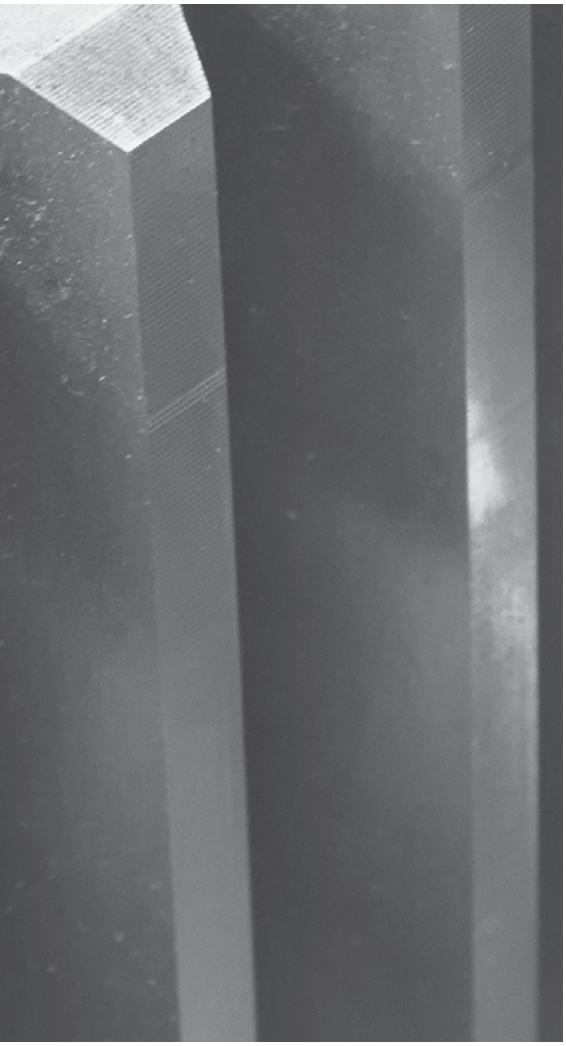

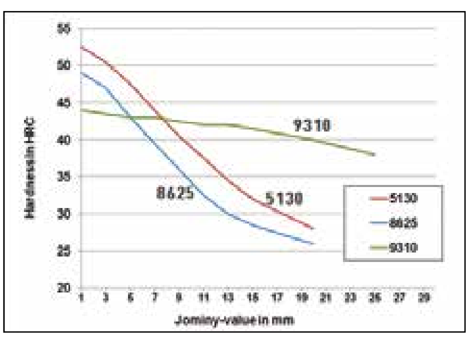

Figure 1: Typical Jominy-curves of case hardening steels (hardness as a function of the Jominy-distance)

maximum quench conditions, still reaches 50-percent martensite in the core [1]. This means that a high DI-value corresponds with a good hardenability of the steel.

The use of Jominy-curves is popular in Europe. The Jominy hardenability curve is a standardized test as described in ASTM A255 [2] using cylindrical specimen with Ø25 mm and 100 mm height as test probes. After austenitizing, the probe is hung vertically and quenched with a water jet of well-defined intensity. The water jet is directed toward the lower face of the cylindrical specimen. This means that with increasing distance from this face, the quench rate inside the probe is continually reduced.

After completion of the quench, the hardness profile is measured in an axis-parallel line with 0.4 mm distance to the surface. The resulting curve is called the Jominy-curve. This curve describes the relation between the distance from the lower face of the probe in millimeters or in 1/16 of an inch (called the Jominy-value) and the achieved hardness in HRC. Besides the experimental method as earlier described, the curve can be calculated from the chemical composition of the steel grade as well. Figure 1 shows typical Jominy-curves of case hardening steels.

Each standardized steel grade has a defined range of hardenability, meaning that each grade has a minimum and maximum Jominy-curve. However, many producers have restricted this range further. Doing so will result in the following benefits:

- Improved distortion control
- Reduced variation of core hardness and case hardening depth (CHD) after heat treatment
- Reduced variation of microstructure (e.g., avoiding bainite formation in the surface area) after heat treatment

Over recent years, in many applications the hardenability range was restricted to the upper end of the standard range. The tightest range, which can be supplied by the steel industry today, is a band of 4 HRC. Figure 2 shows an example of the grade 18CrNiMo7-6 with the standard range and with the restricted hardenability. The HH-grade (high hardenability) has a range of hardenability that is restricted to the upper third of the standard range.

In the following three examples, successful restrictions of hardenability are given.

Levers made of 8620H material were initially supplied using the standard range with a minimum DI = 1.7 inches (see Figure 3). This resulted in significant variations of core hardness and case hardening depth. After restricting the material to a minimum DI = 2.6 inches, these variations were minimized and a consistent quality was achieved after heat treatment.

Shafts made of 28MnCrB7-2 material were initially supplied in a rather wide range of hardenability with DI = 2.2 to 3.4 inches (see Figure 4). This led to significant variations in core hardness and resulted in problems achieving consistent microstructure after heat treatment. After restricting the hardenability to a range of DI = 2.7 to 3.1 inches, those variations were eliminated successfully.

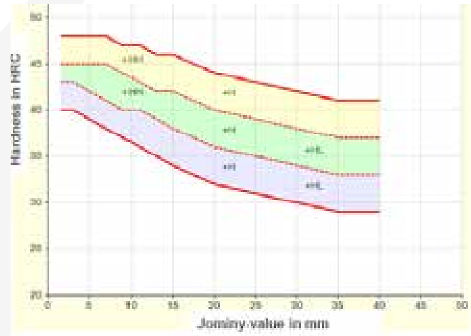

Figure 2: Standard range and restricted range of hardenability for the case hardening steel 18CrNiMo7-6

Figure 3: Lever made of 8620H material

Figure 4: Shafts made of 28MnCrB7-2 material

Figure 5: Final drive ring gear made of 4121M material

Final drive ring gears made of 4121M material were initially supplied with DI-values ranging from 2.7 to 3.1 inches (see Figure 5). This led to significant variations in core hardness. After improving the hardenability to a range of DI = 2.9 to 3.3 inches, those variations were reduced and core hardness specification (28 HRC min.) was safely reached.

ADVANCED HEAT TREATMENT TECHNOLOGY

The high demands regarding service life of transmission components for most applications can be reached only by the

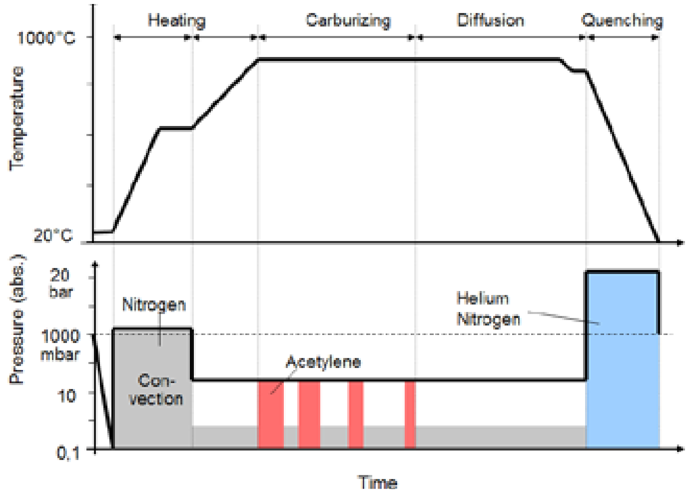

Figure 6: Schematic diagram of the low pressure carburizing (LPC) and high pressure gas quenching (HPGQ) process

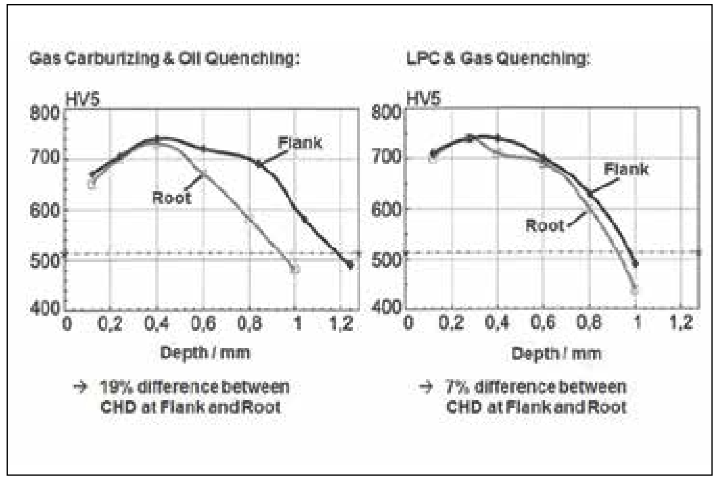

Figure 7: Hardness profiles of tooth flank and tooth root and comparison of gas carburizing and LPC [7]

application of a customized case hardening. This case hardening process results in a wear-resistant surface layer in combination with a tough core of the component. Over the past 15 years, the technology of low pressure carburizing (LPC) and high pressure gas quenching (HPGQ) was established in serial production. LPC is often referred to as vacuum carburizing. Typical applications include gear parts, machine components, and bearing components, as well as injection systems for engines.

The LPC process takes place in a pressure range between 5 mbar and 15 mbar and a temperature range between 870°C and 1050°C. In most cases, the carburizing temperature is between 940°C and 1000°C. During the complete process, the treated components are not exposed to any traces of oxygen [3].

Figure 6 shows the LPC process in a schematic diagram. First, the charge enters the furnace chamber under vacuum, followed by convective heating under a nitrogen atmosphere close to 1 bar. Convective heating offers a quicker and more homogenous heating of the load compared to vacuum heating alone. Subsequently, another heating phase under vacuum takes place. The actual carburizing and diffusion starts after all parts have reached the specified carburizing temperature. Carburizing takes place by applying a routine of alternating pulses and diffusion steps. Acetylene is used in most applications as the carbon source.

Once the targeted carbon profile is obtained, the parts are quenched. Quenching can be initiated either from carburizing temperature or from a lower hardening temperature. In most cases, HPGQ with either nitrogen or helium is applied after LPC [4]. In a few applications, oil quenching is applied after LPC.

Application	Material	Treatment-temperature	CHD	Treatment time* LPC	Treatment-time* Gas carburizing
Internal gear	28Cr4 (ASTM 5130)	900 °C	0.3 mm	0.75 h	1.5 h
Gear	16MnCr5	930 °C	0.6 mm	2 h	2.75 h
Shaft	16MnCr5	930°C	0.8 mm	2.75 h	4 h
Gear	18CrNiMo7-6	960°C	1.6 mm	7.5 h	9.5 h

* Treatment time = Carburize + Diffuse + Lower to hardening temperature

Table 1: Comparison of treatment times for LPC and atmospheric gas carburizing

The high mass transfer of carbon into the components during LPC leads to significantly shorter treatment times compared to conventional gas carburizing (see Table 1).

When combining LPC with HPGQ, the process provides the following advantages compared to gas carburizing combined with oil quenching:

- Excellent carburizing homogeneity even for components with complex shapes
- Avoiding intergranular oxidation (IGO) and surface oxidation
- Shorter cycle times
- Potential for further reduction of cycle time when applying high temperature LPC
- Possibility to integrate heat treatment into the production line [5]
- No conditioning of the equipment necessary (meaning no stepwise heating-up and no saturation of the furnace insulation necessary)
- Clean surfaces of parts after heat treatment and no washing of parts necessary
- Environmentally friendly process (small consumption of resources and no disposal of oil or salt bath residues)
- Potential to reduce heat treat distortion [6]

Altena studied, in particular, the field of carburizing homogeneity. Figure 7 shows the hardness profile after LPC and HPGQ compared to gas carburizing and oil quenching [7]. When using LPC and HPGQ, the hardness profile at the root is almost identical to the profile at the flank.

CARBURIZING TEMPERATURE AND MICROALLOYED STEEL GRADES

The costs of the heat treatment process are largely driven by the cycle time. As shown in Table 1, the high-mass transfer of carbon into the components results in significantly shorter treatment times of LPC compared to atmospheric gas carburizing. The advantage of LPC can be further enhanced by increasing the carburizing temperature. With increasing carburizing temperature, the diffusion rate rises sharply, thus carburizing time is significantly reduced (see Figure 8).

Furthermore, the limit for carbide precipitation shifts to higher values. According to the iron-carbon diagram, the precipitation limit is increased in unalloyed steel (i.e., C15) from 1.3%C at 930°C to 1.65%C at 1030°C. Consequently, high temperature carburizing allows one to target higher surface carbon contents in each carburizing

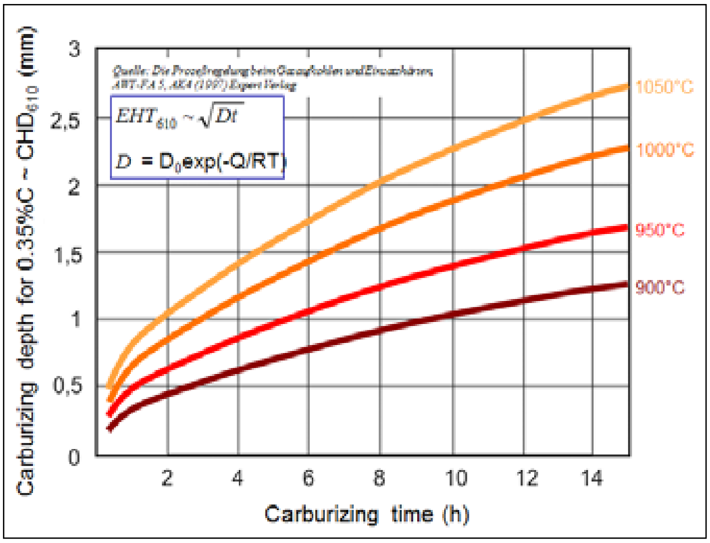

Figure 8: Carburizing depth as a function of carburizing temperature and duration (without heating and with case hardening depth $CHD_{610} = EHT_{610}$ defined at 610 HV) [9]

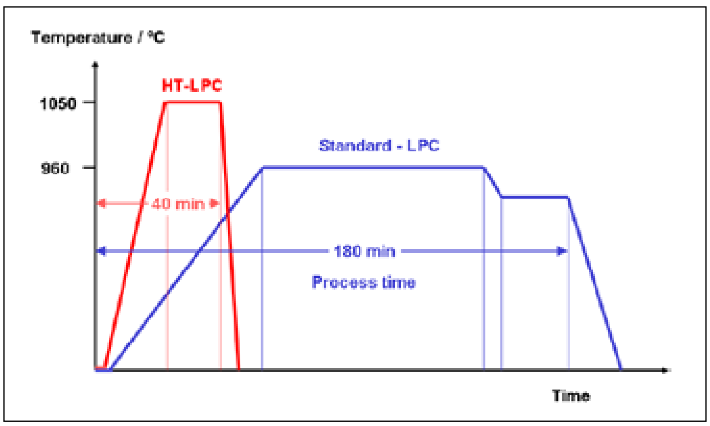

Figure 9: Process cycle of LPC and high temperature–low pressure carburizing (HT-LPC); CHD = 0.65 mm for both cases [5]

Low pressure carburizing CD = 1.5 mm - 18CrNiMo7-6		Treatment temperature 930 °C	980 °C	1030 °C
Loading	hrs.	0.25	0.25	0.25
Heating	hrs.	1.5	1.75	2
Carburizing and diffusion	hrs.	8.5	5	3
Lowering to hardening temp.	hrs.	0.75	1	1.25
Quenching and unloading	hrs.	0.5	0.5	0.5
Door → Door	hrs.	11.5	8.5	7
Total reduction of treatment time			**~ 25 %**	**~ 40 %**

Table 2: Treatment times for LPC of 18CrNiMo7-6 at different temperatures (CD = 1.5 mm)

pulse. The now higher concentration gradient leads to a further reduction of treatment time. This additional reduction of carburizing time is not even reflected in Figure 8.

Table 2 illustrates the treatment times for LPC of 18CrNiMo7-6 at different temperatures for a case depth of 1.5 mm. It shows that the total process time is reduced by 40 percent if carburizing temperature is elevated from 930°C to 1030°C.

The potential for improvement is increased with higher case depth requirements. For material 15CrNi6 and a case depth of 3 mm, for example, a total process time reduction of 55 percent was verified when the carburizing temperature was increased from 950°C to 1050°C [8].

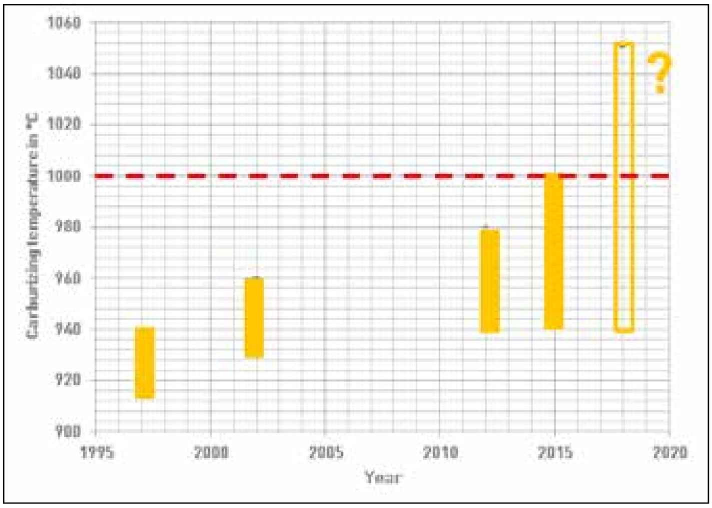

Figure 10: Commonly used carburizing temperature over the past years when applying LPC

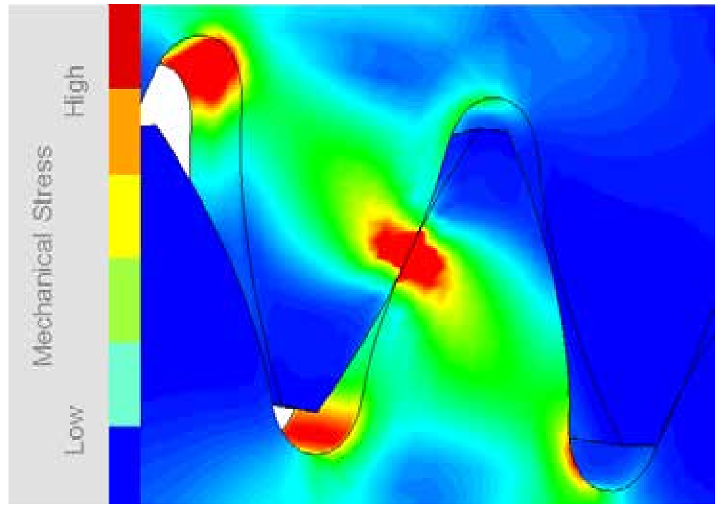

Figure 11: Stress on running gears (source: WZL-RWTH Aachen)

Figure 9 shows the comparison between a conventional LPC process at 960°C and a high temperature LPC process (HT-LPC) at 1050°C. For a given CHD of 0.65 mm, the cycle time is reduced from 180 min. to 40 min. Combined with gas quenching, the HT-LPC process offers a rapid case hardening process with low values of heat treat distortion.

Over recent years, the carburizing temperatures rose steadily (see Figure 10). This led to enormous cost reductions and dramatic savings of energy.

However, when using today's conventional case hardening steels, there are limitations. When applying high carburizing temperatures above the range of 980°C to 1000°C, this may lead to an unwanted grain growth. Components with coarse or mixed grains have the following disadvantages:

- Higher macroscopic heterogeneity
- Less toughness, especially in the carburized area
- Lower tooth root bending strength

Especially for dynamically loaded parts, the formation of coarse grains can reduce service life substantially. As a countermeasure, steel suppliers started several years ago to develop new microalloyed steel grades to prevent unwanted grain growth [10, 11]. These microalloying elements form precipitates during the steel production process that act as grain boundary pinning particles and thus inhibit abnormal grain growth during heat treatment at high temperatures.

For high temperature carburizing up to 1050°C, such steels often have a controlled amount of nitrogen, N (120–170 ppm) and aluminum, Al (250–350 ppm). Furthermore, a small amount of niobium, Nb (320–400 ppm) is being added to the steel. The steel production process route is controlled in a way that an optimum size and distribution of the Al(N) and Nb(C,N) precipitates

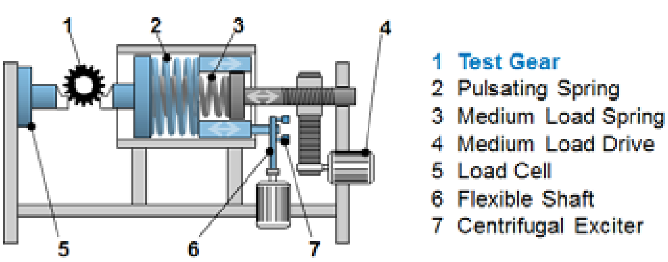

Figure 12: Setup of Imbalance-Excited Resonance Pulsator (test) (source: WZL-RWTH Aachen)

are being secured. Several microalloyed steel grades have been developed and successfully tested jointly by steel suppliers and gear manufacturers [12, 13].

Currently, several gear manufacturers are in the process of adjusting their material specifications to use these materials in high temperature heat treatment. No negative influence of micro-alloying on the gear machining processes has been reported.

Furthermore, the material needs to have a sufficient and controlled hardenability to allow for quenching with moderate quench intensities. High quench intensities should be avoided to facilitate a cost-effective gas quench process. Typical steel grades suited for that process are 20MnCr5-HH, 23MnCrMo5, 27MnCr5, 18CrNiMo7-6 or 20NiMoCr6-5, 5120, 5130, or 9310.

The use of microalloyed materials is necessary to exploit the vast potential of process time reduction through high temperature carburizing by means of LPC.

IMPROVEMENTS IN FATIGUE RESISTANCE

Figure 11 illustrates the stress distribution on running gears. The highest stress appears at the flank and the root of the teeth.

One popular test method to quantify tooth root fatigue is the Imbalance-Excited Resonance Pulsator — also called the Pulsator test. Figure 12 shows the setup of the test rig.

The tested gear is part of a mechanical oscillation system with a sinusoidal load applied. The components are tested with different loads, and as a result, the S/N curve (Wöhler curve) is generated. This curve assigns — for a certain failure probability — the achievable number of load cycles to each load level.

The German drivetrain research association (FVA) has determined S/N curves in order to compare test gears heat treated with gas carburizing and oil quenching and test gears treated with LPC and HPGQ [14]. These S/N curves were determined by using the Pulsator test. The components were not shot-peened. Figure 13 shows a comparison of the tooth root bending strength in the range of limited fatigue life at $N = 3 \cdot 10^4$ load cycles for 50-percent failure probability. Two different materials were tested. For both materials 20MnCr5 and 18CrNiMo7-6, the gears treated with LPC demonstrated higher bending strength than the gas carburized ones. When comparing the gears made of 18CrNiMo7-6 treated with LPC at 940°C with those treated at 1050°C, the later ones showed significantly lower strength. This can be explained with the grain growth that occurred dur-

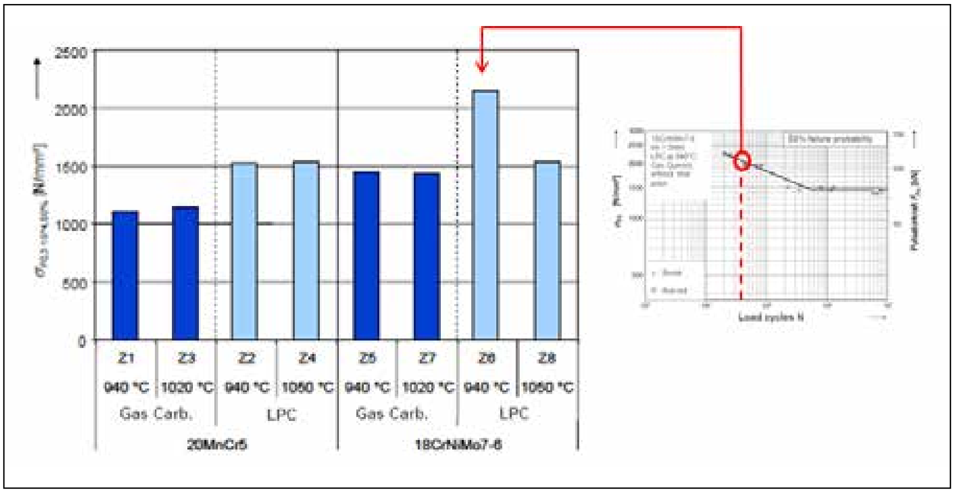

Figure 13: Tooth root bending strength in the range of limited fatigue life at N = 3 x 10^4 load cycles; 50-percent failure probability; derived from Pulsator test; comparison of gas carburizing and oil quench and LPC and gas quench and different carburizing temperatures [14]

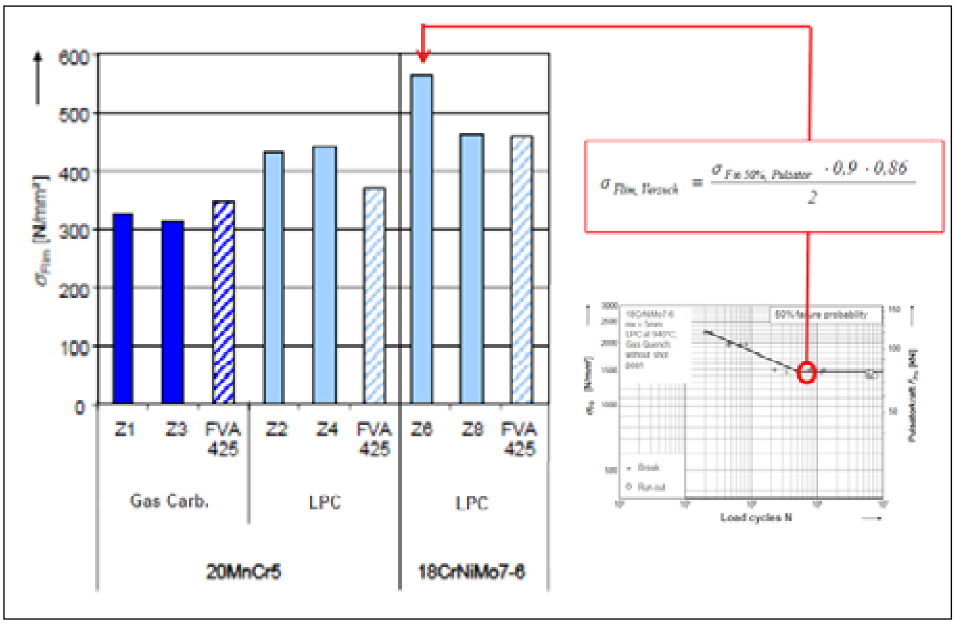

Figure 14: Nominal bending stress number (endurance limit); derived from Pulsator test; comparison of gas carburizing and oil quench and LPC and gas quench [14]

ing treatment at 1050°C. The test gears were made of a standard grade without microalloys, therefore, formation of large grains was not avoided.

The nominal bending stress number (endurance limit) is given in Figure 14. Again, the LPC-treated gears demonstrate higher strength compared to the gas carburized gears.

A summary of the tooth root endurance limit as a function of the carburizing method and the carburizing temperature is given in Figure 15. Clearly, the LPC-treated gears demonstrate higher tooth root endurance limit (meaning strength against tooth break at the tooth root) compared to gas carburized gears. When analyzing pitting on the tooth flank, the same results were obtained when comparing LPC-treated and gas carburized test gears [14].

CONCLUSION

Improvements in heat treatment technology and improvements of material are key factors to enhance the fatigue resistance for gear components. A clear trend toward a restriction of hardenability of the steel and an increase of hardenability of the steel could be observed over recent years. As a result, the variations in core hardness and case hardening depth (CHD) after heat treatment were significantly reduced. Another important benefit when restricting material hardenability is an improvement of distortion control, which was described in earlier publications.

The application of advanced heat treatment technologies such as LPC in combination with HPGQ offers many benefits. One of them is an enhancement of tooth root bending strength compared to the technology of gas carburizing with oil quenching.

With the introduction of newly developed microalloyed case hardening steels, the LPC temperatures can be increased up to 1050°C (1920°F) and even higher. Raising carburizing temperature results in a dramatic reduction of cycle time and therefore in great savings of production costs and energy.

REFERENCES

1. Herring, D.: Fundamentals of heat treating: Ideal diameter. In: Industrial heating Sept. 2005, pp. 18–20.
2. ASTM A255-10 (2014), Standard Test Methods for Determining Hardenability of Steel, ASTM International, West Conshohocken, PA, 2014.
3. Heuer V.: Chapter "Low-Pressure Carburizing." In: ASM handbook Volume 4A, 2013; pp. 581–590.
4. Heuer V.: Chapter "Gas Quenching." In: ASM handbook Volume 4A, 2013; pp. 222–231.
5. Heuer, V; Loeser , K; Schmitt, G.; Ritter, K.: Integration of case hardening into the manufacturing line: "One Piece Flow"; AGMA Technical Paper 11FTM23, 2011. (ISBN 978-1-61481-023-0).
6. Heuer, V.; Loeser, K.; Faron, D.R.; Bolton, D.: Low distortion heat treatment of transmission components; AGMA Technical Paper 10FTM04, 2010. (ISBN 978-1-55589-979-0).
7. Altena H.: Niederdruckaufkohlung mit Hochdruckgasabschreckung. In: HTM 57 (2002), 4.
8. Koch, A., Steinke, H., Brinkbäumer, F., Schmitt, G.: Hochtemperatur-Vakuumaufkohlung für große Aufkohlungstiefen an hoch belasteten Rundstahlketten. In: Der Wärmebehandlungsmarkt 4/2008, S. 5–7.
9. Autorenkollektiv AWT-FA 5; AK4: Die Prozeßregelung beim Gasaufkohlen und Einsatzhärten; Expert Verlag 1997.
10. Hippenstiel, F. et al: Innovative Einsatzstähle als maßgeschneiderte Werkstofflösung zur Hochtemperaturaufkohlung von Getriebekomponenten; In: HTM 57 (2002), S. 290ff.
11. Hippenstiel, F.: Tailored Solutions in Microalloyed Engineering Steels for the Power Transmission Industry. In: Materials Science Forum Vols 539-543 (2007); S. 4131–4136.

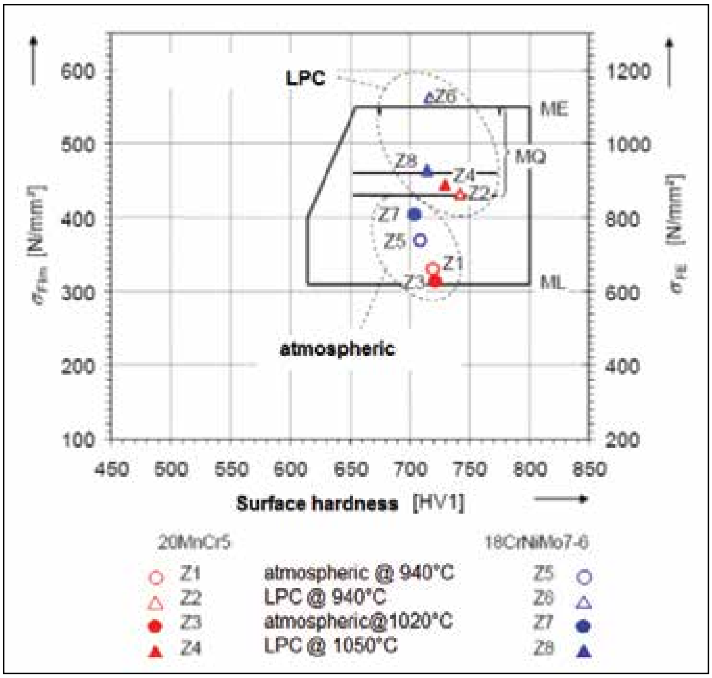

Figure 15: Tooth root endurance limit (nominal bending stress number) as a function of the carburizing method and the carburizing temperature [14]

12. Hoch, S.; Kleff, J.; Kellermann, I.; Schulz, M.: Temperature – the key to optimize cost and result in carburizing vehicle driveline parts: Proceedings of the Intern. Conf. on Steels in Cars and Trucks, June 5 to 10, 2005, Wiesbaden pp. 245–255 (ISBN 3-514-00718-7).
13. Klenke, K.; Kohlmann, R., Reinhold P., Schweinebraten, W.: Kornwachstumsverhalten des Einsatzstahles 20NiMoCr6-5 (VW4521+Nb) für Getriebeteile beim Hochtemperaturaufkohlen, HTM J. Heat Treatm. Mat. 63 (2008) 5, pp. 265–275.
14. FVA-Abschlussbericht zum FV-448 Hochtemperaturaufkohlen; authors: Steinbacher, M.; Stenico, A. Heft 800, 2006.

ABOUT THE AUTHORS: Dr. Ing. Volker Heuer studied metallurgy and material science at RWTH Aachen Technical University in Germany. Then he worked as a scientist for TU Freiberg Technical University in the department of Mechanical Engineering and for Cambridge University (U.K.) in the department of Materials Science and Metallurgy. In 1999, he completed his Ph.D. at TU Freiberg. Starting in 1999, he worked as a research engineer at ALD-Vacuum Technologies GmbH in Hanau, Germany. He was involved in the development of low pressure carburizing, plasma-carburizing, and high-pressure gas quenching. Since 2007, he has been the director of R&D for ALD Vacuum Technologies GmbH.

Dr. Ing. Klaus Loeser studied mechanical engineering at the Technical University of Darmstadt in Germany. Then, he worked at the Institute of Technology and Materials at TU Darmstadt. In 1991, he completed his Ph.D. Starting in 1991, he worked as a research engineer at Leybold-Durferrit GmbH (later ALD Vacuum Technologies GmbH) in the division of process and furnace development. From 2001 to 2006, he was the director of R&D. From 2007 to 2015, he held the position of vice president of heat treatment. Since 2016, he is the senior vice president of heat treatment for ALD Vacuum Technologies GmbH.

Dipl. Ing. Gunther Schmitt studied materials technology at the University of Applied Sciences in Giessen-Friedberg, Germany. In 1987, he started as materials engineer for Degussa AG in Hanau. In 1991, the division was renamed to Leybold Durferrit (later ALD Vacuum Technologies GmbH), and he was responsible for the metallurgical laboratory. In 1992, he worked as application engineer for heat treatment. Since 2008, he has been the senior process engineer for ALD Vacuum Technologies GmbH. He is strongly involved in the development of low pressure carburizing and high pressure gas quenching.

Analysis of Heat Treat Growth on Carburized Ring Gear and Multivariate Regression Model Development

By Olga K. Rowan and Thomas J. Yaniak

A developed set of predictive models to anticipate ring gear dimensional changes that occur during carburizing and hardening may eliminate the need for heat treat test lots and reduce gear development lead time and cost.

In gear manufacturing and machine assembly, dimensional stability of each component and conformance to print requirements are of critical importance. During processing, dimensional changes associated with each manufacturing step must be consistent and predictable so that the final part size conforms to the print tolerances and assembles properly. Misalignment of the assembled components may cause excessive noise during operation and premature failure of the mating components [1, 2]. Typical industrial ring gear manufacturing includes green (i.e., prior to heat treat) machining that may involve lathing, hobbing, or grinding, followed by a carburizing and hardening heat treatment to enable desired mechanical properties, and finally, hard grinding to ensure dimensional conformance to print [3]. Like most other heat treatments, the carburizing and hardening process is known to introduce dimensional changes and gear distortion [4]. If these size and shape changes can be anticipated and controlled, it is possible to eliminate post–heat treatment machining by designing ring gears that would allow for the heat treat change. Such gear manufacturing would significantly reduce cost and machining-to-assembly time, both of which are critical in a commercial environment and large-scale production.

To establish proper green gear size, a heat treat test lot (HTTL) is generally conducted

Proceedings of the 28th ASM Heat Treating Society Conference. October 20–22, 2015, Detroit, Michigan. Reprinted with permission of ASM International.

that involves processing gears through their entire manufacturing path with the addition of high accuracy dimensional measurements before and after heat treatment [3, 4]. Heat treat size change is then calculated for the critical geometrical features, and the desired green gear size is determined based on the final print requirements and observed heat treat growth. HTTLs are typically performed when developing new gears or implementing various design or process modifications on current production gears, such as changes in supplier, case depth, material, and process changes. While HTTL data provide the information needed, they are expensive and time-consuming and may take many weeks to complete. For new gear development, an initial attempt to estimate the desired green size is frequently based on an engineering estimate and historical data for similarly designed gears. As a result, two to three HTTLs are often required to establish the optimal green gear size and may add many months to the process development and validation timeline. Therefore, the ability to predict and account for the gear dimensional changes during heat treat could be of great benefit and yield substantial cost savings.

Several publications have addressed the distortion issues during surface hardening. Bahnsen et al. [5] studied the influence of carburizing case depth, surface carbon, and process temperature on shaft distortion behavior and reported that carburizing case depth has the most dominant effect. Bomas [6] experimentally confirmed that the dimensional changes in carburized samples can be related to the carburized depth-to-wall thickness ratio. Clausen et al. [7] reported that changes in length of the carburized shaft are inversely proportional to the carburized depth-to-radius ratio and total carbon flux. Other researchers [8-10] studied the effect of material hardenability, quench oil temperature, and velocity on flat rings geometry. While all researchers agreed that size and shape changes in the carburized components are multivariate in nature, these studies reported design of experiments (DoE) results on basic simplified geometry parts and are not comprehensive enough to deduce any predictive models for heat treat changes as a function of the key geometrical features and process characteristics.

This development work considered a wide range of ring gear sizes and geometries and was based on the extensive statistical analyses of the HTTL data collected concurrently with large-scale ring gear manufacturing. The main objective was to develop a better tool for predicting heat treat changes during carburizing to help determine the optimal green size based on various gear design features and process parameters. Ultimately, the heat treat growth model would be used to reduce and potentially eliminate the need for the HTTL, thus reducing time and cost associated with ring gear development and validation.

EXPERIMENTAL PROTOCOL

An extensive database was created from the existing HTTL data. The first data set included 10 part numbers (146 gears total) of various gear geometry and green hardness data. Additional historical HTTL data were available that did not contain green hardness measured on gears prior to heat treatment. Thus, a larger database was also populated and consisted of 19 part numbers (314 gears total) with similar data structure, but without green hardness available. From the authors' previous experience, green hardness — reported in this paper as the diameter of the hardness impression (HBD) — appeared to be an important parameter influencing gear growth during carburizing. Therefore, analyzing both datasets was advantageous, allowing green hardness to be one of the predicting factors, as well as providing a wider range of gear sizes and geometries.

All gears were measured in the metrology lab before and after heat treatment using CMM/PMM measurements with 2-micron accuracy. The gears were carburized in gas-fired pusher-type furnaces to produce a target hardened depth within a 0.6 to 1.2 mm range. The typical carburizing cycle consisted of a boost at 927°C and 1.1 wt.% carbon potential, a diffuse at 850°C and 0.85 wt.% carbon potential, and direct quenching in agitated oil. Carburizing cycle time was adjusted for each part number based on the print-required case depth.

The gears were made of AISI 4120 and AISI 4122 medium-alloy gear steel with slight modifications in Mo and Cr content yielding nominal hardenability ideal diameters (DIs) of 52, 70, and 89 mm. The range of ring gear geometry included:

- OD: 326-900 mm
- Tip diameter: 284-874 mm
- Root diameter: 300-927 mm
- Height: 47-266 mm
- Gear cross-section: 12.4-55.4 mm
- Mid-tooth thickness: 6.3-1.2 mm

Statistical data analyses were performed using Minitab [11]. Input factors included material hardenability, the aforementioned key geometrical characteristics, and case depth (defined as the depth from the part surface to the depth where the material carbon content is 0.35 wt.%) calculated from the heat treat cycle history and finite difference carburizing process modeling. Although heat treat growth was measured on all key geometrical features, the initial model development presented here is focused on modeling heat treat growth of the measurements between pins (MBP), as this determines the ability of the gear to be assembled and fit for application. In the future, similar models will be developed to predict heat treat growth during carburizing and hardening on the rest of the critical geometrical features of the ring gear.

RESULTS AND DISCUSSION

Figure 1 shows the matrix plot for the MBP percent change versus various geometrical characteristics and process parameters. High-level correlation (shown as strong linear trends) of several of the geometrical characteristics reflect similarities of some of the gear designs, e.g., larger OD and tip diameter gears tend to be taller and have greater mid-tooth thickness. Such gears are typically carburized to deeper case depths and tend to be made of a steel grade with greater hardenability. While the trend in MBP percent change is multivariate in nature, it appears to be proportional to gear cross-section and inversely proportional to gear mid-tooth thickness. Ring gears with greater green hardness (softer) tend to grow more, which agrees well with the observations made in the previous studies performed on several ring gear part numbers.

Analysis with green hardness data

Table 1 shows the results of the ANOVA analysis for the dataset with green hardness data. The model with the selected predictors proved to be statistically significant with p-value approaching zero. Of all the factors considered, ring gear tip diameter, material hardenability and height were found to be the most significant in influencing the degree of gear MBP growth. Variance inflation factors (VIF) were analyzed to help identify multi-collinearity, which will influence the regression results and the fitted parameters. Ring gear mid-tooth thickness, tip, and root diameter were found to be highly correlated

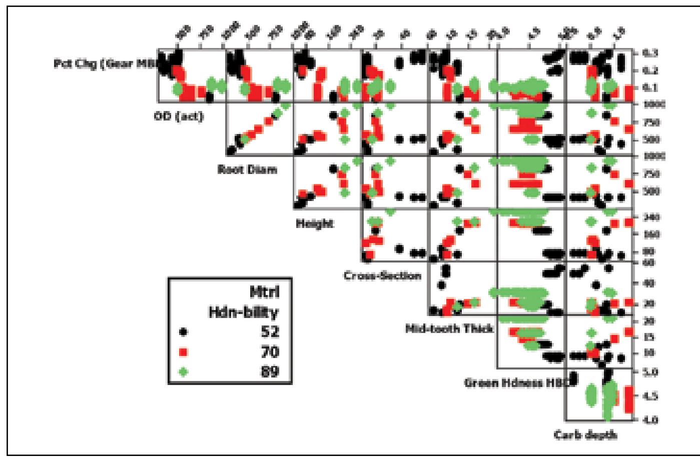

Figure 1: Matrix plot of the gear MBP percent change during carburizing and hardening of various geometry ring gears

Analysis of Variance

Source	DF	SS	MS	F	P
Regression	8	1.00734	0.12592	1481.13	0.000
Residual Error	137	0.01165	0.00009		
Total	145	1.01898			

Source	DF	Seq SS
Mtrl Hdn-bility	1	0.20836
OD (act)	1	0.16553
Tip Diam	1	0.39434
Root Diam	1	0.02792
Height	1	0.20340
Mid-tooth Thick	1	0.00597
Green Hdness (HBD)	1	0.00145
Carb depth	1	0.00037

Predictor	T	P	VIF
Constant	-6.35	0.000	
Mtrl Hdn-bility	18.90	0.000	36.194
OD (act)	32.02	0.000	163.425
Tip Diam	6.09	0.000	208826.021
Root Diam	-6.88	0.000	229425.611
Height	-32.21	0.000	37.186
Mid-tooth Thick	7.36	0.000	434.374
Green Hdness (HBD)	3.50	0.001	3.714
Carb depth	2.09	0.038	3.394

Table 1: ANOVA results for the 10 part numbers dataset with green hardness data

Vars	R-Sq	R-Sq(adj)	Mallows Cp	S	Mtrl Hdn-bility	Tip Diam	Root Diam	Height	Cross-Section	Carb depth	Green Hdness HBD
1	59.8	59.5	3338.3	0.053350				X			
1	50.7	50.4	4123.4	0.059061					X		
2	84.2	83.9	1231.2	0.033604				X	X		
2	77.4	77.0	1819.2	0.040168	X			X			
3	96.9	96.9	127.2	0.014830	X			X	X		
3	85.0	84.7	1156.6	0.032767				X	X	X	
4	97.5	97.5	77.3	0.013347	X			X	X	X	
4	97.3	97.2	101.0	0.014071	X		X	X	X		
5	98.2	98.1	21.5	0.011438	X		X	X	X	X	
5	98.2	98.1	22.5	0.011475	X	X		X	X	X	
6	98.3	98.3	12.0	0.011044	X	X	X	X	X	X	
6	98.2	98.2	20.6	0.011372	X		X	X	X	X	X
7	98.4	98.3	8.0	0.010852	X	X	X	X	X	X	X

Table 2: Best subset model for gear MBP percent change with various combinations of the predicting factors

Vars	R-Sq	R-Sq(adj)	Mallows Cp	S	Mtrl Hdn-bility	Tip Diam	Root Diam	Height	Cross-Section	Carb depth	Green Hdness HBD
1	44.8	44.4	1594.1	0.22267					X		
1	18.2	17.6	2430.8	0.27107						X	
2	51.1	50.5	1396.9	0.21024	X				X		
2	49.2	48.5	1457.0	0.21431					X	X	
3	73.4	72.8	698.7	0.15567	X			X	X		
3	70.0	69.4	805.5	0.16531		X	X	X			
4	91.8	91.6	120.7	0.086537	X		X	X	X		
4	91.5	91.2	132.6	0.088521	X	X		X	X		
5	95.0	94.8	24.5	0.068243	X	X	X	X	X		
5	94.5	94.3	39.5	0.071388	X		X	X	X	X	
6	95.4	95.2	13.5	0.065612	X	X	X	X	X		X
6	95.3	95.1	14.4	0.065814	X	X	X	X	X	X	
7	95.6	95.4	8.0	0.064130	X	X	X	X	X	X	X

Table 3: Best subset model for actual gear MBP growth in millimeters with various combinations of the predicting factors

Analysis of Variance

Source	DF	SS	MS	F	P
Regression	7	1.93990	0.27713	394.22	0.000
Residual Error	306	0.21511	0.00070		
Total	313	2.15501			

Source	DF	Seq SS
Mtrl Hdn-bility	1	0.85176
OD (act)	1	0.21039
Tip Diam	1	0.54451
Root Diam	1	0.01203
Height	1	0.31713
Mid-tooth Thick	1	0.00254
Carb depth	1	0.00154

Predictor	T	P	VIF
Constant	8.41	0.000	
Mtrl Hdn-bility	0.95	0.345	8.151
OD (act)	8.67	0.000	136.253
Tip Diam	-11.68	0.000	12097.539
Root Diam	10.01	0.000	14699.737
Height	-19.08	0.000	14.039
Mid-tooth Thick	-1.98	0.049	14.469
Carb depth	-1.48	0.140	2.588

Table 4: ANOVA results for the extended dataset without green hardness

Vars	R-Sq	R-Sq(adj)	Mallows Cp	S	Mtrl Hdn-bility	OD (act)	Tip Diam	Root Diam	Height	Mid-tooth Thick	Carb depth
1	60.5	60.4	901.0	0.052236					X		
1	55.4	55.2	1058.1	0.055521			X				
2	73.8	73.7	493.9	0.042574		X	X				
2	73.3	73.1	511.2	0.043031		X		X			
3	82.5	82.3	231.7	0.034920			X	X	X		
3	82.1	81.9	243.4	0.035297		X	X		X		
4	89.5	89.4	16.7	0.027013		X	X	X	X		
4	85.8	85.6	132.8	0.031525			X	X	X		X
5	89.8	89.7	9.8	0.026677		X	X	X	X		X
5	89.8	89.7	9.8	0.026677	X	X	X	X	X		
6	90.0	89.8	6.9	0.026509		X	X	X	X	X	X
6	89.9	89.8	8.2	0.026565	X	X	X	X	X	X	
7	90.0	89.8	8.0	0.026514	X	X	X	X	X	X	X

Table 5: Best subset model for gear MBP percent change as a function of various combinations of the predicting factors

with the other factors. As a result, mid-tooth thickness was removed from the model.

Like in most other multivariate regression systems, the response variable (heat treat growth during gas carburizing and hardening) can be described by using various combinations of the predicting factors. Tables 2 and 3 show the best subset model results for the gear MBP percent change and the actual MBP growth, expressed in millimeters, as a function of various combinations of the geometrical and process parameters. The same factors were used in each best subset model to assess which response variable correlated better with the measured results.

Gear MBP percent change revealed a higher R^2 and greater predicting power than the actual gear MBP growth. This can be explained by the "normalizing" effect of MBP percent change, which takes a ratio of the observed heat treat growth to the actual gear size. This is particularly beneficial given the wide range of gear sizes used in this study. As follows from Tables 2 and 3, just three factors — material hardenability, height, and gear cross-section — explain most of the observed heat treat growth variation. From the principle of parsimony, this model may be considered as the optimal, as it utilizes the minimum number of predicting factors to explain the maximum degree of variation. However, this model reveals a high Mallows' Cp value, a statistical factor commonly used to help choose between compelling multiple regression models [11]. A Mallows' Cp value that is close to the number of the predicting factors plus the constant indicates a more optimal model that is relatively precise and unbiased in estimating the true regression coefficients and predicting future responses. Thus, the best subset analysis identified the model that yields 98.3-percent R^2_{adj} and utilizes seven parameters — material hardenability, tip diameter, root diameter, height, cross-section, carb depth, and green hardness — as best able to predict heat treat growth, expressed in terms of gear MBP percent change.

Figure 2 shows the results of the residuals analysis for the best subset model. The normal probability plot (Figure 2-a) with p-value of 0.754 passes the test for normality, though some deviation is observed in

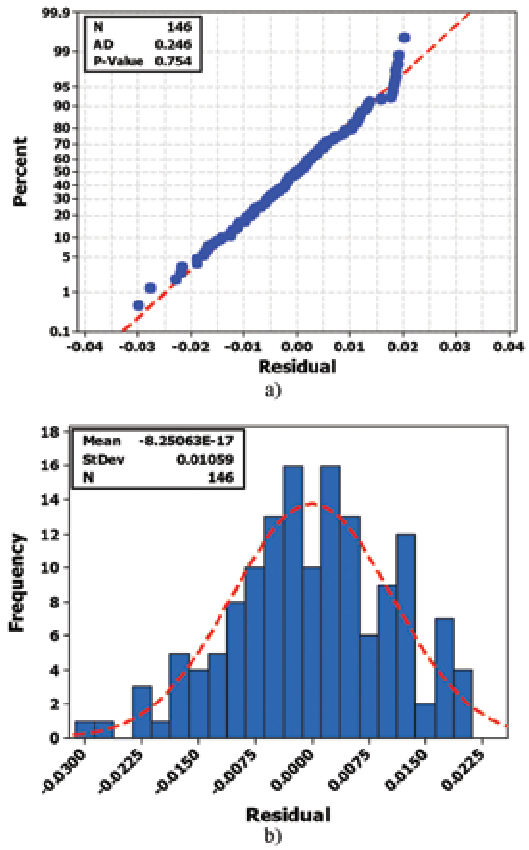

Figure 2: Residuals analysis results for the best subset model with seven predicting factors

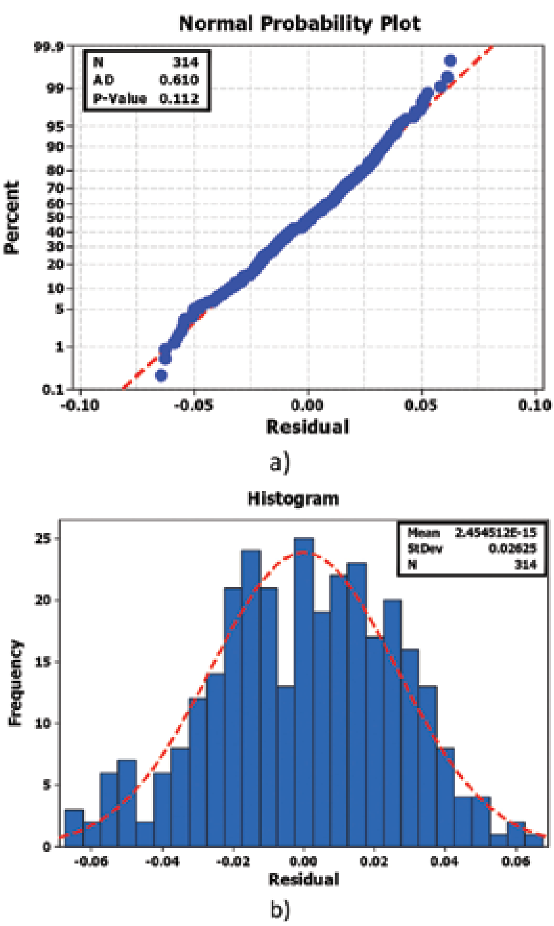

Figure 3: Normal probability plot and residuals distribution histogram for the best subset model with seven predicting factors

the tails. The histogram of the residuals with the fitted normal distribution probability curve (Figure 2-b) shows the spread and confirms some deviation from normality in the tails. These may be resolved as more HTTL data in this ongoing project become available and a larger gear geometry and size range are considered.

Analysis without green hardness data

Table 4 shows the results of the ANOVA analysis on the larger dataset (19 part numbers, 314 gears) without green hardness available. The model with the selected predictors was found to be statistically significant with p-value approaching zero. OD, tip diameter, and height of the ring gear had the largest contribution to the gear MBP heat treat growth. Similar to the previous analysis, tip and root diameter were also found to be highly correlated and influencing the regression results and fitted parameters.

Table 5 shows the results of the best subset model analysis. As with the previous dataset analysis, gear MBP percent change revealed higher R^2 and greater predicting power over the actual gear MBP growth. A model with three factors — tip and root diameter and height — explained 82.3 percent of the overall observed variation but showed high Mallows' Cp. In general, several models with five to seven factors provide 89.7-percent R^2_{adj} with relatively low Mallows' Cp factors. From practical considerations and the authors' experience, material hardenability is known to be significant in influencing ring gear heat treat response. However, based on the high p-value for this factor (Table 4), the model selected as best is the one with six factors with 89.7-percent R^2_{adj} that excludes material hardenability. The addition of future data to this analysis may provide clarity as to the effect of this factor on MBP growth.

Figure 3 shows the results of the normal probability plot and residuals distribution histogram for the best subset model. Both indicate a satisfactory test for normality and confirm validity of the multiple regression analysis.

To validate the multiple regression models developed from both datasets, the regression equations were used to calculate the predicted gear MBP percent change. Figure 4 shows the predicted heat treat growth on gear MBP plotted against the experimentally observed gear MBP percent change. Note that displayed R^2 for the predicted versus actual gear MBP heat treat response in Figure 4 is calculated differently from the R^2 parameter in the multiple regression analysis (Tables 2 and 5). The observed agreement is quite good confirming the models validity.

As mentioned previously, one hypothesis to be explored in this investigation was whether green hardness had a significant impact on the change in MBP. What can be observed in the model that includes green hardness is that it is a statistically significant factor that is not strongly adding or detracting from the model. It is important to reiterate, though, that the dataset with green hardness has relatively limited data consisting of 10 gear part numbers at the time of this paper's publication. Further study of this factor may be warranted.

CONCLUSION

Ring gear HTTL database was developed to quantify and predict gear MBP growth after carburizing and hardening. Gear MBP percent change revealed greater predicting power than the gear MBP growth expressed in millimeters as it normalizes the observed heat treat growth to the actual green size of the gear. The multiple regression model developed from the smaller dataset with green hardness data revealed 98.3-percent R^2_{adj} and utilized seven factors: material hardenability, tip and root diameter, height of the gear, cross-section, carb depth, and green hardness. The second model was developed from the larger dataset without green hardness and included a wider range of the ring gear size and geometry. The best subset model revealed 89.8-percent R^2_{adj} and included OD, tip and root diameter, height of the gear, mid-tooth thickness, and carb depth. This is an ongoing work, as the authors continue collecting and analyzing the HTTL data and refining the model parameters. Ultimately, the use of these models is projected to reduce and possibly eliminate the need for HTTL, thus reducing gear development lead time and cost.

ACKNOWLEDGMENTS

The authors appreciate the assistance of the Caterpillar metrology lab personnel staff in performing the CMM/PMM measurements. The authors would also like to thank Robert Hertenstein Jr., Chad Siebenaler, Md. Maniruzzaman, and Ying-Liang R. Lee for their assistance and valuable discussions.

REFERENCES

1. Whitney, Daniel E. (2004). Mechanical Assemblies - Their Design, Manufacture, and Role in Product Development. Oxford University Press.
2. Davis, J.R. (2005). Gear Materials, Properties, and Manufacture. ASM International. "Fatigue and Life prediction," p. 163-226, 293-309.
3. Dossett, Jon L. Totten, George E. (2014). ASM Handbook, Volume 4D - Heat Treating of Irons and Steels. "Selection of Carburizing Steels," p. 68-75.
4. Michalec, G.W., Sanchez, M.I., Predicting Heat Treat Growth, American Machinist, p. 99-10, 1965.
5. Bahnsen, C., Clausen, B., Hoffmann, F., Zoch, H.-W. (2006), Influence of Carburising on Distortion Behaviour, Mat.-wiss.u.Werkstofftech, 37 (1), p. 58-62.
6. Bomas, H., Lubben, Th., Zoch, H.-W., Mayr, P. (1990), Harterei-Tech. Mitt., 45, p. 188.
7. Clausen, B., Surm, H., Hoffmann, F., Zoch, H.-W. (2009), The Influence of Carburising on Size and Shape Changes, Mat.-wiss.u.Werkstofftech, 40 (5-6), p. 414-419.
8. Kristoffersen, H., Segerberg, S. (1995), Designed Experiments to Study Distortion, Hardness and their Variations in Hot-oil-quench Carburising, Heat Treatment of Metals, 2, p. 39-42.
9. Clausen, B., Frerichs, F., Kohlhoff, T., Lubben, Th., Prinz, C., Rentsch, R., Solter, J., Surm, H., Stobener, D., Klein, D. (2009), Identification of Process Parameters Affecting Distortion of Disks for Gear Manufacture, Part II: Heating, Carburizing, Quenching, Mat.-wiss.u.Werkstofftech, 40 (5-6), p. 361-367.
10. Jurci, P., Stolar, P., Stastny, P., Podkovicak, J., Altena, H. (2008), Investigation of Distortion Behaviour of Machine Components due to Carburizing and Quenching, p. 27-3.
11. Minitab® 17 Statistical Software Manual (2010).

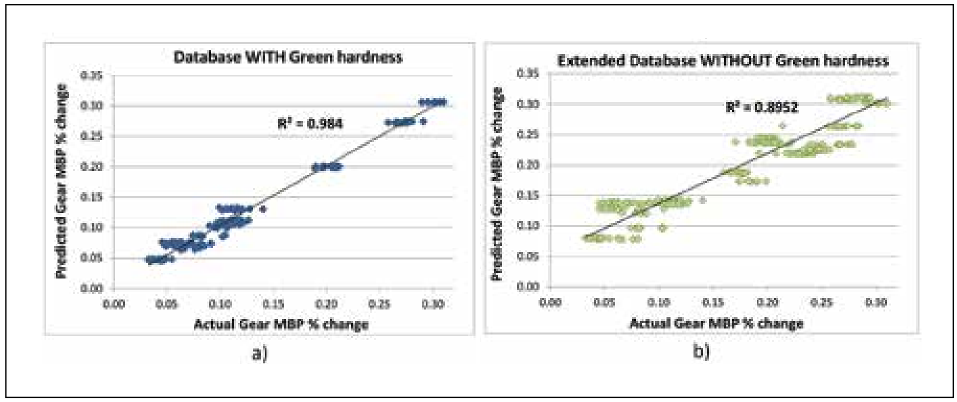

Figure 4: Initial validation of the models' prediction versus experimentally observed gear MBP percent growth after carburizing and hardening

ABOUT THE AUTHORS: Olga (Olly) Rowan is a senior engineer in the Advanced Materials Technology division of Caterpillar Inc. She received her M.S. in Industrial Engineering from Texas Tech University (2004) and Ph.D. in Materials Science from Worcester Polytechnic Institute in 2007. She joined Caterpillar in 2007 where she has been working in heat treat R&D, production support, and supplier development. Rowan has co-authored two articles in the 11th edition of the ASM Handbook Vol. 4A (2013) and published 19 peer-review journal articles and conference publications on gas atmosphere and vacuum carburizing, heat treat process control, and optimization.

Thomas J. Yaniak is an engineering specialist in the Advanced Materials Technology division of Caterpillar Inc. He joined Caterpillar in 2006 where he has been working in various production support and R&D projects related to heat treatment and castings. Prior to this, he was chief metallurgist for the Engine Air Management division of Eaton, Inc. in Saginaw, Michigan. He began his career with Metaltek International where he held various positions in engineering and production management. He received his B.S. in Materials Engineering from the University of Wisconsin-Milwaukee in 1990.

Coupling CFD and Oil Quench Hardening Analysis of a Gear Component

By Zhichao (Charlie) Li and B. Lynn Ferguson with David Greif, Zlatko Kovacic, Simon Urbas, and Rok Kopun

The coupling of CFD and heat treatment analyses provides a more robust application of computer modeling to predict the latent heat release, distortion, and residual stresses during the quench hardening process.

Today, powertrain development is driven in the direction of weight reduction by replacing heavier components with low-cost or higher strength alloys for industries such as automotive, aerospace, and process engineering. Accurate prediction and optimization of the heat treatment process of metal parts is important to achieve optimum material properties or to increase the magnitude of surface compressive residual stress from local thermal gradients and solid phase transformation timing during hardening processes, thereby extending component life during operation. Among all other heat treatment techniques, the immersion quenching process has long been identified as one of the most important methods to fulfill the aforementioned requirements. In order to achieve the desirable microstructure and mechanical properties of the metal piece, steel components are heated to an austenitization temperature, followed by immediate submerging into quenching media [1]. The common austenitization and soaking temperature of steel gears is approximately above 900°C. The temperature varies based on the steel grade. During quenching hardening of steel components, the latent heat released during solid phase transformations affects the cooling significantly, which needs to be considered in heat treatment process modeling.

The paper features the results of the Eulerian multi-fluid model implemented within the commercial CFD code AVL Fire coupled with DANTE®, using the Abaqus/Standard finite element solver. The coupled modeling is capable of considering the solid phase transformation kinetics, which affects the microstructure, thermal, and mechanical properties. Phase transformation during quench hardening also involves releasing latent heat, which is considered in this study.

Proceedings of the 28th ASM Heat Treating Society Conference. October 20–22, 2015, Detroit, Michigan. Reprinted with permission of ASM International.

In this paper, a test gear component made of Pyrowear® 53 is simulated, and the modeling results include the entire history of the part response during hardening including heating, carburization, and quenching. The temperature gradients predicted by the presented model reproduce the latent heat release during the phase transformation. It is clear that neglecting the additional heat source would result in very different thermal gradients and consequently very different thermal stresses and surface properties of the treated component.

THEORETICAL BACKGROUND AND SIMULATION SETUP

The Eulerian multi-fluid model considers each phase as interpenetrating continua coexisting in the flow domain, with interfacial transfer terms accounting for phase interactions where conservation laws apply [2]. The averaged continuity, momentum, energy, and boiling models equations are well-described in works of Srinivasan et al. [3] and Greif et al. [4]. The methodology is applied in an industrial environment as described by Jan et al. [5] and Mulayim Kaynar et al. [6].

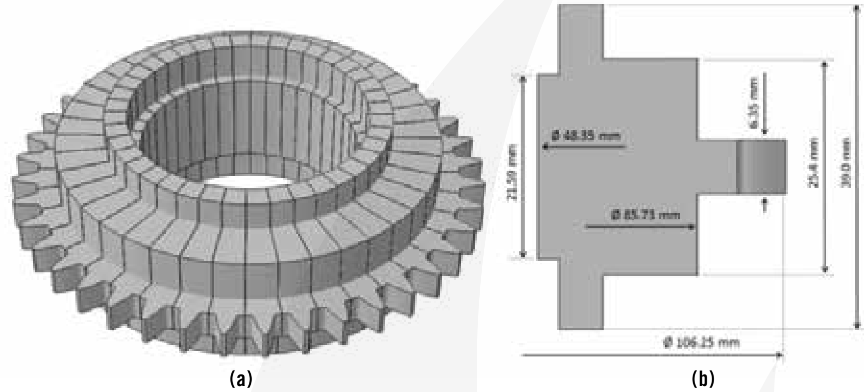

Figure 1: (a) CAD model and (b) the dimensions of the gear

The gear geometry is shown in Figure 1. The bore diameter of the gear is 48.35 mm, the tip diameter is 106.25 mm, and the total number of teeth is 41.

Figure 2 shows finite element meshing of the computational model. In this coupled model, the fluid and the solid structure are modeled by different computational codes, and their geometries are shown in Figure 2. It is assumed that all the gear teeth behave the same during quenching, so the gear is modeled using a single tooth with cyclic symmetry boundary conditions.

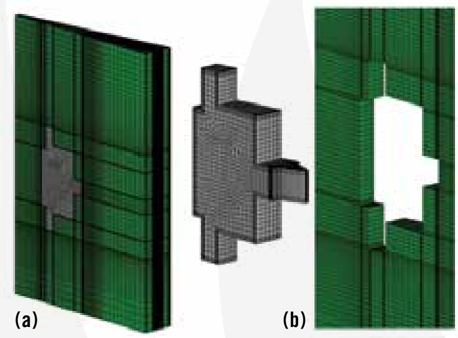

Figure 2: (a) computational model and (b) coupled solid domain using DANTE and liquid domain using AVL Fire

CFD SIMULATION RESULTS AND DISCUSSION

The modeling results shown in Figure 3 are the volumetric fraction of oil to illustrate the boiling process and the temperature distribution of the solid gear at four different time snapshots during quenching. The results are shown on the planar cut through the fluid domain (top row) and on the surface of the structure. The gear temperature prior to quenching is 915°C.

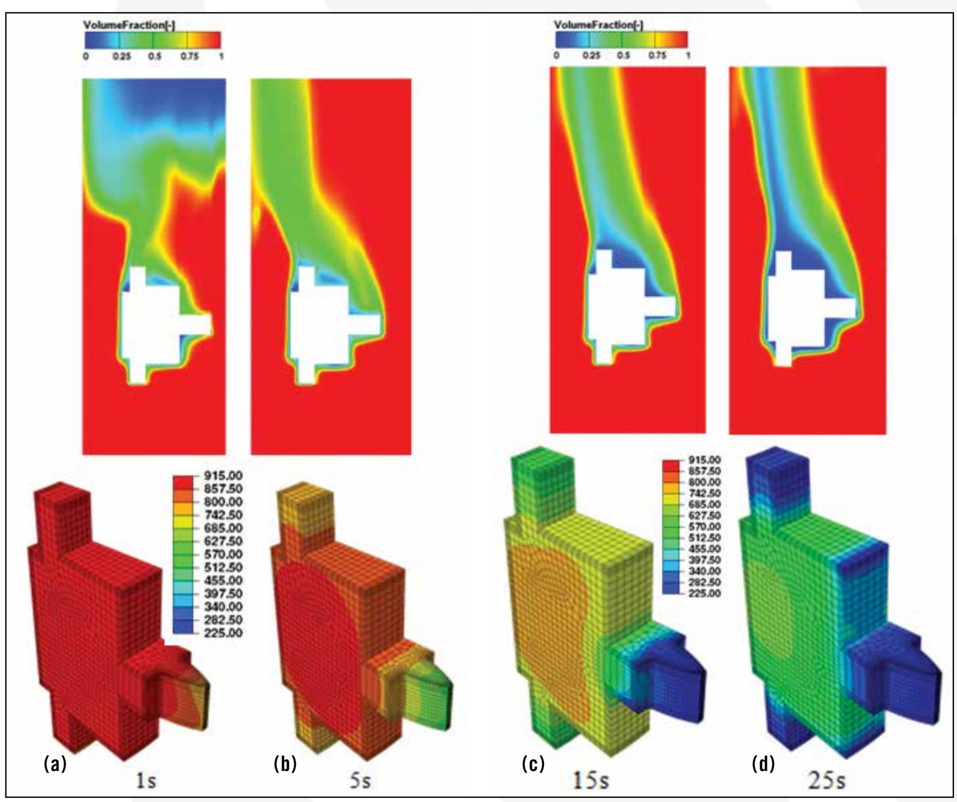

Figure 3: Oil phase volume fractions and solid gear temperature distributions at four different times during quenching: (a) 1.0 second, (b) 5.0 seconds, (c) 15 seconds, and (d) 25 seconds

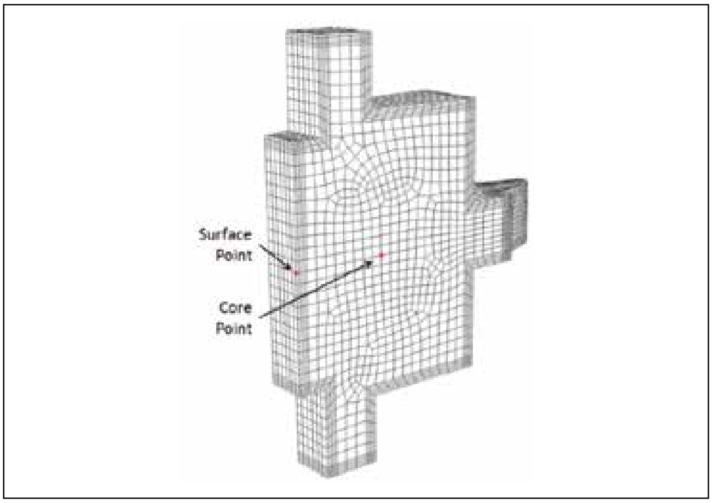

Figure 4: Surface point and core point selected to study the cooling history of the gear during quenching

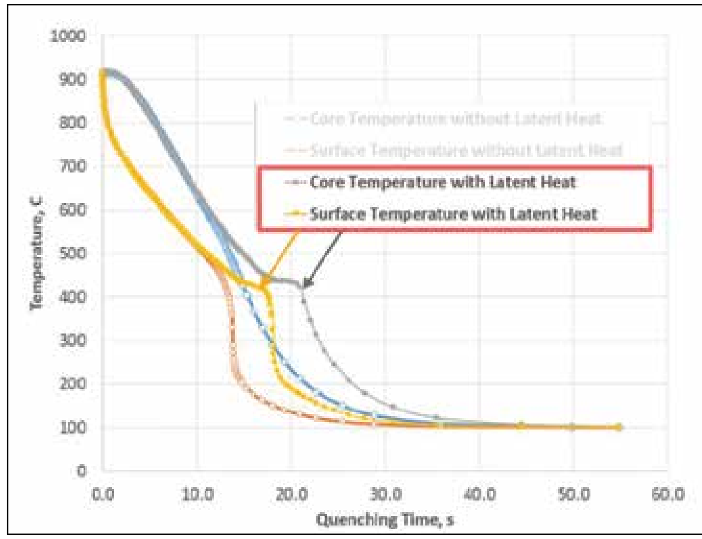

Figure 5: Temperature profiles at monitored locations

Figure 4 shows two points selected to study the cooling history of the gear during quenching. The surface point is located at the bore surface, and the core point is located at approximately the center of the cross-section.

The thermal properties during quenching are affected by the temperature, as well as the phase transformations because different phases have different thermal properties. The overall thermal properties are calculated from the volume fractions of individual phases and their properties. The cooling history of the part is also significantly affected by the latent heat released due to phase transformation. By turning off the latent heat in the quenching model but still including the phase transformations, the effect of latent heat is shown in Figure 5. The bump in the time-temperature profile after 15-20 seconds represents the latent heat release. Slower cooling is clearly visible (yellow and gray profile), thus affecting the local cooling and overall temperature gradients. Orange and blue curves show the case without latent heat consideration.

THERMAL AND STRESS MODELING USING DANTE

Prior to quench hardening, the gear tooth is gas carburized with all other surfaces being copper plated. After carburization, the gear is reheated for hardening. It is important to include the carbon distribution profile in the quench hardening model because the carbon content has a significant effect on the phase transformation kinetics. The carbon distribution profile after carburization is shown in Figure 6.

The heating process is modeled by applying a uniform heat transfer coefficient on the gear surface with the furnace temperature at 915°C. Figure 7 shows temperature, austenite, and circumferential stress distributions at 673 seconds during heating. The tooth tip has a higher heating rate, and the austenite transformation occurs earlier at the tip.

Figure 8 is a snapshot of the gear at 820 seconds during heating. The austenite distribution clearly shows the effect of carbon on the austenite formation. The growth of the gear due to heating is also shown.

At the end of heating, the gear temperature is 915°C, and it is fully austenitic. The radial growth is 0.431 mm.

Using the predicted temperature from coupled AVL Fire and DANTE thermal model, the stress model of the quenching process is executed. Figure 10 shows the temperature, martensite, and circumferential stress distributions at 3.7 seconds during quenching. When austenite transforms to martensite, the material volume increases because martensite has a lower density. As shown in Figure 10, the region with martensite forming shows a compression stress, and its neighbor is under tension to balance the stress.

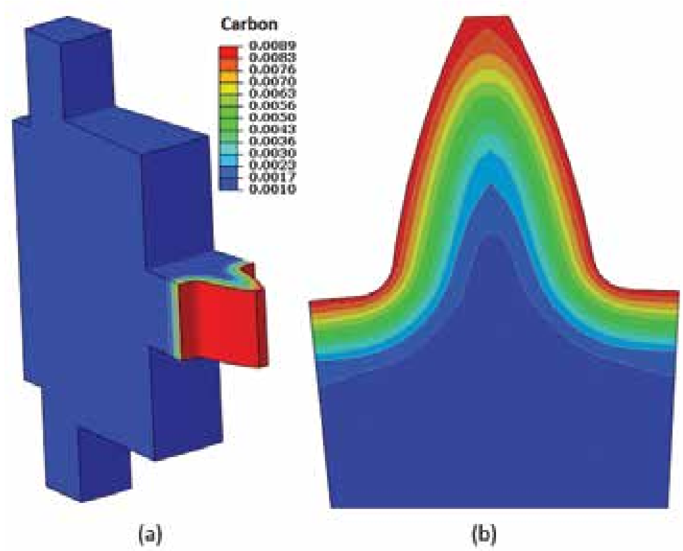

Figure 6: Carbon distribution after the gas carburization process: (a) overall view and (b) magnified view of the tooth section

At the end of quenching, the volume fraction of martensite and residual stress in the circumferential direction is shown in Figure 11. Pyrowear 53 has high hardenability, and the austenite transforms only to martensite during quenching. The gear tooth is carburized, and the retained austenite at the gear tooth case is about 12 percent due to the lower Ms and Mf temperatures of the high carbon content of the case.

CONCLUSION

The applied CFD code AVL Fire is coupled with DANTE to predict the latent heat release, distortion, and residual stresses during the quench hardening process. The latent heating release has a significant effect on the temperature distribution during quenching, which will affect the rate of phase transformation, distribution, and residual stresses of the quenched part. The study shows the possibility of coupling CFD transient analysis with the heat treatment model of a solid part, which is valuable in understanding the cooling uniformity around the part and its effect on the part response during liquid quenching processes.

REFERENCES

1. R. Kopun, R., Greif, D., Zhang, D., Stauder, B., Škerget, L., Hriberšek, L., Advances in Numerical Investigation of immer-

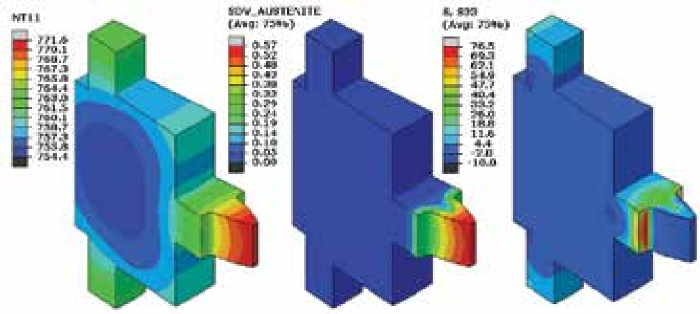

Figure 7: Temperature, austenite, and circumferential stress of the gear at 673 seconds during heating

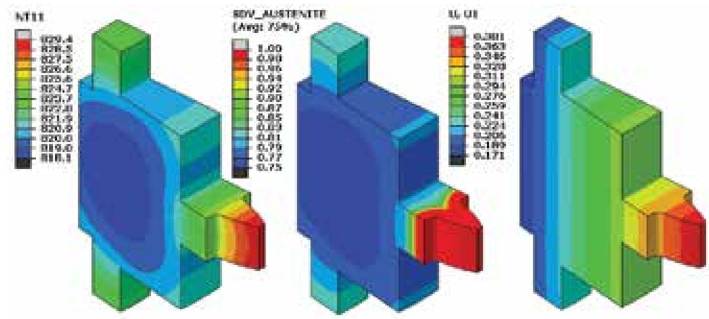

Figure 8: Temperature, austenite, and radial displacement at 820 seconds during heating

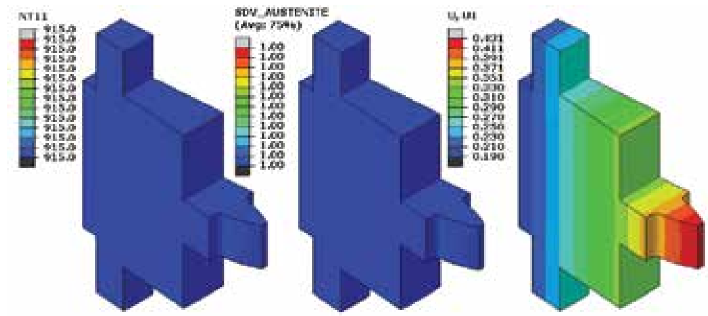

Figure 9: Temperature, austenite, and radial displacement at the end of heating (3,600 seconds)

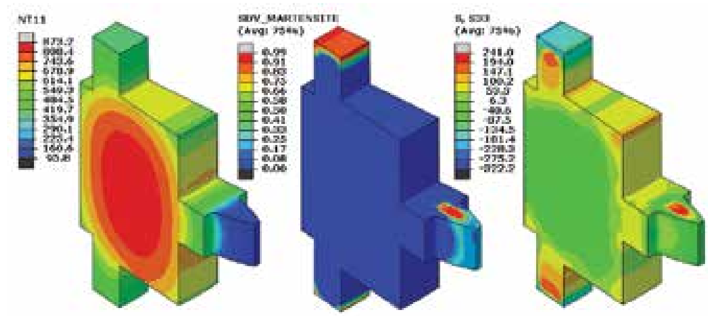

Figure 10: Temperature, martensite, and circumferential stress at 3.7 seconds during quenching

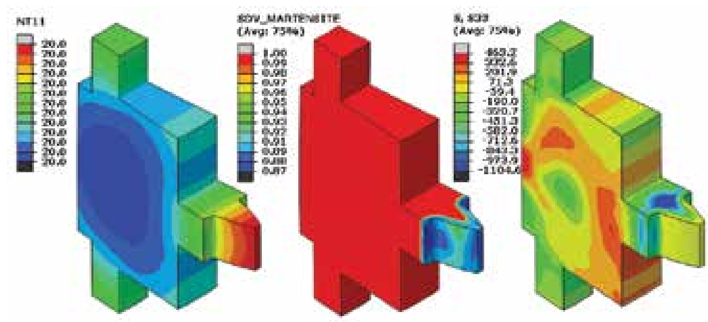

Figure 11: Temperature, martensite, and circumferential stress at the end of quenching

sion Quenching at Different Pool temperatures, SAE Brasil under revision.

2. AVL List GmbH, Fire® CFD Solver, Eulerian Multi-fluid model. Solver Theory Guide. 2013, Graz, Austria.
3. Srinivasan, V., Greif, D., Basara, B., On the heat and mass transfer modeling to simulate quenching heat treatment process, 6th International Quenching and Control of Distortion Conference, Chicago (2012).
4. Greif, D., Kovacic, Z., Srinivasan, V., Wang, D.M., Suffa, M., Coupled numerical analysis of quenching process of internal combustion engine cylinder head, BHM Journal, Vol. 154 (2009).
5. Jan, J., Prabhu, E., Lasecki, J., Weiss, U., Mulayim Kaynar, A., Eroglu, S., Development and Validation of CFD Methodology to Simulate Water Quench, Proceedings of the ASME 2014 International Manufacturing Science and Engineering Conference.
6. Mulayim Kaynar, A., Eroglu, S., Weiss, U., Prabhu, E., Jan, J., Lasecki, J., Kopun, R., Greif, D., Experimental and Numerical Investigation of Water Quench Cooling of Aluminum Cylinder Heads, 5th International Conference on Thermal Process Modeling and Computer Simulation, June 16-18, 2014, Florida.

ABOUT THE AUTHORS: Zhichao (Charlie) Li is a principal at DANTE Solutions, Inc. where he focuses on DANTE software applications to the heat treat industry. He is a Ph.D. mechanical engineer from Wright State University. His interests center around process modeling of carburizing and quench hardening of steel parts.

B. Lynn Ferguson, also a principal at DANTE Solutions, Inc., is a Ph.D. materials engineer from Drexel University. He has over 40 years of industrial experience in thermal and mechanical processing of steel parts and has been a leader in application of mathematical modeling of heat treatment processes.

David Greif is a product manager at AVL-AST in Maribor, Slovenia. He graduated with a B.Sc. degree in Mechanical Engineering from the University of Washington, Seattle, in 1996 and continued toward his M.Sc. degree at the Montana State University, Bozeman, which he completed in 1998. In 2012, he received his Ph.D. from the University of Maribor, Slovenia. The area of his doctoral thesis was numerical modeling of cavitating flows in high pressure injection equipment accounting for cavitation erosion effects. As product manager, Greif is responsible for the CFD product AVL Fire, focusing on the multiphase topics.

Zlatko Kovacic has been an analysis engineer at AVL-AST in Maribor since 1996. He graduated with a B.Sc. degree in Mechanical Engineering from the University of Maribor, Slovenia, in 1980 and obtained his M.Sc. degree from the same university in 1993. He has more than 20 years of experience in the modeling and simulation of combustion engine structures using the Finite Element Analysis method.

Simon Urbas works as a support engineer at AVL-AST in Maribor, Slovenia. He graduated with a B.Sc. in 2011 and continued toward his M.Sc. degree at the University of Maribor in 2010, which he completed in 2013. The area of his M.Sc. work was spray bomb multi-component CFD simulation of gasoline fuel. Urbas is responsible for the support and services worldwide for the CFD product AVL Fire, focusing on the multiphase topics.

Rok Kopun works as an analysis engineer at AVL-AST in Maribor, Slovenia. He graduated with a B.Sc. degree in Mechanical Engineering from the University of Maribor in 2010 and continued at the same faculty toward his Ph.D. The area of his doctoral thesis was numerical modeling of the immersion quenching process using an Eulerian multi-fluid modeling approach. As analysis engineer, Kopun is responsible for the product AVL Fire, focusing on the multiphase topics.

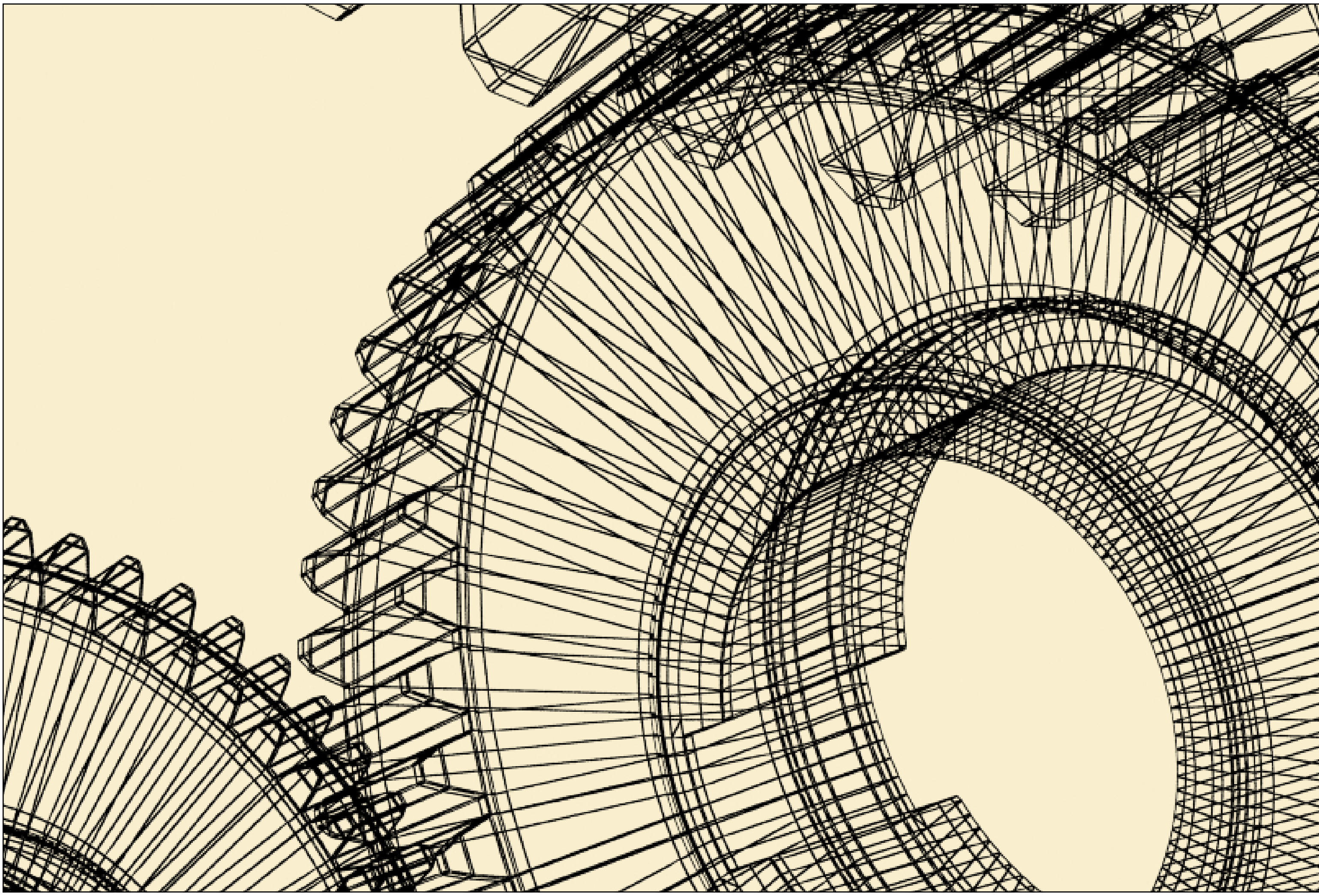

Residual Stress Distribution in an Induction Hardened Gear

By Dmitry Ivanov, John Inge Asperheim, and Leif Markegård

Results of a full-scale 3D simulation is utilized to evaluate the complete distribution of residual stress in an induction hardened aeronautic gear component.

A vast majority of steel gears are heat treated in order to obtain the desirable properties of a final product such as a high wear resistance and a long fatigue life. There are numerous heat treating techniques available today. Which one is chosen depends on many factors including the required hardening pattern, allowable distortion, post-heat-treatment machining, energy consumption, and production line requirements [1].

One of the widespread techniques is induction hardening of gears, usually associated with high flexibility and controllability allowing the minimization of the final product distortion and the possibility to control, to a certain extent, the distribution of the residual stress [2]. Despite the apparent flexibility, adjustment of the induction heating parameters is a challenging problem originating from the complexity of the hardened gear's geometry, highly non-linear steel properties in the range of heat treatment, and complex nature of the electromagnetic interaction in the system. The complexity is magnified even further if the optimization of stress distribution or distortion of the component is considered as a goal function. The analytical models are significantly limited in this case, whereas numerical simulations are of great importance. Numerous impressive investigations have been done in the last couple of decades, simulating the induction hardening of gears [3–7]. Some of the published works include the mechanical effects [8, 9].

One of the actual problems today is to verify the existing models and compare the simulation results with reliable and comprehensive experimental data. It looks promising to use the recently published papers concentrating on the experimental investigation of induction hardening of an aeronautic gear [10, 11]. Alongside in-process measurement of the

Proceedings of the 28th ASM Heat Treating Society Conference. October 20–22, 2015, Detroit, Michigan. Reprinted with permission of ASM International.

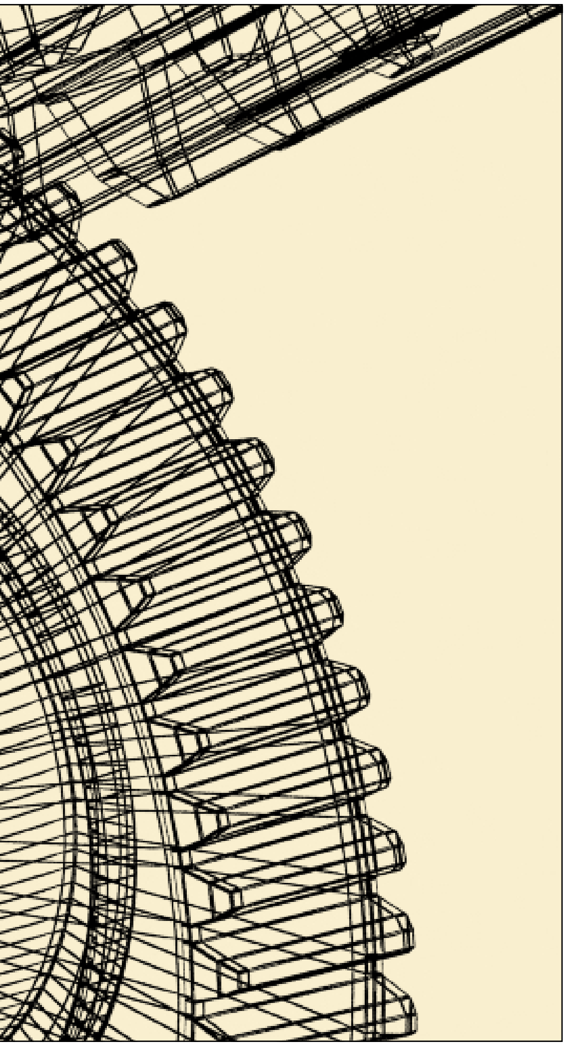

isotherms [10], the exhaustive measurement of the residual stress with a novel technique is available [11]. Larregain's et al. work has been already used for verification of magneto-thermal computations, and the results have been published as two master theses [12, 13].

This paper concentrates on a coupling of the commercial software package Cedrat Flux 3D v12 [14] for electromagnetic and thermal simulations with an open source package EDF Code Aster v12.2 [15] for the following phase transformations and stress-strain computations of the induction hardening of the aeronautic gear. Obtained simulation results are compared with the experimental published results [10, 11].

EXPERIMENTAL CASE

The geometry, material, and process parameters for simulation have been adopted from the original experimental investigations [10, 11]. As shown in Figure 1, only a quarter of the gear tooth is enough for the following procedure due to the symmetry of the geometry. The number of teeth is 48, therefore, the sector of 3.75° represents the features of gear shape entirely. Figure 1 introduces the designations of the geometry planes being used further as a reference and presentation of the simulation results.

The material of the gear is steel AMS 6414 (similar to AISI 4340) [11]. Prior to induction heat treatment, the material is quenched and tempered (Q&T) to a homogeneous initial hardness of 415 ±24 HV microstructure.

Case B from the Savaria's et al. paper was chosen for simulation since the same induction heat treatment parameters and geometry have been used previously in Larregain's et al. work for in-process measurement of isotherms [10, 11]. In the selected case, the induction coil of 110 mm inner diameter and a 6 mm thickness was connected to a generator, designed by EFD Induction AS, with dual simultaneous medium and high frequencies. The gear was preheated with medium frequency (10 kHz, 15.75 kW generator power) in 4.5 seconds. After a short dwell of 0.2 seconds, a final high frequency shot (190 kHz, 99 kW) was run. After heating, the gear was rapidly quenched with a water and liquid polymer spray solution (12 percent).

Shortly after the induction hardening, the gear was tempered in a furnace at 150°C for two hours.

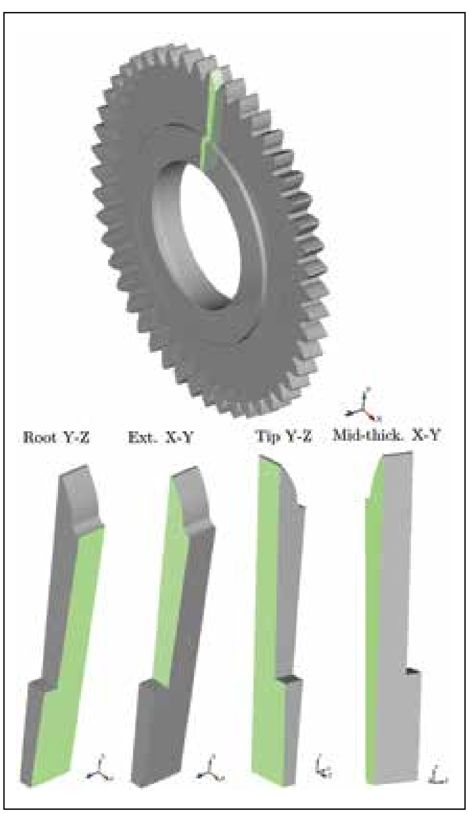

Figure 1: Spur gear geometry — domain selected to be used in simulations and designations of planes

APPROACH TO SIMULATION

Magneto-thermal simulations

A simulation flow chart is shown in Figure 2. Firstly, magneto-thermal computations have been run in Cedrat Flux 3D v12 [14]. Dependency of electric conductivity and magnetic permeability on temperature have been taken into account. Electromagnetic and thermal properties for low-alloyed medium carbon steel have been adopted for simulation. Symmetry boundary conditions have

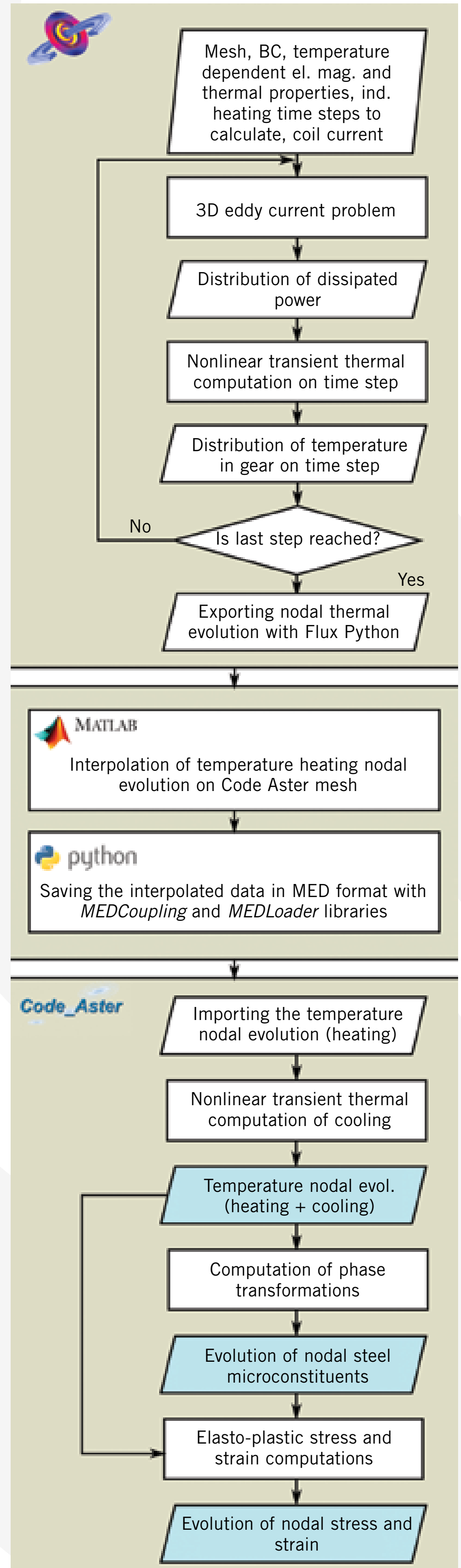

Figure 2: Simulation flow chart

been exposed on the planes: Root Y-Z, Tip Y-Z, and Mid-thick. X-Y (see Figure 1). The geometry also includes the coil, surrounding air, and an infinite box.

As a result of simulation, nodal evolution of temperature at the induction heating stage is obtained and exported for post-processing using Flux Python.

Coupling of Cedrat Flux and Code Aster

The finite element meshes used for the electromagnetic and mechanical computations are optimized taking into account the physics of simulated phenomena. The high frequencies used for induction heating in this case require the FEM electromagnetic problem to be created with a very fine mesh. Characteristic length not exceeding 0.1 mm is used for the regions closest to the surface. The total number of nodes used in the current investigation for discretization of the gear domain in Cedrat Flux 3D was 341429. The discretization density can be reduced for the phase transformation and stress-strain simulation. At the same time, the distribution of element sizes should be more uniform in this case as high stress is not limited by the hardening region due to mechanical integrity of the gear. The total number of nodes used in Code Aster simulation is 72021. In order to use the result of electromagnetic simulation, the nodal temperature evolution must be interpolated to a mesh used for a computation of the subsequent cooling, phase transformations, stress, and strain. This operation has been done in the Mathworks MATLAB environment [16]. The result of interpolation (projection) was exported then to a MED format as it is supported by Code Aster [17].

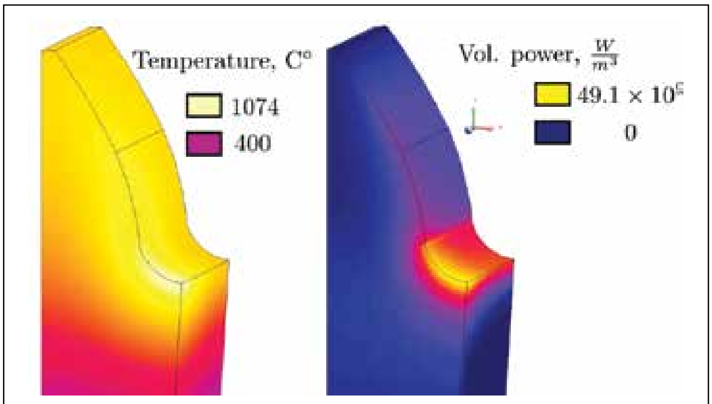

Figure 3: Distribution of temperature and volumetric power at the very end of the final shot

Phase transformations and stress-strain simulation

The resulting MED-file was imported by Code Aster. The last time step of induction heating simulation has been used for subsequent quenching calculation as initial temperature distribution. A concatenated list of nodal temperature evolutions during induction heating and quenching is input data for phase transformation computation. One can see that Code Aster runs metallurgical computations in a post-processing mode. In other words, no modification of thermal material properties caused by phase transformations are possible [18]. Therefore, latent heat of transformation should be included as a part of heat capacity.

The parameters of an austenitization model have been fitted to obtain the same hardening pattern as shown in referenced experimental works [10, 11]. The measured data indicates that the transformation is completed in a temperature range 704-816°C. See Figure 11 in Reference [10]. A simple austenitization model with constant Ac1 and Ac3 temperatures has been accepted due to a lack of experimental data. The model does not take into account an influence of heating rate on transformation kinetics. Adjustment of the model parameters results in Ac1 = 740°C and Ac3 = 760°C. The obtained apparent transformation range looks implausible from the metallurgical point of view, substantially because of its narrowness. Despite that, as it will be possible to see later, utilization of the apparent Ac1-Ac3 values allowed to obtain the hardening pattern conform to that observed in the experiments. Further investigations on reverse transformation to austenite of Q&T AMS 6414 steel is required to enrich the model with effects from taking the heating rate into account.

Resulting nodal evolution of temperature and micro-constituents, alongside mesh and boundary conditions, are the initial data for stress and strain computations. As in the magneto-thermal simulations, the symmetry boundary conditions have been imposed on the planes: Root Y-Z, Tip Y-Z, and Mid-thick. X-Y (see Figure 1). The model takes into account the transformation plasticity, von Mises classic plasticity, and isotropic hardening (relation META_P_IL_PT) is applied [19].

Material properties for the gear being used for the simulations correspond to Ck45 steel [20]. The initial Q&T structure is described by martensite properties. The very high yield limit of martensite drops down drastically during the final shot because of the transformation to soft austenite. This shows up as the source of the model's significant non-linearity.

RESULTS

Despite the high frequency of 190 kHz used for the final shot, the peak of volumetric power is located in the root of the gear, as shown in Figure 3. This type of the power distribution is observed through the process and confirmed by similar simulations [12, 13]. The peak is shifted to the exterior plane due to the configuration of the magnetic field generated in the system. Such power distribution results in significant asymmetry in a Z-direction underlining the importance of full 3D-simulation in this case.

A comparison of the simulated surface isotherms with ones obtained in Larregain's et al. experiment is shown in Figure 4. Note that simulated and experimental tooth shapes are slightly different — the tooth flank of simulated geometry is more convex. Apparently, this deviation is conditioned by a chosen method of CAD gear model construction according to the specified parameters.

Conformity of in-process isotherms with simulated results is acceptable. No serious deviation is visible, except for the gradient in the temperature range of 704-927°C. It appears that simulation shows a shallower gradient, especially in the root area. A possible cause of that is the magnetic properties of the steel and the way they are treated in computation. Fine tuning of the AMS 6416 steel properties should be done in future work.

The comparison of simulated hardening pattern with the etched part is shown in Figure 5. An excellent match can be seen for the exterior surface, whereas the mid-thickness pattern is slightly shallower in the simulation.

The simulated distribution of residual stress is shown in Figure 6. A very high tensile peak of σ_x and σ_y can be seen in the transition zone down the root area with a maximum value in the mid-thickness plane. A tensile peak of such magnitude is possible due to the accepted yield limit of Q&T microstructure corresponding to the yield limit of martensite.

Distribution of σ_y and σ_z along the tooth surface is rather complex. Moderate compression can be seen at the root area starting from the

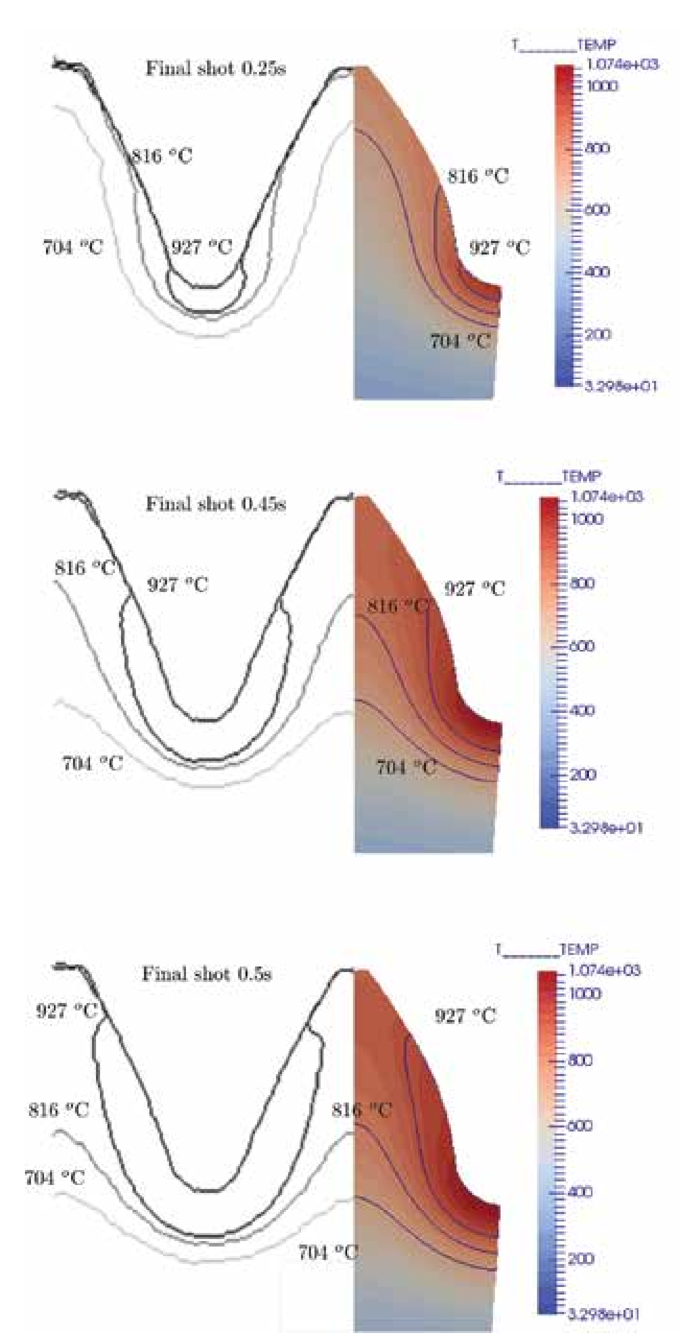

Figure 4: Experimental in-process isotherms compared to simulation

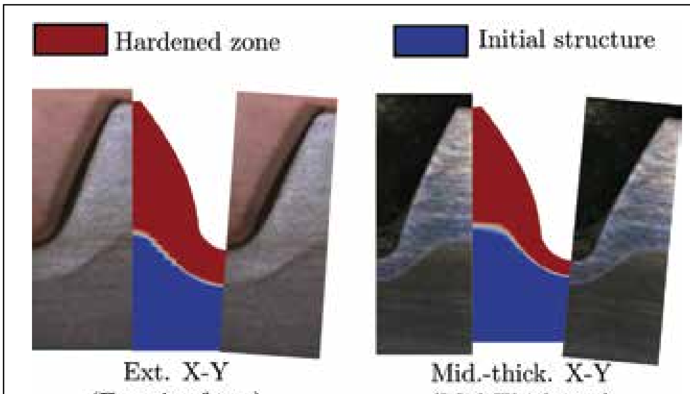

Figure 5: Comparison of experimental and calculated hardening pattern

mid-thickness plane. The compression gradually turns into a moderated tension moving both up to the tooth flank and toward the exterior faces along the root. The distribution of stress at the pitch area is more uniform.

The result of the residual stress simulation was compared with experimental measurements done by Savaria et al. on a final part after grinding [11]. The same locations as in the original work have been defined in a geometric model. The locations and in-depth direction of measurement are shown in Figure 7. (See Figure 4 in [11] for definition and comments in the original work.) The measured axial component of stress tensor (stresses σZ1 and σZ3 accordingly for zones 1 and 3) corresponds to axis Z in the current work. The orientation of the measured component B in the original work is nearly parallel to axis Y in the current investigation. Therefore, the Y-component of stress is exported from the simulation and the pairs σB1-exp — σY1-sim, σB2-exp — σY2-sim, and σB3-exp — σY3-sim are to be compared.

Figure 8 shows the experimental and simulation data for zones 1 and 2. In contrast to simulation, the experimental distributions σB1-exp, σZ1-exp, and σB2-exp have the drop toward the more compressive stress at the very surface. As it was explained in the original work, this drop can result from the grinding operation applied after induction hardening and before stress measurement.

It is accepted that the measurements are affected by the grinding down to a depth of 0.1 mm. It is worth noting that zones 1 and 2 are located in a stress transition area (from tension to compression) as shown in Figure 6. The actual values of stress distribution obtained from simulation are very sensitive to zone position, especially for zone 1. Taking into account that fact and accuracy of measurement (±40 MPa), one can see an acceptable conformity of experimental result and simulation.

The simulation result fits the experimental data even better if zone 3 is considered (see Figure 9). Again, the surface stress drop in experimental lines σB3-exp and σZ3-exp can be related to grinding operation. The rest of the results obtained from simulations are in a good agreement with experimental measurements. In contrast to zones 1 and 2, zone 3 is located in the area with a stable stress distribution and not as sensitive to location of measurement.

CONCLUSION AND FURTHER WORK

Despite the accepted simplifications, the simulation results appear to reflect the real distribution of residual stress in the investigated spur gear after the induction hardening process. It makes it possible to consider the optimization of stress distribution by varying the process parameters using the provided approach to simulations.

As the part of future work, fine tuning of material parameters should be done. In particular, the parameters identification of the austenitization model dependent on the heating rate is of great interest. In addition, more accurate electromagnetic, thermal, and mechanical properties of Q&T AMS 4340 steel (or similar) is an open question.

Finally, the experimental work done by Savaria et al. contains the results for three other combinations of process parameters including the dual-frequency processes. Reconstruction of these experiments in numeric simulations is the short-term target, as it allows fine tuning of the simulation tools being used on a daily basis at EFD Induction.

ACKNOWLEDGMENTS

The authors are grateful to Dr. Vincent Savaria and Professor Philippe Bocher for providing the details of their work.

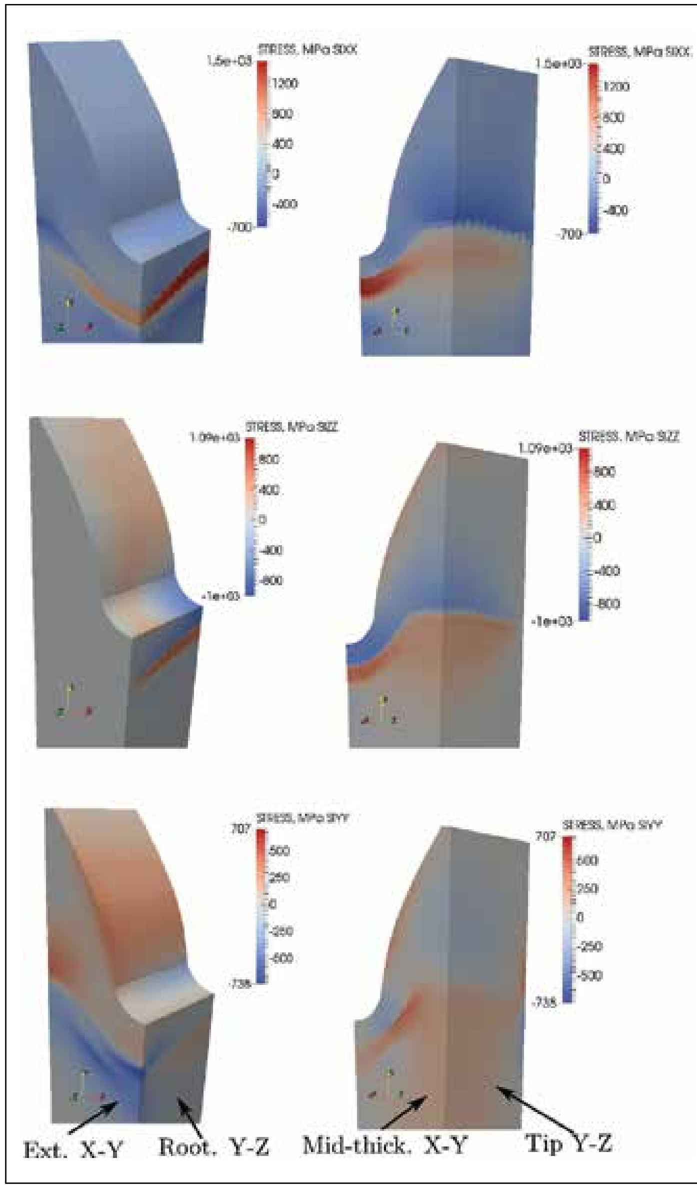

Figure 6: Calculated distribution of residual stress

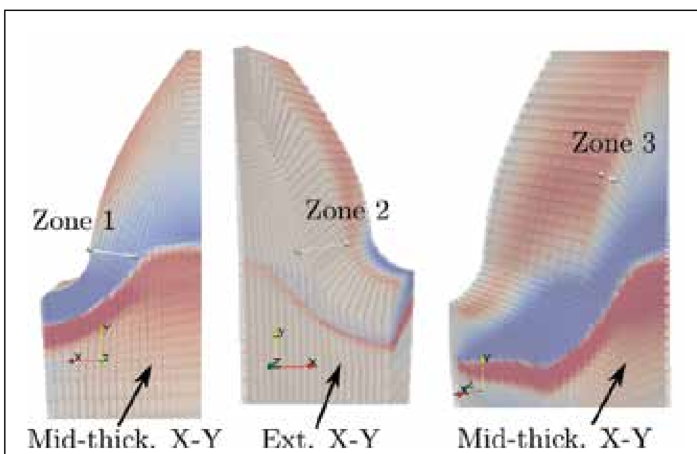

Figure 7: Location of stress measurement zones

REFERENCES

1. Nicholas Bugliarello et al. "Heat Treat Process For Gears." In: Industrial Heating (1995).
2. Valery Rudnev. "Induction hardening of gears and critical components." In: Gear Technology (2008), pp. 58–63.
3. E. Wrona, B. Nacke, and D. Resetov. "3DModelling of the Transient Heating Process for Induction Surface Hardening."

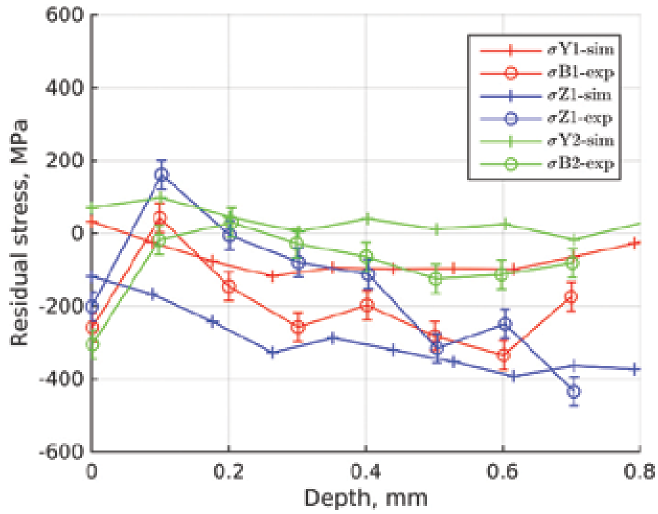

Figure 8: Comparison of simulated and measured in-depth distributions of residual stress in zones 1 and 2

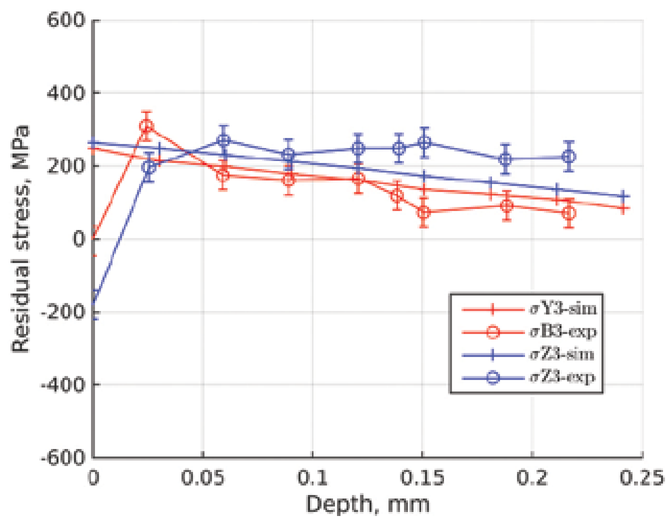

Figure 9: Comparison of simulated and measured in-depth distributions of residual stress in zone 3

In: MEP-International Scientific Colloquium Modelling for Electromagnetic Processing, Hanover. 2003, pp. 119–123.

4. Dietmar Höomberg, Thomas Petzold, and Elisabetta Rocca. "Analysis and simulations of multifrequency induction hardening". In: Nonlinear Analysis: Real World Applications 22 (2015), pp. 84–97.
5. Alessandro Candeo et al. "Multiphysics modeling of induction hardening of ring gears for the aerospace industry." In: Magnetics, IEEE Transactions on 47.5 (2011), pp. 918–921.
6. Thomas Petzold. "Modelling, analysis and simulation of multifrequency induction hardening." Ph.D. thesis. Technische Universität Berlin, 2014.
7. Steffen Klonk. "Numerical modelling of induction heating for complex geometrical parts." Ph.D. thesis. Ecole Nationale Supérieure des Mines de Paris, 2013.
8. Zhichao Li and B. Lynn Ferguson. "Controlling gear distortion and residual stresses during induction hardening." In: American Gear Manufacturers Association Technical Paper, 11FTM25 (2011).
9. D. Hömberg et al. "Simulation of multifrequency-induction-hardening including phase transitions and mechanical effects." In: WIAS Preprint 1975 (2014).
10. Benjamin Larregain et al. "Method for accurate surface temperature measurements during fast induction heating." In: Journal of materials engineering and performance 22.7 (2013), pp. 1907–1913.
11. Vincent Savaria et al. "Measurement and correction of residual stress gradients in aeronautical gears after various induction surface hardening treatments." In: Journal of Materials Processing Technology 220 (2015), pp. 113–123.
12. Damiano Mingardi. "Numerical models for induction hardening of gears." MA thesis. Universita Degli Studi Di Padova , 2013.
13. Lorenzo Ciccarone. "Models and tests of induction contour hardening process." MA thesis. Universita Degli Studi Di Padova, 2014.
14. Cedrat. Flux - electromagnetic and thermal finite element software. 2015. url: http://www.cedrat.com/en/software/flux. html.
15. EDF R&D. Code Aster - Analysis of structures and thermomechanics for studies and research. url: http://www.code-aster.org/V2/UPLOAD/DOC/Presentation/ plaquette_aster_en.pdf (visited on 06/30/2015).
16. MATLAB. 8.4.0.150421 (R2014b). The MathWorks Inc., 2014.
17. Open Cascade, EDF, and CEA. MED data model. 2015. url: http://www.salomeplatform.org/user-section/about/med (visited on 06/30/2015).
18. Jean Angles. Notice dutilisation pour des calculs thermo-métallo-mécaniques sur des aciers. 2012. url: http://http://www. code-aster.org/V2/doc/v11/fr/man_u/ u2/u2.03.04.pdf.
19. Jean Angles. Modélisation élasto (visco) plastique prenant en compte des transformations métallurgiques. 2012. url: http://www. code-aster.org/V2/doc/v11/fr/man_r/ r4/r4.04.02.pdf.
20. Hubertus Josephus Maria Geijselaers. "Numerical simulation of stresses due to solid state transformations: the simulation of laser hardening." Ph.D. thesis. University of Twente, Enschede, 2003, p. 142.

ABOUT THE AUTHORS: Dr. Dmitry Ivanov graduated from Belarussian State University of Informatics and Radioelectronics with a specialist degree in electrical engineering. In 2005, he commenced his Ph.D. research in the laboratory of Prof. Dr. Kundas. His thesis is dedicated to development of robust models for simulation of stress and strain effects in induction hardening processes. In 2009, he was awarded his doctorate degree in Minsk, Belarus, and continued his research in the Kundas' laboratory as a post-doc. He joined EFD Induction in 2009 and works on process development, simulations of stress and strain, metallurgical phenomena in induction heating processes, and microstructural analyses in EFD's R&D department.

John Inge Asperheim received his M.S. in electrical engineering in 1994 at the Technical University of Trondheim (NTNU). He started his work in 1995 at Elva Induksjon, which is now EFD Induction. After a short period as a test engineer, he joined the R&D team to start EFD's FEM computations effort. The main focus of the work has been on design and development of various induction heating processes and applications, including induction tube welding, seam annealing, and a wide variety of heat treatment applications.

Leif Markegård received his M.S. in electrical engineering in 1974 at the Technical University of Trondheim (NTNU). He started his work at Sintef with Professor Dr. Odd Todnem at NTNU where he worked with the development of a method for thermal straightening of steel sheet constructions after welding based on induction heating. He followed the project to the industry and was one of a small group that in 1981 started a new company (today, named EFD Induction) where he is still working. He has concentrated on different applications of induction heating, including heat treatment where residual stress and distortion are areas of concern.

Laser hardening of a crane pivot

Case Study: Laser Hardening

By Markus A. Ruetering

The hardening of materials by laser is a specialized and fast-growing field, as it offers improved wear resistance, expansion of component life, and increased strength and fatigue limits of the material.

To increase the hardness of a steel material, there are basically three required steps in the hardening process. Step one is to heat the material, step two is to keep the temperature above a certain hardening temperature level for a certain time (dwell time), and step three is the quick cooling of the part, often referred to as quenching. During the dwell time, which is always higher than 1333°F (723°C), α-iron (ferrite) changes to γ-iron (austenite). Austenite can dissolve a higher amount of carbon than ferrite. Quickly cooling the material after the dwell time leads to a freezing of the carbon in the fine grain structure, creating a body-centered tetragonal structure. This structure is called martensite, and the non-crystallographic structure represents the hard material.

Today, hardness is measured in Rockwell (HRC), Vickers (HV), and Brinell (HB); the most commonly used are HV and HRC. All are based on the resistance of a part to the penetration of a counter body. A test specimen with a defined force for a defined time will leave a mark on the surface of the component to be measured. Typical HRC values for materials can range from 50 to 60 and sometimes achieve values slightly above 60.

Martensite is formed between an upper and lower material-specific temperature range. The higher the cooling rates, the more martensite is created in the material. Martensite, based on its crystal structure, increases the volume of a part, which can cause cracks, tension, and damages in the piece, and it requires a certain amount of rework after the hardening process to achieve the specified mechanical measurements of the hardened part. In almost all hardening techniques known to the industry — e.g., oven hardening, flame hardening, and induction hardening — milling, shaping, and grinding are necessary after hardening. Hence, the necessary material removal, the wear of the tools, and the calculated additional material before hardening add up to a high cost factor.

A COST-EFFICIENT PROCESS

It is possible to lessen the aforementioned cost factors with the use of laser hardening. However, laser hardening cannot be considered for every application, as it has its limits, too. The following discussion presents comparisons of laser hardening to other applications.

Figure 4: Crane and position of the pivot to be hardened

Figure 1: A 21-ton gear wheel for case hardening (source: Härterei Reese Bochum GmbH and Horsburgh & Scott in Cleveland, Ohio)

The first example is shown in Figure 1, a 21-ton part that is heated in the oven to create a hardening. Here, it's important to consider the amount of energy that is deposited into the part and the quick cool-down needed to create martensitic structures. Also, consider the necessary rework, the cost of energy, and carbon footprint. Nevertheless, the hardening was done this way most likely because of the hardening depth required in such a huge part and its use in the industry.

Hardening is applied from the surface to the inner of a part, and the hardening depth depends on the technology applied. In other words, the correct technology should be applied for a certain depth. The example shown in Figure 1 requires a hardening depth of several inches, whereas the laser is limited to 0.03-0.08". However, the limited hardening depth can be the necessary advantage, as it does not require milling in the hard status unlike oven, flame, and induction. A German OEM using various hardening technologies claims it can save up to 20 percent in the total cost of production after changing from induction to laser just by eliminating the machining in the hard status.

The schematics of laser hardening is shown in Figure 2. A focused laser beam is moved slowly over a section of the workpiece to heat it up quickly, keeping the temperature above hardening level during the dwell time and allowing the part to cool by self-quenching after the laser beam moves on. The high rise and fall time of the temperature with the sharp laser beam is specific, as well as the selective heating of the functional surfaces only. Therefore, distortion is avoided, rework is eliminated or reduced to a minimum, and no specific cooling media is required as the heat conduction of a small amount of energy is easily managed into the part itself. The latter leads to the self-quenching effect. Aerosols, water, or gases are not necessary, which translates into cost savings.

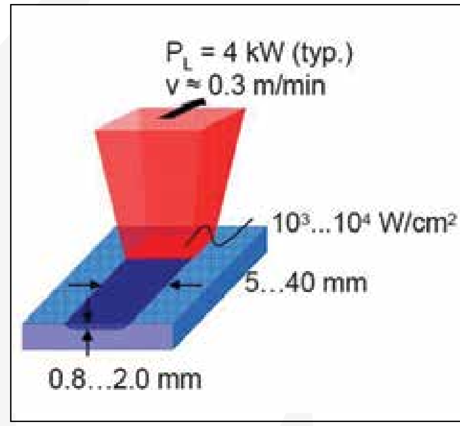

Figure 2: Schematics of laser hardening

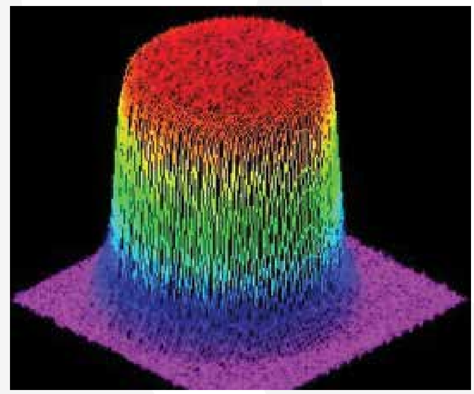

Figure 3: Top-hat energy distribution of a Laserline diode laser

A FIBER COUPLED DIODE LASER

The laser sources typically use a power level from 2 kW upwards, and the industry has seen installations with 15 kW and higher. Most efficient is a laser applied in a top-hat beam distribution (even in all directions) with a wavelength that allows high absorption into the metals treated. This all leads to a fiber coupled high power diode laser, which is the core development and product of Laserline GmbH.

A diode laser with a wavelength in the near infrared light, ranging from 900 to 1100 nm, allows the best absorption in metal — typically a factor of 10 to 15 percent higher compared to other lasers — and does not offer the top-hat energy distribution.

Higher speeds in the overall process are faster and more precise, which saves production time as well.

Laser hardening is not limited to small parts or fine structures; it can be helpful even for bigger structures and heavy-duty parts. Users might assume that the depth of just 0.06" is not enough, but with the fastest heating and quenching, the hardness is higher and the wear is lower, hence, even big parts should be considered. Some examples from Laserline's customers — ALOtec Dresden GmbH (ALOtec) in Germany and LaserTherm spol.s.r.o. (LaserTherm)

Figure 5: Laser hardening of a crane pivot

in Czech Republic — are presented in the following section. Both companies are offering job-shop work for hardening as well as turnkey solutions for customers ready to buy a system.

LESS DISTORTION WITH LASER HARDENING

LaserTherm was involved in beds of heavy lathe for processing parts in the range of maximum 12 x 4 x 1 m³ (40 x 13 x 3 ft³) that required hardening of 660 HV (58 HRC) in a depth of > 1 mm (0.04"). Conventional methods such as induction and flame hardening required an over-measure of 0.08-0.12" and a hardening depth of 0.12-0.20".

"We have seen a distortion of over 0.08" per yard length using the conventional methods," said Ondřej Soukup, managing director at LaserTherm.

After applying finite element calculations in combination with empiric results, the distortion could be reduced to 0.11" over a total length of 11.9 yards.

"As our calculations from the FEM ended up with 0.12" distortion, which was applied in pre-machining the bed in soft status, it compensated perfectly and left us with no rework," said Soukup.

The hardness in this laser-applied example is up to 700 HV (60.1 HRC) and has a depth of 0.04" with over 660 HV as specified.

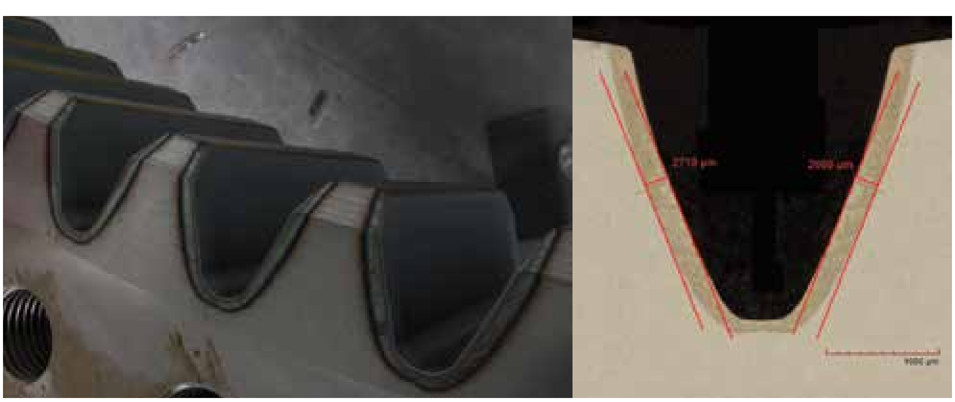

Figure 6: Hardening results for crane pivot

Another example from LaserTherm is the heavy-duty pivot ring of a crane. Figure 4 shows the crane and the position of the gear wheel in question. The wheel is over 14 feet in diameter and weighs 5.3 metric tons. The material is a 42CrMo4, which can be effectively laser hardened due to its 4.2-percent carbon content. Only materials with above 0.2-percent carbon content are to be considered.

Figure 5 shows the hardening process by laser. Within six hours, the teeth of the wheel are hardened to a hardness of over 520 HV in a depth of 0.08", reaching a hardness of over 600 HV on the surface. The results are shown in Figure 6 with a cross-section of the gear wheel. The hardness of the base material is only seen in a depth of almost 3 mm (0.12"). The spot sizes of the diode laser were applied by a zoom homogenizing optic, another product from Laserline. The optic allows changing the spot size from the smallest 8 x 8 mm² to the largest 50 x 50 mm² — always keeping the spot in a top-hat distribution and homogenized. This allows LaserTherm to apply the perfect spot size to every geometry and create unflawed results.

"High power diode laser techniques can be applied in many sectors of heavy industry in order to make the manufacturing of machine parts more efficient and to improve its overall quality and productivity," said Soukup.

Figure 7: A laser-hardened chain sprocket

Figure 8: Worm shaft, selectively hardened

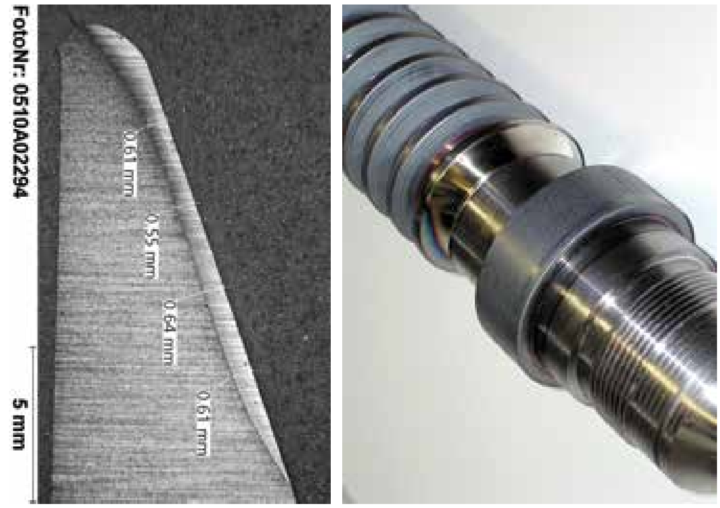

LASERS CAN BE ADAPTED TO A RANGE OF GEOMETRIES

In addition to LaserTherm, ALOtec is also using the diode laser from Laserline. ALOtec offers toothed racks, worm shafts, worm gear wheels, gear shafts, gear wheels, and pinion shafts, as well as conical gear wheels, chain sprockets, and clutch grooves. For this discussion, we selected three examples: the chain sprocket (Figure 7), the worm shaft (Figure 8), and the conical gear wheel (Figure 9). For all of these parts, the low distortion, the selective hardening only where needed, the depth of 0.02 to 0.08", and the resulting hardness of 60 HRC in all samples in absence of a coolant were results from laser hardening. Some of the parts would not have been possible with any other method; others would have been more costly with non–laser based applications.

The conical gear wheel achieves a hardening depth of 0.075", takes 55 seconds per flank, and only requires a laser power of 2 kW. The distortion is not possible to measure, there is no rework, and the wheel is machined to its final measurements before hardening. With the zoom optics, ALOtec would be able to adapt the spot to any version of the wheel.

The complexity of the worm shaft is covered by the freedom of a six-axis robot and an additional turning axis. ALOtec is experienced in applying the laser and its heat to the material. It must be considered that an overlap of the already-hardened section with another heat treatment should be avoided. The martensite will start to fall apart, depending on the material used at temperatures of 300°F and above. Hitting a surface twice will create a soft section.

An advantage of laser hardening is that the laser can be applied selectively, so the operator of the robot or system can ensure that the overlap does not happen. Using the zoom optics and the corresponding power into the spot allows new approaches and unveils new options for customers. In the past, the limit was 4 kW, thus the spot size was limited to approximately 40 x 10 mm^2, but Laserline now offers lasers up to 25 kW, and it has 40 kW and higher in its labs. With such high power, the spot can be made larger, and where two lines had been necessary in the past, the heat can now be applied in just one path, with a width of 4 inches now possible. This avoids a softened area in the overlap section. Having the 40 kW from the lab at the doorstep of factories and production floors, more applications are possible, and lasers are taking more market share.

As laser hardening is a temperature-guided process, it is highly recommended to apply a closed-loop temperature control to the process, such as a pyrometer or a camera-based system. Applying this closed-loop temperature-guided application allows precise hardening sections, as shown in Figure 7 for the chain sprocket.

Setup and programming is typically part of the three-day commissioning for a turnkey solution.

"Today's diode lasers are simply black boxes in a hardening system, covered with warranties up to five years for their diodes, installed in less than three hours, and have a standardized interface," said Dr. Hensel, founder and CEO of ALOtec.

CONCLUSION

With laser hardening, designers and engineers as well as managers and operators on the production floor have the option to optimize their heat treatment processes. Rework in the hard status can be eliminated

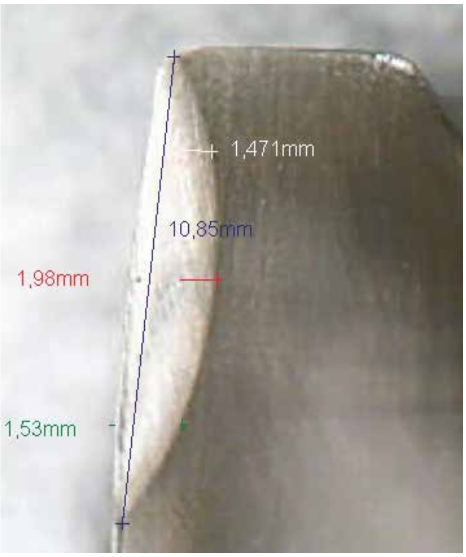

Figure 9: Conical gear wheel after hardening

or reduced to one grinding process. Lasers can harden selectively and avoid distortion and high levels of over-measure. Diode lasers themselves can be adapted to almost all geometries and have the best-suited beam and wavelength combined with an unparalleled wall plug efficiency to reduce the carbon footprint in production. Finally, these lasers can be guided by optical fibers to make them a versatile and flexible tool, which can be combined with both robots and CNCs, and existing hardware can be upgraded.

ABOUT THE AUTHOR: Markus A. Ruetering studied physical engineering at the University for Applied Science in Wedel, Germany, and holds a degree as Diplom-Ingenieur. In 1989, he joined Rofin-Sinar Laser GmbH, a major manufacturer of lasers. From 1989 to 1992, he was an R&D engineer for solid state lasers and held various sales positions. In 2011, Ruetering joined Laserline GmbH, which has offices in Santa Clara, California, and Plymouth, Michigan, and is headquartered in Mülheim-Kärlich, Germany. Ruetering is currently sales manager for Germany. For more information, go to www.laserline.de.

Heat Treat Equipment – REF #101
Phone: 734-331-3939 • Fax: 734-331-3915
Email: john@heattreatequip.com
Website: www.heattreatequip.com

Premier Furnace/BeaverMatic Inc. – REF #102
23850 Freeway Park Drive
Farmington Hills, Michigan 48335
Phone: 248-596-9000 • Fax: 248-596-9001
Email: sales@premierfurnace.com

The W.H. Kay Company – REF #103
30925 Aurora Road, Cleveland, OH 44139
Phone: 440-519-3800 • Fax: 440-519-1455
Email: sales@whkay.com
Website: www.whkay.com

Park Thermal – REF #104
257 Elmwood Ave #300, Buffalo, NY 14222
Phone: 905-877-5254 • Fax: 905-877-6205
Email: jmistry@parkthermal.com
Website: www.parkthermal.com

BATCH OVENS & BOX TEMPERING FURNACES

54" wide x 72" long x 84" high, Despatch Walk-In Oven Gas, 500 F. .... **REF #102**
8" 18" 8" Lucifer Elec. 1250 F. .... **REF #103**
12" 16" 18" Lindberg Elec. 1200 F. .... **REF #103**
12" 16" 18" Lindberg (3) Elec. 1250 F. .... **REF #103**
30" 48" 22" Dow Elec. 1250 F. .... **REF #103**
34" 19" 33" Poll.Ctrls Burnoff Gas 900 F. .... **REF #103**
36" 36" 35" Despatch Elec. 400 F. .... **REF #103**
36" 36" 120" Steelman Elec. 450 F. .... **REF #103**
36" 48" 36" Grieve Elec. 350 F. .... **REF #103**
36" 60" 36" CEC (2) Elec. 650 F. .... **REF #103**
37" 19" 25" Despatch Elec. 500 F. .... **REF #103**
37" 25" 37" Despatch Elec. 850 F. .... **REF #103**
37" 25" 50" Despatch Elec. 500 F. .... **REF #103**
38" 20" 24" Blue-M Elec. 1200 F. .... **REF #103**
38" 26" 38" Grieve Elec. 1000 F. .... **REF #103**
48" 24" 48" Blue-M Elec. 600 F. .... **REF #103**
48" 30" 42" Despatch Gas 850 F. .... **REF #103**
48" 48" 48" CEC (N2) Elec. 1000 F. .... **REF #103**
48" 48" 60" Gasmac Burnoff (2) Gas 850 F. .... **REF #103**
48" 48" 72" Despatch (2) Elec. 500 F. .... **REF #103**
48" 48" 72" Lydon Elec. 500 F. .... **REF #103**
54" 108" 72" Despatch Elec. 500 F. .... **REF #103**
56" 30" 60" Gruenberg Elec. 450 F. .... **REF #103**

BOX FURNACES

J.L. Becker Slot Forge Furnace, 1986, Brand New, Never Used .... **REF #101**
L & L Special Furnace Electrically Heated Box Furnace, 1991 .... **REF #101**
J.L. Becker Box Temper Furnace, 1989 .... **REF #101**
Sunbeam Electric Box Furnace, good running condition **REF #101**
Surface 30-48-30 Electric Temper Furnace, good/ very good condition .... **REF #101**
Atmosphere Furnace Co. 36-48-30 Electric Temper Furnace, good/ very good condition .... **REF #101**
Atmosphere Furnace Co. 36-48-30 Electric Temper Furnace, good/ very good condition .... **REF #101**
Atmosphere Furnace Co. 36-48-30 Electric Temper Furnace, good/ very good condition .... **REF #101**
Surface Combustion 30-48-30 Gas Fired Temper Furnace, good/ very good condition .... **REF #101**
Surface 30-48-30 Gas Fired Temper Furnace, good/ very good condition .... **REF #101**
24" wide x 48" long x 18" high, Lindberg batch temper, Gas, 1400 F. .... **REF #102**
30" wide x 48" long x 26" high, BeaverMatic batch temper, Gas, 1400 F. .... **REF #102**
8" 18" 8" Blue-M Elec. 2000 F. .... **REF #103**
12" 24" 8" Lucifer-Up/Down (Retort) Elec. 2150/1400 F. .... **REF #103**
12" 24" 8" C.I. Hayes (Atmos) Elec. 1800 F. .... **REF #103**
12" 24" 12" Hevi-Duty (2) Elec. 1950 F. .... **REF #103**
12" 24" 12" Lucifer-Up/Down Elec. 2400/1400 F. .... **REF #103**
3" 24" 12" Electra-Up/Down Elec. 2000/1200 F. .... **REF #103**
15" 30" 12" Lindberg (Atmos) - Retort Elec. 2000 F. .... **REF #103**
17" 14.5" 12" L & L (New) Elec. 2350 F. .... **REF #103**
22" 36" 17.5" Lindberg (Atmos) Elec. 2050 F. .... **REF #103**
24" 36" 18" Thermnlyne (2) - Unused Elec. 1800 F. .... **REF #103**
36" 48" 24" Sunbeam (N2) Elec. 1950 F. .... **REF #103**
36" 72" 42" Eisenmann Kiln (Car) Gas 3100 F. .... **REF #103**
60" 48" 48" Recco (1998) Gas 2000 F. .... **REF #103**
60" 96" 60" Park Thermal Elec. 1850/2200 F. .... **REF #103**
126" 420" 72" Drever "Lift Off"-Atmos (2 Avail) Gas 1450 F. .... **REF #103**
13" 14" 12" ELECTRIC 1300°F .... **REF #104**
10" 10" 18" ELECTRIC 2000°F .... **REF #104**
22" 36" 22" ELECTRIC 1600°F .... **REF #104**
12" 6" 8" ELECTRIC 2000°F .... **REF #104**
12" 8" 18" ELECTRIC 2800°F .... **REF #104**
20" 13" 36" ELECTRIC 1850°F .... **REF #104**
12" 18" 18" ELECTRIC 1250°F .... **REF #104**
4" 10" 4" ELECTRIC 2000°F .... **REF #104**
22" 10" 8" ELECTRIC - C/W STAND 1250-2000°F .... **REF #104**
15" 8" 30" ELECTRIC - ATMOSPHERE 1950°F .... **REF #104**
11" 11" 17" ELECTRIC - CABINET 2000°F .... **REF #104**
33" 40" 48" ELECTRIC 500°F .... **REF #104**
18" 18" 30" ELECTRIC - GLO BAR 2900°F .... **REF #104**
30" 30" 54" ELECTRIC - AGING 500°F .... **REF #104**
30" 30" 54" R ELECTRIC - AGING 500°F .... **REF #104**
30" 30" 54" ELECTRIC 500°F .... **REF #104**
24" 18" 24" NATURAL GAS - BATCH FURNACE .... **REF #104**
24" 18" 24" NATURAL GAS - BATCH FURNACE .... **REF #104**
36" 30" 84" ELECTRIC 1200°F .... **REF #104**
24" 24" 24" ELECTRIC 2000°F .... **REF #104**
29" 22" 36" NATURAL GAS 1250°F .... **REF #104**
12" 11" 24" ELECTRIC - BOX 2000°F .... **REF #104**
24" 24" 24" ELECTRIC - GAS MAC 850°F .... **REF #104**
18" 12" 12" ELECTRIC 2100°F .... **REF #104**
48" 30" 36" ELECTRIC - ATMOSPHERE TEMPERING .... **REF #104**
50" 24" 29" NATURAL GAS 1250°F .... **REF #104**
36" 18" 24" ELECTRIC 1250°F .... **REF #104**
17" 17" 36" NATURAL GAS 1250°F .... **REF #104**
15" 6" 10" ELECTRIC 1850°F .... **REF #104**
6" DIA 48" ELECTRIC - TUBE FURNACE 1200°C .... **REF #104**
7" 4" 14" GAS .... **REF #104**
10" DIA 18" GAS - FORGE FURNACE .... **REF #104**
9" 6" 15" GAS - FORGE FURNACE .... **REF #104**
6" 6" 15" GAS - FORGE FURNACE .... **REF #104**
12" 10" 20" ELECTRIC - SPEEDY MELT FURNACE 2000°F .... **REF #104**
12" 9" 18" ELECTRIC .... **REF #104**
12" 12" 18" NATURAL GAS 1250°F .... **REF #104**
14" 14" 18" ELECTRIC - GLOBAR 2500°F .... **REF #104**
17" 17" 17" ELECTRIC - HITEMP KILN 2200°F .... **REF #104**
35" 24" 60" ELECTRIC 1430°F .... **REF #104**
10" 9" 14" ELECTRIC - FRONT DOOR LOADING 2000°F .... **REF #104**
12" 12" 24" ELECTRIC - 13KW 2300°F .... **REF #104**
12" 12" 24" ELECTRIC - 20KW 2000°F .... **REF #104**
18" 12" 24" ELECTRIC 2000°F .... **REF #104**
36" 24" 56" ELECTRIC 800°F .... **REF #104**
24" 24" 36" ELECTRIC - CYCLONE 1250°F .... **REF #104**
24" 36" 30" ELECTRIC RE-CIRC. BOX FURNACE 2000°F .... **REF #104**
18" 20" 45" ELECT. RE-CIRC. W/ FLAME CURTAIN & BASKET 2000°F .... **REF #104**
12" 12" 18" ELECT. RE-CIRC. BATCH (MATCH PAIR WITH I3958) 1250°F .... **REF #104**
12" 12" 18" ELECT. RE-CIRC. BATCH (MATCH PAIR WITH I3957.) 1250°F .... **REF #104**

CAR BOTTOM FURNACES

Holcroft 48-144-48 Car Bottom Furnace .... **REF #101**
Sauder 48-144-48 Car Bottom Furnace .... **REF #101**
48" 48" 72" GAS FIRED CAR BOTTOM 2000°F .... **REF #104**
130" 72" 216" GAS FIRED CAR BOTTOM 2000°F .... **REF #104**
130" 72" 215" GAS FIRED CAR BOTTOM 2400°F .... **REF #104**
108" 36" 192" GAS FIRED CAR BOTTOM 2400°F .... **REF #104**
72" 48" 216" GAS FIRED CAR BOTTOM 2000°F .... **REF #104**

CHARGE CARS

Surface Combustion 30-48 Charge Car (Double Ended), fairly good condition .... **REF #101**
Atmosphere Furnace Company 36-48 Charge Car (Double Ended) .... **REF #101**
Surface Combustion 30-48 Charge Car (Double Ended) **REF #101**

CONTINUOUS ANNEALING FURNACES

Wellman Continuous Mesh Belt Annealing Furnace .... **REF #101**
Aichelin-Stahl Continuous Roller Hearth Furnace & Conveying System, 1996 .... **REF #101**
Park Thermal Continuous Mesh Belt Furnace, 2005, Excellent Condition – New – Never been used .... **REF #101**

CONTINUOUS HQT FURNACES

Tokyo Gasden Ro Continuous Mesh Belt HQWT Furnace Line, 1989 .... **REF #101**

CONTINUOUS TEMPERING FURNACES

Surface Combustion Mesh Belt Temper Furnace .... **REF #101**
J.L. Becker Conveyor-Type Temper Furnace with Ambient Air Cool Continuous Belt, 1997 IQ Furnaces .... **REF #101**
Surface Combustion 30-48-30 Pro-Electric IQ Furnace **REF #101**
AFC 36-48-30 IQ Furnace with Top Cool .... **REF #101**
AFC 36-48-30 IQ Furnace .... **REF #101**
Surface Combustion 30-48-30 IQ with Top Cool, Excellent Condition, 2000 .... **REF #101**
Surface Combustion 30-48-30 IQ Furnace, Excellent Condition .... **REF #101**

DRAW TEMPER FURNACES

24" wide x 48" long x 18" high, Lindberg batch temper, Gas, 1400 F .... **REF #102**
30" wide x 48" long x 26" high, BeaverMatic batch temper, Gas, 1400 F (NEW) .... **REF #102**
18" 12" 30" ELECTRIC 1250°F .... **REF #104**
16" 15" 12" ELECTRIC - BOX DRAW 1250°F .... **REF #104**
36" 16" 24" ELECTRIC - BOX DRAW 1250°F .... **REF #104**
12" 18" 16" ELECTRIC - BOX DRAW 1400°F .... **REF #104**
30" 20" 48" ELECTRIC - BOX DRAW 1250°F .... **REF #104**
24" 18" 36" NATURAL GAS ROLLER DRAW 1400°F .... **REF #104**
30" 30" 48" NATURAL GAS 1200°F .... **REF #104**
60" 40" 60" NATURAL GAS - DRAW FURNACE 800°F .... **REF #104**
29" 16" 36" ELECTRIC - DRAW/TEMPER 1400°F .... **REF #104**
54" 54" 150" ELECTRIC 900°F .... **REF #104**
24" 18" 10 FEET ELECTRIC 500°F .... **REF #104**
30" 24" 72" GAS - GRAVITY FEED DRAW 1350°F .... **REF #104**
12" 14" 12" ELECTRIC - WATER COOLED FAN 1200°F .... **REF #104**

ENDOTHERMIC GAS GENERATORS

Lindberg 1500 CFH Endothermic Gas Generator, 1992, good condition .... **REF #101**
Lindberg 1500 CFH Endothermic Gas Generator, 1996, excellent condition .... **REF #101**
Surface Combustion 5600 CFH Endo. Gas Generator ... **REF #101**
Surface Combustion 5600 CFH Endo. Gas Generator ... **REF #101**
Surface Combustion 5600 CFH Endo. Gas Generator ... **REF #101**
Surface Combustion 5600 CFH Endo. Gas Generator ... **REF #101**
Rolock Inc. 2000 CFH Endothermic Gas Generator........ **REF #102**

EXOTHERMIC GAS GENERATORS

J.L. Becker 12,000 CFH Exothermic Gas Generator w/ Dryer, w .... **REF #101**
Thermal Transfer 30,000 CFH Exothermic Gas Generator, 1994, excellent condition .... **REF #101**
Seco Warwick 2000 CFH Exothermic Gas Generator...... **REF #102**
Sunbeam 2000 CFH Exothermic Gas Generator .... **REF #102**
Alhern 6000 CFH Exothermic Gas generator .... **REF #102**
J L Becker 6000 CFH Exothermic Gas Generator........ **REF #102**
JL Becker 6000 CFH Exothermic Gas Generator........ **REF #102**

FLUIDIZING BED FURNACE

14" 30 DIA 5" ELECTRIC 1600ºF .... **REF #104**

FREEZERS

Webber 36-48-36 Chamber Freezer, 1980 .... **REF #101**
Cincinnati Sub Zero 36-48-36 Chamber Freezer, 1995 . **REF #101**

MESH BELT FURNACES

17" 8" 10' ELECTRIC 600ºF .... **REF #104**
23" 4" 10' NATURAL GAS 1250ºF .... **REF #104**
24" 12" 96" ELECTRIC 500ºF .... **REF #104**

MESH BELT BRAZING FURNACES

Lindberg Continuous Mesh Belt Brazing Furnace .... **REF #101**
J.L. Becker 26" Mesh Belt Brazing Annealing Furnace, 2007 .... **REF #101**
10" J.L. Becker Mesh Belt Furnace with Muffle, 1988 . **REF #101**
24" J.L. Becker Mesh Belt Furnace .... **REF #101**
Premier Furnace 14" wide mesh belt Aluminum Brazing Furnace 1400 F........ **REF #102**
Alhern 20" wide mesh belt Copper Brazing, Annealing Furnace 2100 F........ **REF #102**
J L Becker 20" wide mesh belt Copper Brazing, Annealing Furnace 2100 F. .... **REF #102**
JL Becker 20" wide mesh belt Copper Brazing, Annealing Furnace 2100 F. .... **REF #102**
Alhern 28" wide mesh belt Copper Brazing, Annealing Furnace 2100F. .... **REF #102**

MISC. EQUIPMENT

Atmosphere Furnace Co. 36-48 Stationary Holding Stations, 1987, 36"W x 48"L work area .... **REF #101**
Atmosphere Furnace Co. 36-48 Stationary Holding Stations, 1987, 36"W x 48"L work area .... **REF #101**
Atmosphere Furnace Co. 36-48 Stationary Holding Stations, 1987, 36"W x 48"L work area .... **REF #101**
Atmosphere Furnace Co. 36-48 Scissors Lift Holding Stations, 1987, 36"W x 48"L work area .... **REF #101**
Atmosphere Furnace Co. 36-48 Scissors Lift Holding Stations, 1987, 36"W x 48"L work area .... **REF #101**
Surface Combustion 30-96 Stationary Load Tables, 96-inch rail length, 15-inch rail centers .... **REF #101**
Surface Combustion 30-96 Stationary Load Tables, 96-inch rail length, 15-inch rail centers .... **REF #101**
Surface Combustion 30-96 Stationary Load Tables, 96-inch rail length, 15-inch rail centers .... **REF #101**
Surface Combustion 30-48 Scissors Lift Table, 48-inch rail length .... **REF #101**
Airco Flo meter panel# 1 .... **REF #102**
Airco Flo meter panel# 2 .... **REF #102**
Smart Skim unit........ **REF #102**
8xxx 2.400 CFH 12 oz (2) North American 1/3HP .... **REF #103**
8xxx 3.000 CFH 12 oz (3) North American 1/2HP .... **REF #103**
8xxx 5.400 CFH 4 oz North American 1/3HP .... **REF #103**
8236 12.000 CFH 12oz (3) North American 1/2HP ..... **REF #103**
8712 15.600 CFH 37 oz, North American 5HP .... **REF #103**
8193 19.500 CFH 32 oz, Spencer 5HP .... **REF #103**
8245 23.400 CFH 8 oz. North American 1,5HP .... **REF #103**
8185 24.000 CFH 24 oz. Buffalo Forge 7.5HP .... **REF #103**
8251 45.600 CFH 16 oz. Spencer 5HP .... **REF #103**
8252 66.000 CFH 24 oz . Snencer(New) 10HP .... **REF #103**
8253 66.000 CFH 24 oz. Spencer 10HP .... **REF #103**
8250 150.000 CFH 16 oz. Hauck 15HP .... **REF #103**

OVER - UNDER FURNACES

12" 11" 48" GLO BAR ELECTRIC 3000ºF .... **REF #104**
9.5" 9.5" 18" COILED ELEMENTS ELECTRIC 2300ºF . **REF #104**
22" 11" 14" COILED ELEMENTS ELECTRIC 2200ºF ... **REF #104**
12" 7" 30" ELECTRIC - CRESS .... **REF #104**
18" 12" 24" ELECTRIC 2100/1250ºF .... **REF #104**
12" 12" 36" ELECTRIC 2300/1250ºF .... **REF #104**

PARTS WASHERS

J.L.Becker Gas-Fired Tub Washer .... **REF #101**
48-72-48 Gas Fired Spray Washer .... **REF #101**
Dow Furnace Co. 30-48-30 Electrically Heated Spray, Dunk & Agitate Washer .... **REF #101**
Atmosphere Furnace Co. 36-48-30 Spray/Dunk Washer **REF #101**
Atmosphere Furnace Co. 36-48-30 Spray/Dunk Washer **REF #101**
Surface Combustion 30-48-30 Electrically Heated Spray Dunk/ Dunk Washer .... **REF #101**
Surface Combustion 30-48-30 Electrically Heated Washer .... **REF #101**

PIT FURNACES

Lindberg 28" x 28" Pit-Type Temper Furnace .... **REF #101**
14" 60" Procedyne - Fluidised Bed Elec. 1850 F. .... **REF #103**
16" 20" Lindberg Elec. 1250 F. .... **REF #103**
22" 26" L & N Elec. 1200 F. .... **REF #103**
28" 48" Lindberg Elec. 1400 F. .... **REF #103**
38" 48" Lindberg Elec. 1400 F. .... **REF #103**
40" 60" L & N -Steam/N2 Elec. 1400 F. .... **REF #103**
40" 60" Wellman-Steam/N2 Elec. 1400 F. .... **REF #103**
48" 48" Lindberg (Atmos) - Fan Elec. 1850 F. .... **REF #103**
20" 48" ELECTRIC 1200ºF .... **REF #104**
30" 36" NATURAL GAS 1250ºF .... **REF #104**
24" 30" ELECTRIC 1400ºF .... **REF #104**
16" 18" GAS - CYCLONE 1300ºF .... **REF #104**
28" 96" NATURAL GAS 1400ºF .... **REF #104**
24" 28" ELECTRIC - HOMO CARBURIZING 1400ºF ..... **REF #104**
16" 30" ELECTRIC SALT POT 1650ºF .... **REF #104**
22" 36" 22" ELECTRIC SQUARE PIT 1600ºF .... **REF #104**
6" 4" 16" ELECTRIC VACUUM PIT 2400ºF .... **REF #104**
24" 24" ELECTRIC 1400ºF .... **REF #104**
12" dia 18" ELECTRIC - HOMO PIT 1200ºF .... **REF #104**
30" 30" 30" ELECTRIC 800ºF .... **REF #104**
30" DIA 30" ELECTRIC - PIT CYCLONE 1250ºF .... **REF #104**
12" 20" ELECTRIC - KEYHOLE 1250ºF .... **REF #104**
4.5" 24" 4" ELECTRIC - SQUARE PIT .... **REF #104**
24" 48" 24" ELECTRIC - SQUARE PIT 1200ºF .... **REF #104**
18" 18" 18" ELECTRIC - TOP LOAD 2000ºF .... **REF #104**
16" Dia. 20" ELECTRIC - CYCLONE 1250ºF .... **REF #104**
22" Dia 26" ELECTRIC - CYCLONE 1250ºF .... **REF #104**
22"Dia 26" ELECTRIC 1250ºF .... **REF #104**
8"dia 9"deep ELECTRIC - TEMPERING 1250ºF .... **REF #104**
35" 60" GAS .... **REF #104**
28"DIA 28" ELECTRIC - CYCLONE PIT 1250ºF .... **REF #104**

VACUUM FURNACES

Brew/Thermal Technology Vacuum Furnace .... **REF #101**
Abar Ipsen 2-Bar Vacuum Furnace, 1986, good condition .... **REF #101**
24"W x 36"D x 18"H Hayes (Oil Quench) Elec. 2400 F. . **REF #103**
48" Dia 60" High Ipsen (Bottom Load) Elec. 2400 F. .. **REF #103**

ATMOSPHERE GENERATORS

750 CFH Endothermic Dow Elec. .... **REF #103**
750 CFH Endothermic Insen Gas .... **REF #103**
1000 CFH Exothermic Gas Atmosphere .... **REF #103**
1000 CFH Ammonia Dissociator Lindberg Elec. .... **REF #103**
1000 CFH Ammonia Dissociator Drever Elec. .... **REF #103**
1500 CFH Endothermic (Air Cooled) Ipsen Elec. .... **REF #103**
1500 CFH Endothermic Ipsen Gas .... **REF #103**
3000 CFH Endothermic air Cooled) Lindberg Gas .... **REF #103**
3000 CFH Endothermic (Air Cooled) Lindberg (2) Gas .. **REF #103**
3000 CFH Endothermic (Air Cooled) Lindhera Gas .... **REF #103**
3600 CFH Fnclothermic (Air Cooled) Surface (2) Gas ... **REF #103**
3600 CFH Endothermic Surface Gas .... **REF #103**
5600 CFH Endothermic Surface (3) Gas .... **REF #103**
6000 CFH Nitrogen Generator (2000) Gas Atmospheres Gas .... **REF #103**
10 000 CFH Exothermic Seco-Warwick Gas .... **REF #103**

INTERNAL QUENCH FURNACES

24 inch wide, 48 inch long, 18 inch high, Lindberg, Gas, 1850 F........ **REF #102**
24"W 36"D 18"H Dow (Slow Cool) Line Elec. 2000 F. . **REF #103**
24"W 36"D 1 8"H Ispen T-4 - Air Cooled Gas 1850 F. .. **REF #103**
24"W 36"D 18"H Ispen T-4 - Air Cooled Gas 1850 F. .. **REF #103**
24"W 36"D 18"H Isoen T-4 - Air Cooled Gas 1850 F. .. **REF #103**
24"W 36"D 18"H Ispen T-4 - Air Cooled Gas 1850 F ... **REF #103**
30"W 48"D 30"H Surface Allcase Elec. 1750 F. .... **REF #103**
30" 30" 48" NATURAL GAS 1750ºF .... **REF #104**
12" 10" 24" ELECTRIC - BABY PACEMAKER 1850ºF .. **REF #104**
45" 40" 72" ELECTRIC - ALUMINUM QUENCH 1250ºF **REF #104**
12" 9" 18" IPSEN 2000ºF .... **REF #104**
87" 36" 87" SURFACE COMBUSTION W/ 12,500G. QUENCH 1850ºF .... **REF #104**
62" 36" 62" SURFACE COMBUSTION W/ 9,500G. QUENCH 1850ºF .... **REF #104**
62" 36" 62" SURFACE COMBUSTION W/ 9,500G. QUENCH 1850ºF .... **REF #104**
15" 12" 30" Electric c/w load carts 1850ºF .... **REF #104**

CONTINUOUS/BELT FURNACES + OVENS

5"W 36"D 2"H BTU Systems (Inert Gas) Rec. 1922ºF . **REF #103**
12"W 48"D 2"H Lindberg (Inert Gas) Elec. 1022ºF. .... **REF #103**
12"W 15'D 4"H Sargent&Wilbur'94(Mufflel) Gas 2100ºF. .... **REF #103**
16"W 24'D 4"H Abbott-Retort (1996) Elec 2400ºF. ..... **REF #103**
24"W 12'D 6"H Heat Industries Elec. 750ºF. .... **REF #103**
24"W 40'D 18"H Despatch Elec. 500ºF. .... **REF #103**
60"W 45'D 12"H Roller Hearth Annealer (Atmos) Gas 1700ºF .... **REF #103**

MARKETPLACE

Manufacturing excellence through quality, integration, materials, maintenance, education, and speed.

AD INDEX

COMPANY NAME	PAGE NO.

BILL STUEHR
PRESIDENT AND CEO, INDUCTION TOOLING, INC.

PLEASE TELL US HOW INDUCTION TOOLING BEGAN.

In 1975, I was working as a process design engineer with a local commercial heat treating company. Several customers were coming to me and requesting tooling specific to their internal heat treating needs. My boss rejected the idea to build tooling, so I set out to begin my own business in 1976, which I started in my parents' garage. Today, I have a 30,000-square-foot facility in North Royalton, Ohio, with 20 employees.

WHAT PRODUCTS DOES INDUCTION TOOLING OFFER?

Our team designs and manufactures high-quality tooling for the induction heat treat industry, specializing in selective hardening quick-change inductors for the automotive, aerospace, medical, agricultural, and metal industries. We build high-quality inductors, bus bars, quick-change adapters, and other products. We are also a certified commercial testing laboratory accredited to ISO 17025 by the American Association for Laboratory Accreditation (A2LA) for the services provided by our metallurgical lab.

DESCRIBE INDUCTION TOOLING'S CAPABILITIES.

Our design approach is unique for each and every project in that we closely analyze and continually improve the quality, performance, and durability of our products. We develop and use the latest in computer technology — including FEA computer modeling, CAD/CAM software tools, surface and solid modeling, and 2- through 5-axis CNC machining applications — to validate our inductors. And along with controlled documentation, we can assure repeatable tooling to the closest tolerances in the industry.

In addition to our induction R&D laboratory, our commercial metallurgical laboratory integrates a complete package of testing services for our customers. Our lab manager, Sandra Midea, is a registered professional engineer with over 25 years of heat treating and testing experience. Our modern fully equipped metallurgical lab includes the ability to section and machine larger cross-section parts, including large bearing races and gears.

WHAT SETS INDUCTION TOOLING APART FROM OTHERS IN THE INDUSTRY?

We are recognized worldwide as a premier manufacturer of tooling for induction hardening, commonly called "inductor coils." We are also the largest facility in the world that engineers this tooling for selective hardening.

No one else offers customers a full-circle process like we do. We engineer the tooling, we build it in our production facility, and we test it in our induction laboratory to specific frequencies that our customer may have, either captive or in a commercial environment.

We are able to take the specification of a part, which is built into the basic structure, and hit the exact median in between the maximum requirement and the minimum requirement of selective hardness required on the component itself. This will allow for the deviation in their process when they do the heat treating. We build the tooling so that it hits that median.

Then, after the testing process, we characterize the tooling so that it is able to qualify. Once the characterization is done, we run parts in our induction lab, section the part, mount samples, and do the metallurgical evaluation. Sandra writes a report and submits it to the customer so that either they do it in-house with their equipment, send it out to a local heat treater, or order the equipment from the generator manufacturer with specifications to their part using our qualified inductors.

WHAT ARE YOUR BIGGEST CHALLENGES RELATED TO INDUCTION HEATING?

Our biggest challenge is with training new people entering our industry and quickly teaching the process of induction heat treating as it applies to selective hardening. Selective hardening is often applied to areas that will be case hardened by the induction heating method. The entire part itself is not heated, which makes it a green energy process. It takes a lot of training to understand how to apply the application, and it takes a lot of experience. There are safety issues, too, because it's an electrical process and we are working with high electrical currents at high frequency.

Training at our facility involves hands-on instruction utilizing the machine controls, understanding the concept of load tuning, capacitance, and the relationship of LC circuits (inductive capacitive circuits). Training also includes learning about the generator supplying power to the load tuning circuit and the inductor. The result shows how the heated part reacts to the inductor. Our team offers training programs at our facility and in our laboratory. When trainees move on to the factory environment where they are heating a part using the induction process, they need to feel prepared and comfortable.

WHAT BENEFITS DO YOU OFFER TO CUSTOMERS?

In addition to the design and fabrication of world-class tooling, we provide inductors that are capable of producing the required induction hardening pattern immediately when put into production. We also provide ISO-compliant commercial test lab reports that validate the results for our customers. The benefit is significantly reduced time to get a new process into production or ready to PPAP while using fewer company resources. We also use the induction development lab to solve problems, do research and development, and to invent new or novel methods for selective hardening. Our met lab also provides commercial testing services specially geared toward induction heat treating evaluations.

FOR MORE INFORMATION on Induction Tooling, go to www.inductiontooling.com.